UC San Diego

UC San Diego Electronic Theses and Dissertations

Title

Microtubule tethers at kinetochores and spindle poles : essential mitotic components

Permalink

https://escholarship.org/uc/item/1q60175p

Author

Silk, Alain Daniel

Publication Date

2008

Peer reviewed|Thesis/dissertation

eScholarship.org Powered by the California Digital Library
University of California

UNIVERSITY OF CALIFORNIA, SAN DIEGO

Microtubule tethers at kinetochores and spindle poles: essential mitotic components

A dissertation submitted in partial satisfaction of the

requirements for the degree Doctor of Philosophy

in

Biomedical Sciences

by

Alain Daniel Silk

Committee in charge:

Don W. Cleveland, Chair
Steven F. Dowdy
Xiang-Dong Fu
Lawrence S. B. Goldstein
Bruce A. Hamilton

2008

The dissertation of Alain Daniel Silk is approved, and it is acceptable in quality and form for publication of microfilm:

_____

_____

_____

_____

_____

Chair

University of California, San Diego

2008

Table of Contents

SIGNATURE PAGE..... iii

TABLE OF CONTENTS..... iv

LIST OF FIGURES..... viii

LIST OF TABLES..... x

ACKNOWLEDGEMENTS..... xi

VITA..... xiii

ABSTRACT..... xiv

CHAPTER 1: INTRODUCTION.....1

1.1 ANEUPLOIDY AND TUMORIGENESIS 1

1.1.1 Prevention of aneuploidy by the mitotic checkpoint.....1

1.1.2 Links between aneuploidy and tumorigenesis 2

1.1.3 CENP-E heterozygosity as a model to investigate aneuploidy in vivo 5

1.2 NON-MOTOR STRUCTURAL PROTEINS IN MITOTIC SPINDLE ASSEMBLY AND STRUCTURE 9

1.2.1 Cell-cycle specific roles for NuMA 10

1.2.2 Identification and Initial Characterization of NuMA..... 11

1.2.3 NuMA function at mitotic spindle poles..... 13

1.2.3.1 Initial characterization in mammalian cells..... 13

1.2.3.2 Mechanism of NuMA function elucidated in *Xenopus* egg extracts..... 14

1.2.3.3 Stoichiometry of spindle factors may dictate the NuMA phenotype 16

1.2.4 The mitotic function of NuMA in mammalian cells is not established..... 18

1.2.5 Additional features and functions of NuMA during mitosis..... 21

1.2.5.1 Modification by poly-ADP-ribosylation..... 21

1.2.5.2 Asymmetric cell division 22

1.2.6 Organization of the interphase nucleus..... 25

1.2.7 NuMA is a candidate nuclear structural component..... 28

CHAPTER 2: ANEUPLOIDY ACTS BOTH ONCOGENICALLY AND AS A TUMOR SUPPRESSOR 31

2.1 INTRODUCTION 31

2.2 ANEUPLOIDY CONTRIBUTES TO TUMORIGENICITY *IN VIVO* 32

2.3 ANEUPLOIDY DRIVES TUMORIGENESIS *IN VIVO* 33

2.4 ANEUPLOIDY INHIBITS TUMORIGENESIS IN TISSUES PRONE TO TUMOR FORMATION 34

2.5 DISCUSSION 36

CHAPTER 3: DISTINCT REQUIREMENTS FOR NUMA IN THE ESTABLISHMENT AND MAINTENANCE OF MAMMALIAN SPINDLE POLES DEMONSTRATED WITH INDUCIBLE GENE INACTIVATION 43

3.1 INTRODUCTION 43

3.1 NUMA EXPRESSION PATTERN INDICATES A POTENTIAL INTERPHASE FUNCTION 46

3.2 EXON MAPPING FUNCTIONAL DOMAINS OF MURINE NUMA 47

3.3 CREATION OF CONDITIONAL AND DELETION ALLELES OF NUMA 48

3.4 EFFICIENT TAMOXIFEN-REGULATED CRE-MEDIATED DELETION OF NUMA 50

3.5 NUMA IS REQUIRED FOR THE PROLIFERATION OF PRIMARY EMBRYO FIBROBLASTS 52

3.6 SPINDLE DEFECTS CAUSED BY LOSS OF MITOTIC NUMA FUNCTION 54

3.7 SPINDLE BIPOLARIZATION PRECEDES CENTROSOME DETACHMENT IN THE ABSENCE OF NUMA 56

3.8 REDUCED LEVELS OF NUCLEAR NUMA SUPPORT ALL ESSENTIAL INTERPHASE FUNCTIONS 58

3.9 NUMA IS REQUIRED FOR THE MAINTENANCE OF CENTROSOME-SPINDLE COUPLING IN BIPOLAR SPINDLES UNDER TENSION 60

3.10 STABLE KINETOCHORE-MICROTUBULE INTERACTIONS ARE REQUIRED FOR CENTROSOME SEPARATION DURING PROMETAPHASE 63

3.11 KINETOCHORE FIBERS ARE NOT REQUIRED FOR NUMA ACCUMULATION AT SPINDLE POLES 65

3.12 DISCUSSION 66

3.12.1 Mechanisms of microtubule focusing *67*

3.12.2 Function of Eg5 in prometaphase centrosome separation *71*

3.12.3 Centromere reorientation and chromosome segregation in the absence of focused poles *73*

CHAPTER 4: CONCLUSIONS AND FUTURE DIRECTIONS **93**

4.1 CONSEQUENCES OF ANEUPLOIDY 93

4.1.1 How does aneuploidy drive tumorigenesis? *93*

4.1.2 Aneuploidy therapy for cancer *95*

4.1.3 The myth of normal diploidy *96*

4.2 MITOTIC SPINDLE ARCHITECTURE 98

4.2.1 The relationship between centrosomes and spindle poles *98*

4.2.2 Separation of centrosomes in prometaphase *100*

4.2.3 In support of a spindle "matrix" *101*

4.3 FUNCTIONAL ORGANIZATION OF THE MAMMALIAN NUCLEUS 102

METHODS **105**

REFERENCES **118**

List of Figures

Figure 2.1 Aneuploidy Due to CENP-E Heterozygosity Contributes to Tumorigenicity 39

Figure 2.2 Aneuploidy promotes tumorigenesis. 40

Figure 2.3 Aneuploidy inhibits tumorigenesis 41

Figure 3.1 NuMA is broadly expressed in mouse tissues and present in nuclei of post-mitotic neurons 75

Figure 3.2 Efficient spindle-pole localization of NuMA requires exon 22 76

Figure 3.3 Creation of Conditional and Disrupted NuMA alleles 77

Figure 3.4 Aberrant splicing disrupts expression from the $NuMA^{Neo}$ Allele 78

Figure 3.5 Tamoxifen induced disruption of NuMA inhibits proliferation of primary embryo fibroblasts 79

Figure 3.6 Spindle defects result from homozygous NuMA disruption 80

Figure 3.7 Spindle phenotypes in NuMA-deleted cells are apparent in metaphase 81

Figure 3.8 Normal dynein localization and K-fiber stability in aberrant spindles following NuMA disruption 82

Figure 3.9 Bipolar spindle formation precedes centrosome detachment in the absence of NuMA 83

Figure 3.10 Normal cellular function and viability following *in vivo* motor neuron specific NuMA exon22 deletion 84

Figure 3.11 Prometaphase centrosome separation and centrosome independent spindle-pole focusing require NuMA 85
Figure 3.12 Creation and characterization of wild-type and cytoplasmic NuMA-GFP expressing stable HeLa cell lines 86
Figure 3.13 Kinetochore-fiber independent localization of NuMA to centrosomes 87
Figure 3.14 Kinetochore-microtubule attachments are required for centrosome separation in prometaphase 88
Figure 3.15 Functions of NuMA in centrosome-dependent and –independent spindle pole focusing 89
Figure 3.16 Two models for Eg5 mediated centrosome separation 90

List of Tables

Table 3.1 Genotype Incidence and Frequencies of Pups and Embryos from $NuMA^{Neo/+}$, $NuMA^{flox/+}$, and $NuMA^{\Delta/+}$ Heterozygous Crosses 91

Acknowledgements

I would first like to acknowledge my advisor, Don Cleveland, for providing me with the opportunity to be a part of the incredible intellectual environment of his lab where I have developed and matured as a scientist. So many lessons I learned from Don, I will carry with me in all aspects of my academic life. I cannot imagine having done my doctoral work in a better lab.

I also want to acknowledge the tremendous support I received from all Cleveland lab members over the many years. From science, to life, to the life of science, there is not a single member of the lab who ever hesitated to take the time to discuss anything I wanted, and provide encouragement when things were rough. Thanks especially to the mitosis crew, and in particular Beth Weaver with whom I had the privilege to work on a productive collaboration and for guiding me through the rigors of graduate school. Also I would like to thank Andrew Holland, for many enlightening discussions and motivation through the final days.

In addition, I am indebted to my family for their continuous support of all my decisions and providing me with a base of curiosity and determination that led me to pursue science. Finally I want to thank my fiancée, Katie Kindt, for always listening to my problems and providing advice, distraction, or solutions as required. I couldn't possibly have done it without her.

Chapters 1 and 2, in part, are reprints of the material as it appears in *Cancer Cell*, 2007(11):25-36, Weaver BA, Silk AD, Montagna C, Verdier-Pinard P and Cleveland, DW. The dissertation author was a major contributing researcher and second author of this paper.

Chapter 3, in part, is in preparation for publication of the material as it may appear in *The Journal of Cell Biology*, 2008, Silk AD, Holland, A and Cleveland DW. The dissertation author was the primary researcher and author of this paper.

Vita

1999 BS, Microbiology and Immunology, McGill University, Montreal, Canada

2008 PhD, Biomedical Sciences, University of California, San Diego

Publications

Silk AD, Holland A, and Cleveland DW. *Distinct requirements for NuMA in the maintenance and establishment of mammalian spindle poles demonstrated with inducible gene inactivation*. In preparation, Journal of Cell Biology, 2008.

Weaver BA, Silk AD, Montagna C, Verdier-Pinard P, Cleveland DW. *Aneuploidy acts both oncogenically and as a tumor suppressor*. Cancer Cell, 2007 (11):25-36.

Weaver BA, Silk AD, Cleveland DW. *Nondisjunction, aneuploidy and tetraploidy*. Nature, 2006 (442) E9-10.

Weaver BA, Bonday ZQ, Putkey FR, Kops GJ, Silk AD, Cleveland DW. *Centromere-associated protein-E is essential for the mammalian mitotic checkpoint to prevent aneuploidy due to single chromosome loss*. Journal of Cell Biology, 2003 (162):551-63.

Putkey FR, Cramer T, Morphew MK, Silk AD, Johnson RS, McIntosh JR, Cleveland DW. *Unstable kinetochore-microtubule capture and chromosomal instability following deletion of CENP-E*. Developmental Cell, 2002 (3):351-65.

ABSTRACT OF THE DISERTATION

Microtubule tethers at kinetochores and spindle poles: essential mitotic components

by

Alain Daniel Silk

Doctor of Philosophy in Biomedical Sciences

University of California, San Diego, 2008

Professor Don W. Cleveland, Chair

Mitosis is the period of the cell cycle during which the duplicated genome is equally partitioned into two daughter cells. This is accomplished by the alignment of paired sister chromatids in metaphase and the accurate segregation of sisters in anaphase. The faithful alignment and segregation of chromosomes relies on the assembly of cytoskeletal elements into the bipolar

mitotic spindle, the productive attachment of spindle fibers to kinetochores on each chromosome, and the focusing and anchoring of microtubule bundles at spindle poles. Errors in these various aspects of mitosis have severe consequences with regards to embryonic development, cellular viability, and tumorigenesis.

Disruption of kinetochore function leading to reduced microtubule attachment and decreased checkpoint signaling results in the gain or loss of whole chromosomes (aneuploidy), which is a hallmark of cancer. However, whether aneuploidy is a cause or effect of tumorigenesis has remained untested since it was first suggested as an agent of carcinogenesis more than 100 years ago. Heterozygosity for the microtubule-binding, kinetochore localized, kinesin-like motor protein, CENP-E, results in the development of aneuploidy in cultured cells and *in vivo* in the absence of additional genomic instability. A variety of studies presented here, using CENP-E heterozygous animals, demonstrate that elevated rates of chromosome segregation errors act in a context dependent manner to either promote or inhibit tumorigenesis.

At the opposite end of spindle microtubules, the poles, the requirement for microtubule associated cross-linking proteins in establishing and maintaining normal spindle structure has remained unclear. Construction and analysis of a conditional, loss-of-mitotic-function allele of the microtubule binding, coiled-coil protein NuMA, in mice and in cultured primary cells demonstrates that NuMA is an essential mitotic component. NuMA makes

distinct contributions to the establishment and maintenance of focused spindle poles. When NuMA function is disrupted, centrosomes provide initial focusing activity, but continued centrosome attachment to bi-polar spindles under tension, and maintenance of focused kinetochore-fibers at spindle poles require NuMA's microtubule binding capacity. Without centrosomes and NuMA function, spindle microtubule focusing completely fails to become established. Thus, microtubule-tethers at kinetochores and spindle poles are essential components for normal progression through mitosis.

Chapter 1: Introduction

1.1 Aneuploidy and tumorigenesis

1.1.1 Prevention of aneuploidy by the mitotic checkpoint

As a cell divides, it is crucial that duplicated identical genomes produced in S phase are transmitted to each daughter cell. This happens in two steps, first through replication of all nuclear DNA, followed by segregation of one copy of each duplicated chromosome into each daughter cell during mitosis. The mechanical separation and movement of chromosomes during mitosis is monitored and regulated by components of the mitotic checkpoint. This checkpoint, also known as the spindle assembly checkpoint, is a major cell cycle control mechanism that prevents chromosome missegregation by delaying advance to anaphase (the final stage of mitosis at which duplicated sister chromosomes are separated and segregated into separate cells) until kinetochores of all chromosomes have attached to spindle microtubules (Cleveland et al, 2003). The mitotic checkpoint requires that sister chromatids are held together until all chromosomes are bi-oriented at metaphase and attached to microtubules emanating from opposite poles of the mitotic spindle. Once all chromosomes are centrally poised in this way, the checkpoint is satisfied, and inhibition of anaphase progression is lifted. Sister chromatids are simultaneously released from each other and one copy of each

chromatid is moved into each new daughter cell. The molecular mechanisms of the mitotic checkpoint involve multiple sensing and signaling proteins, which cause the generation of an inhibitory signal at unattached kinetochores. This signal prevents action of the effector of anaphase progression, the APC/C, an E3 ubiquitin ligase that targets inhibitors of mitotic progression for degradation. A failure of checkpoint signaling results in advance through mitosis prior to the attachment of all chromosomes to the spindle, resulting in inaccurate chromosome segregation and generates aneuploidy – a condition in which daughter cells have an altered whole number of chromosomes relative to the normal diploid number.

1.1.2 Links between aneuploidy and tumorigenesis

It has been well known for more than a century that aneuploidy is a common characteristic of tumors. Indeed, nearly all major human tumor types display some degree of aneuploidy (Lengauer et al., 1998). Based on this correlation, and his observations of the pathological consequences of aneuploidy in fertilized sea urchin oocytes, Theodor Boveri proposed in 1902 and again in 1914 that aneuploidy drives tumorigenesis (Boveri, 1902; Boveri, 1914). With the subsequent discovery of specific genes that serve to drive or inhibit tumorigenesis, the idea that gain or loss of whole chromosomes plays an active role in initiating or promoting the progression of cancer, now known as the aneuploidy hypothesis, has become controversial. Attempts to test this

hypothesis using chemical or genetic manipulations have often been misleading or non-informative. For example, aneuploidy-inducing agents can indeed be carcinogenic, but they also act as DNA mutagens (Li et al., 1997; Quintanilla et al., 1986). Alternatively, highly specific genetic changes have been thought to be sufficient to transform human cells without widespread genetic aneuploidy, for example, due to co-expression of the SV40 T antigen, the telomerase catalytic subunit hTERT, and oncogenic ras (Hahn et al., 1999). However, later examination proved many of these supposedly genetically defined transformed cells to have a non-diploid karyotype (Li et al., 2000).

More recently, *in vivo* tests have made use of genetic animal models in which aneuploidy is generated at an elevated frequency. Reduction in any one of three essential components of the mitotic checkpoint, Mad2 (Babu et al., 2003; Baker et al., 2004; Michel et al., 2001), Bub3 (Babu et al., 2003; Baker et al., 2004; Michel et al., 2001) or BubR1 (Babu et al., 2003; Baker et al., 2004; Michel et al., 2001) causes chromosomes missegregation and has been implicated in tumorigenesis. For example, mice heterozygous for the essential mitotic checkpoint protein MAD2 develop spontaneous, benign, self-limiting lung adenomas with long latencies (18-20 months) (Michel et al., 2001). $BUB3^{+/-}$ mice do not show an increase in spontaneous tumorigenesis but do exhibit a trend toward increased sensitivity to chemically induced lung tumors (Babu et al., 2003; Baker et al., 2006; Kalitsis et al., 2005), while mice with

reduced levels of BubR1 exhibit increased susceptibility to tumors induced by carcinogens (Baker et al., 2006; Dai et al., 2004) or formation of colon polyps caused by mutations in the adenomatous polyposis coli tumor suppressor (Rao et al., 2005). Moreover, germline mutations in BubR1 have recently been identified in patients with the inherited cancer-prone syndrome mosaic variegated aneuploidy (Hanks et al., 2004; Matsuura et al., 2006).

Nevertheless, despite the uniform susceptibility to various types of tumorigenesis in these three animal models and the increased frequency of cancer in humans carrying a checkpoint gene mutation, no conclusion can be firmly drawn from these apparent correlations since each of these mitotic checkpoint contributors is also present in cells throughout interphase and may therefore participate in cellular functions other than chromosome segregation. Mad2 is known to be present at the nuclear envelope and nuclear pores (Campbell et al., 2001; Iouk et al., 2002) and has been implicated in both the DNA replication checkpoint (Sugimoto et al., 2004) and in promoting gross chromosomal rearrangements in yeast (Myung et al., 2004). Bub3 may interact with histone deacetylases, act to repress transcription (Yoon et al., 2004), and act to prevent chromosomal rearrangements (Myung et al., 2004). BubR1 is likely involved in numerous cellular processes in addition to its checkpoint function, including possibly apoptosis (Baek et al., 2005; Kim et al., 2005; Shin et al., 2003), fertility (Baker et al., 2004), megakaryopoiesis (Wang et al., 2004), inhibition of gross chromosomal rearrangements (Myung et al.,

2004) and the response to DNA damage (Fang et al., 2006). The multi-functionality of BubR1 specifically is made abundantly clear in mice which express very low levels of BubR1 and display a premature aging phenotype (Baker et al., 2004). This phenotype is difficult to explain based on deficiencies of checkpoint function, since no other checkpoint mutant mice display this unique phenotype. Thus, the ability of aneuploidy *per se* to drive tumorigenesis remains untested by efforts with reduced levels of any of these multifunctional proteins. Rather, the hypothesis that aneuploidy promotes tumorigenesis remains unproven, as are alternative views that aneuploidy is merely a benign side-effect of transformation or a contributor to tumor progression but not to tumor initiation (Marx, 2002).

1.1.3 CENP-E heterozygosity as a model to investigate aneuploidy *in vivo*

CENtromere associated Protein-E (CENP-E) is an essential, mitosis-specific, cell cycle regulated motor that accumulates primarily in G2, functions in mitosis and is then quantitatively degraded at the end of mitosis (Brown et al., 1994). A large (~312 kD in human) kinesin-like motor protein, CENP-E is conserved in all but the simplest metazoans and plays at least two critical functions during mitosis (Putkey et al., 2002; Wood et al., 1997; Yen et al., 1991; Yucel et al., 2000). First, it participates in making and/or maintaining the interactions between chromosomes and the microtubules of the mitotic spindle (McEwen et al., 2001; Putkey et al., 2002). Second, CENP-E serves a bi-

functional role in the mitotic checkpoint. It first stimulates mitotic checkpoint signaling by serving as an activator of BUBR1 kinase activity (Mao et al., 2003; Weaver et al., 2003) and then turns off production of the BUBR1-dependent “wait anaphase” inhibitor when all chromosomes have made appropriate attachments to spindle microtubules (Mao et al., 2005).

Embryos completely deleted of CENP-E die prior to implantation, and when cultured from E3.5 blastocysts display defects in chromosome alignment. Likewise, primary mouse embryo fibroblasts (MEFs) carrying a Cre-conditional CENP-E gene demonstrate a dramatic increase in misaligned chromosomes, specifically of chromosomes juxtaposed to the spindle pole, after treatment with Cre recombinase (Putkey et al., 2002; Weaver et al., 2003). This phenotype is also manifested *in vivo* after tissue-specific disruption of CENP-E in the liver followed by a liver regeneration protocol to induce mitoses. A dramatic increase in the number of polar chromosomes is found in anaphases of these CENP-E depleted vs. wildtype hepatocytes (Putkey et al., 2002). Daughter cells produced from these anaphases are fated to be aneuploid and contain an abnormal whole number of chromosomes.

Interestingly, aneuploidy expected from complete knockout of CENP-E is also seen in cells and mice that are heterozygous for the gene. CENP-E$^{+/-}$ cells contain half the level of CENP-E protein present in comparable wild type cells and display mitotic errors in which one or a few chromosomes are unable to make stable attachments to microtubules and remained misaligned near

one of the spindle poles (Weaver et al., 2007). As would be expected, the existence of these misaligned chromosomes results in the production of aneuploid progeny. Indeed, quantitation of the degree of aneuploidy in CENP-E heterozygous cells by visualizing chromosome spreads (also known as metaphase spreads) demonstrates that although aneuploidy increases with time in culture for all genotypes, primary MEFs with reduced CENP-E are significantly more aneuploid than wild type MEFs at all time points (Weaver et al., 2007). Examination of tissues or cells harvested directly from mice also shows higher rates of aneuploidy when CENP-E is heterozygous relative to wildtype. Notably, there are no growth defects in mice lacking one copy of CENP-E; whole animal and even individual organ weights are identical to wild-type (Weaver et al., 2007). The apparently normal viability despite development of aneuploidy in these animals makes the CENP-E heterozygous mouse a potentially useful model for investigating the *in vivo* consequences of aneuploidy.

The distinctiveness of aneuploidy resulting from CENP-E haploinsufficiency arises from the fact that unlike all other aneuploidy generating mutations in mice, very strong evidence indicates that the role of CENP-E truly is exclusively mitotic (and meiotic) and that the only cellular defect caused by a reduction in CENP-E function is the accumulation of whole chromosome loss or gain - aneuploidy. Firstly, CENP-E accumulates immediately prior to mitosis, localizes to kinetochores (which assemble at the

centromeric region of mitotic chromosomes) during all phases of chromosome movement, and is degraded during mitotic exit (Brown et al., 1994). It is therefore unlikely to participate in cellular functions other than those in mitosis. Consistent with this, general genomic integrity is preserved in CENP-E heterozygous cells. Secondly, levels of phosphorylated histone H2AX, a marker for DNA damage, are not increased in CENP-$E^{+/-}$ cells, although CENP-E heterozygous cells are responsive to DNA damage: treatment with a DNA damaging agent induces phosphorylation of H2AX to a similar extent in both wild type and CENP-$E^{+/-}$ MEFs (Weaver et al., 2007). Additionally, there are no obvious cancer-associated DNA mutations that accompany CENP-E heterozygous loss, sequencing of the p53 gene in CENP-$E^{+/-}$ cells revealed no mutations, as expected. Most importantly, spectral karyotyping demonstrated that chromosomes in CENP-E+/- cells do not exhibit structural rearrangements, including translocations, insertions or deletions (Weaver et al., 2007). Finally, the type of chromosome segregation error (polar chromosomes) produced by CENP-E haploinsufficiency would not result in DNA damage or activation of pathways that might be induced when mitotic chromosomes are caught in the incoming cytokinetic furrow as might be the case for lagging chromosomes, which are produced by all other genetic methods of generating aneuploidy (Norden et al., 2006; Shi and King, 2005; Weaver et al., 2006). CENP-E heterozygosity thus causes alteration in whole chromosome number in the absence of other defects, and provides a unique

model for investigating the contribution of aneuploidy to the process of tumorigenesis.

1.2 Non-motor structural proteins in mitotic spindle assembly and structure

The mitotic spindle is a molecular machine composed primarily of tubulin subunits polymerized into microtubule filaments. “Plus” ends of spindle microtubules attach to kinetochores in a manner partially dependent on the kinesin-like motor protein CENP-E, as described above. The “minus” ends of microtubules are grouped together at spindle poles, which serve as the final destination for chromosomes segregated in anaphase (Compton, 1998). In normal animal somatic cell mitosis, spindle poles are always coincident with centrosomes, the major cellular microtubule organizing structures. The two centrosomes of a cell appear to dictate spindle formation by nucleating extensive arrays of astral microtubules that transform into the two halves of the mature spindle. However, centrosomes are not absolutely required for spindle, or pole, formation (Khodjakov et al., 2000). Multiple non-motor structural proteins also contribute to the formation of mitotic spindles and may be required for spindle formation in the absence of centrosomes. Some of these components include microtubule cross-linking proteins such as Astrin, TPX2 and NuMA (Manning and Compton, 2008). The nuclear mitotic apparatus protein (NuMA) is a large (>200kD) coiled-coil protein that localizes

to the nucleus in interphase and to the poles of the mitotic spindle during M-phase. Many features of spindle structure that may depend on microtubule crosslinkers such as NuMA, including how kinetochore bundles are captured and focused towards centrosomes, the means for sustained anchoring of kinetochore fibers at spindle poles, and the role of centrosomes in both active focusing and the maintenance of spindle pole integrity are not established.

1.2.1 Cell-cycle specific roles for NuMA

The role of NuMA during mitosis has been studied primarily using the *Xenopus* extract system and in human cells by expression of dominant negative fragments and antibody microinjection approaches. The NuMA protein is poorly amenable to depletion using RNAi approaches and as such, the consequences on spindle assembly and structure of a genetic depletion of NuMA in mammalian somatic cells remain unknown. Although recent work has concentrated primarily on the mitotic function of NuMA at spindle poles, various lines of evidence suggest that NuMA may have additional functions in the nucleus during interphase. It is important to recognize the possibility that NuMA contributes to nuclear function with regards to the design and execution of strategies to specifically investigate the role of NuMA during mitosis. The following overview provides a summary of the current state of knowledge regarding the multiple potential functions of NuMA.

1.2.2 Identification and Initial Characterization of NuMA

The NuMA protein was first identified, and named for its localization pattern in 1980, by Lydersen and Pettijohn, who noticed a conspicuous high molecular weight band in Coomassie stained nuclear fractions of HeLa cell lysates while examining the electrophoretic mobility of nuclear non-histone chromatin proteins. Polyclonal antibodies raised in mice against the partially purified NuMA protein identified a striking staining pattern in human cells: in interphase the protein was nuclear, but during mitosis NuMA was present at the poles of the mitotic spindle (Lydersen and Pettijohn, 1980). This was the first description of an exclusively nuclear protein that associates with the spindle during mitosis, and to this day NuMA remains the only spindle protein with this unique localization pattern (Zeng, 2000).

An advancement of this work waited more than ten years until the Cleveland group serendipitously made an antibody to NuMA while searching to identify novel centromere and kinetochore proteins. Multiple monoclonal antibodies were generated against chromosome scaffolds – non-histone proteins isolated from chromosomes obtained from mitotically arrested cells. Many of these antibodies recognized a double-dot pattern characteristic of centromeres/kinetochores by indirect immunofluorescence on isolated mitotic chromosomes, but a subset of these failed to recapitulate this pattern in unperturbed mitotic cells. In contrast, they strongly stained the poles of the mitotic spindle, and in the case of antibodies from two hybridoma clones, also

showed a bright, diffuse, non-nucleolar staining pattern in nuclei of interphase cells (Compton et al., 1991). NuMA was the antigen recognized by these two antibodies. It is now clear that the kinetochore localization of NuMA (which allowed its identification) is an artefact of mitotic arrest induced by microtubule depolymerizing agents, and NuMA has subsequently never been observed at kinetochores in normally cycling cells by immunofluorescence nor by live imaging using GFP-NuMA (Merdes et al., 2000).

Compton went on to demonstrated that a number of additional monoclonal antibodies contemporaneously generated by others (Kallajoki et al., 1991) (Maekawa et al., 1991) (Tousson et al., 1991) gave similar staining patterns to the novel Cleveland monoclonals by immunofluorescence, identified identically sized bands by immunoblotting, and all recognized the same protein. He isolated the full length human NuMA cDNA using an expression cloning approach, and described the overall structure of the protein as an extended coiled coil with globular ends (Compton et al., 1992). Additionally, a purified fragment of the protein was used to calculate the cellular concentration of NuMA at $2x10^5$ copies per cell. An error in this calculation resulted in a ten fold underestimate of the concentration of NuMA, placing the actual number of molecules per cell in the range of millions, a number corroborated by an independent calculation based on conventional biochemical purification of endogenous NuMA (Kempf et al., 1994).

1.2.3 NuMA function at mitotic spindle poles

1.2.3.1 Initial characterization in mammalian cells

The mitotic localization of NuMA suggested that it may play a part in spindle function and offered the first insight toward investigating and understanding its mitotic role. An early appreciation for the requirement of NuMA in establishing and maintaining bipolar spindle structure during mitosis came from the first set of a series of antibody injection experiments. In these initial studies, anti-NuMA antibodies were microinjected into mammalian cells in interphase or various stages of mitosis. While pre-mitotic cytoplasmic antibody injection had no effect on mitotic entry (as expected), progression through mitosis was inhibited, as cells rounded and maintained a prolonged mitotic arrest for up to 4 hours. Antibody injection during prophase or prometaphase appeared also to result in prometaphase arrest, with microtubules arranged into monopolar spindles. Additionally, NuMA disruption in metaphase cells with normal bipolar spindles caused spindle collapse and convergence of centrosomes, which suggested that NuMA was required both for formation and maintenance of spindle bipolarity. Notably, anaphase antibody injection had no effect on the late stages of chromosome segregation or completion of cytokinesis (Yang and Snyder, 1992).

Further evidence of a requirement for NuMA in mammalian mitosis came from overexpression studies of dominant mutants. Expression of amino

or carboxy terminal truncation mutants resulted in micronucleation phenotypes of varying severity (Compton and Cleveland, 1993) supporting a role for NuMA in establishing and/or maintaining spindle integrity. It is notable that the phenotypes resulting from dominant inhibition of NuMA are distinct from antibody-microinjection with regards to progression through mitosis and effects on chromosome segregation. This is likely to result from the differing manner of NuMA inhibition caused by these alternate approaches, but could also arise from varying requirements for NuMA in diverse cell lines. Subsequent antibody injection experiments have failed to recapitulate the monopolar spindle phenotype and lend more support towards a function for NuMA in tethering microtubules at spindle poles (Gordon et al., 2001; Levesque et al., 2003), however the reasons for the inconsistencies between reports remain unclear and may be related to the uncertainties inherent in antibody-mediated inhibition.

1.2.3.2 Mechanism of NuMA function elucidated in *Xenopus* egg extracts

To further understand the role of NuMA in mitosis and the mechanisms underlying mitotic NuMA function, the effect of NuMA depletion on spindle structure has been examined more directly using the *Xenopus* egg extract system. Depletion of NuMA from mitotic extracts causes an alteration in spindle morphology such that microtubules do not converge at spindle poles. Instead of typical metaphase “football” shaped spindles, NuMA depleted

extracts form elongated irregular or rectangular microtubule structures with poorly defined and unfocused poles, although without any obvious metaphase chromosome alignment defects. These effects are partially rescued by reconstitution with purified NuMA indicating a direct role for NuMA in spindle pole focusing and suggesting that the micronucleation seen under conditions of dominant truncated NuMA overexpression may arise from a failure to maintain tight grouping of anaphase chromosomes during the final stages of mitosis. Mechanistic insight into the mitotic function of NuMA has been gained from the analysis of components bound to NuMA in immunoprecipitates, which include cytoplasmic dynein and dynactin (Merdes et al., 1996).

Tracing the behavior of GFP-NuMA in mitosis using live-cell imaging clarifies the significance of the NuMA-dynein interaction. Early in mitosis and immediately following nuclear envelope breakdown, NuMA is present in non-polar aggregates that are moved in a poleward (minus end) direction at velocities approximating those of dynein dependent transport. Inhibition of dynein in mitotic *Xenopus* extracts results in a reduction of spindle pole accumulation of NuMA, and phenocopies the pole-focusing defect caused by NuMA disruption (Merdes et al., 2000). This has led to a model in which stationary, microtubules attached at the pole serve as tracks for the poleward movement of dynein-NuMA complexes linked to non-anchored microtubules. This model is supported by the presence of a domain in NuMA which directly mediates microtubule binding (Haren and Merdes, 2002) and leads to current

thinking that mitotic NuMA serves as an adaptor protein for dynein, allowing microtubules themselves to be transported as a minus end directed cargo. In addition to the cargo adaptor role of NuMA, the dimeric nature of the protein (Harborth et al., 1995) also supports the idea that a direct microtubule cross-linking function of NuMA may also be responsible for holding non-centrosome anchored microtubules in the vicinity of the pole (Gaglio et al., 1995) (Wong et al., 2006). Various aspects of this model remain to be clarified.

1.2.3.3 Stoichiometry of spindle factors may dictate the NuMA phenotype

The pole-focusing role of NuMA described primarily in the cell-free *Xenopus* extract system has been investigated through the disruption of NuMA in intact mitotic and meiotic cells using a variety of means; however, results are not in complete agreement. Interestingly, in maturing *Xenopus* oocytes, the phenotype of NuMA antibody injection is manifested not as defocusing of microtubules on a bipolar spindle, but instead as spindle multipolarity. This can be explained by the fact that microtubule organizing centers (MTOCs) in this system are formed *de novo* from centrosomal components distributed throughout the oocyte (Becker et al., 2003). In this case, NuMA is involved in the coalescence of the multitude of possible immature centrosome into two distinct mature MTOCs.

The centrosome clustering behavior has been suggested as an explanation for the observation that cancers frequently have an amplification

of the NuMA locus (Huang et al., 2002). This argument follows from the idea that in addition to aneuploidy, cancer cells are also often characterized by multiple centrosomes (Fukasawa, 2005), the structures that nucleate and anchor microtubules in mitosis. While normal cells enter into mitosis with two centrosomes and thereby form bipolar spindles, cells with multiple centrosomes have the potential to form multipolar mitotic spindles. This might be expected to serve as a selective advantage to cancer in the early stages of tumorigenesis by allowing the generation of aneuploidy from multipolar divisions to increase karyotypic diversity within a tumor. In terms of maintaining a stable karyotype, however, a high frequency of multipolar divisions within a tumor would disrupt the maintenance of the cancer genome. Based on this reasoning, it would be expected that multi-centrosomal cell lines that overexpress NuMA should have a high frequency of bipolar spindles relative to equally multi-centrosomal cells that express lower NuMA levels.

However, in contrast to this expectation, and the interpretation that NuMA acts as a centrosome focusing agent, high NuMA levels in some cancer cell lines seem to allow the formation of multipolar spindles from multiple centrosomes, and reducing NuMA to wild-type levels restores spindle bipolarity. Quintyne *et al.* (2005) found that various tumor cell lines with multiple centrosomes also overexpressed NuMA, and that these cells formed multipolar spindles at high frequency. Reduction (but not complete elimination) of NuMA in these cells using siRNA resulted in an elimination of spindle

multipolarity, indicating that in these cells NuMA was required to allow supernumerary centrosomes to develop into mature poles. The same was true when non-transformed cells were induced to become multi-centrosomal: NuMA overexpression licensed the formation of multiple poles (Quintyne et al., 2005). Therefore, while it seems that disruption of NuMA can induce spindle multipolarity in some contexts, the same result can be seen after NuMA overexpression. These experiments indicate that there may be an important dependence on appropriate stoichiometry of non-tubulin spindle elements, such as NuMA, for the establishment and maintenance of normal spindle structure. This idea is supported by multiple observations that altered levels or functionality of other spindle proteins can rescue NuMA phenotypes. For example, while NuMA antibody microinjection results in disorganized poles, this can be rescued by simultaneous antibody mediated disruption of the chromokinesin Kid (Levesque et al., 2003). Also, either overexpression or depletion of the spindle protein Rae1 causes spindle multipolarity, and this can be rescued by respective overexpression of depletion of NuMA (Wong et al., 2006).

1.2.4 The mitotic function of NuMA in mammalian cells is not established

Despite tremendous advances into understanding the mitotic function of NuMA, it remains unclear as to which are the true phenotypes resulting from NuMA loss of function in mammalian cells. Although initial experiments

suggested that NuMA is responsible for the establishment and maintenance of spindle bipolarity (Yang and Snyder, 1992), subsequent efforts recapitulate more closely the *Xenopus* phenotype of defocused poles (Levesque et al., 2003) (Gordon et al., 2001). Although it is tempting to extrapolate results from the extract system to intact cells, it is clear that spindles in *Xenopus* egg extracts are fundamentally different from mammalian cell spindles in terms of assembly and dynamic behavior. Spindle assembly in the *Xenopus* system is likely to be much more strongly driven by a gradient of Ran-GTP emanating from chromosomes than in mammalian cells. Also, chromosome movements in *Xenopus* egg extract spindles rely heavily on microtubule flux, a feature that is essentially absent from mammalian spindles. In addition, bundled microtubules known as kinetochore-fibers (K-fibers), that connect spindle poles to kinetochores and are required for chromosome segregation in mammalian mitosis, are relatively rare in frog extract spindles. Finally, in the *Xenopus* system there is a complete lack of astral microtubules, which play a major role in spindle positioning and function in intact cells, which require these microtubule attachments to the cell cortex to stabilize mitotic spindle positioning.

Uncertainty in resolving the discrepancies reported in studies of mammalian NuMA function is compounded by the observation that NuMA overexpression can result in some of the same phenotypes as inhibition. Additionally, further difficulty in reaching a consensus is introduced since

disruption of NuMA function has been carried out primarily by antibody injection. Although all injected antibodies localize similarly (spindle poles or pole-like foci) each might have distinct function blocking capabilities dependent on epitope, and whether any of these antibodies are truly function blocking at all remains unclear. There are also obvious complications involved in interpreting the effects of using a divalent cross-linking antibody to interrupt the function of a putative cross-linking protein. While an antibody microinjection approach is useful for yielding information about temporal requirements for NuMA throughout consecutive stages of mitosis, inconsistent results and caveats inherent to interpretations of antibody injection experiments have made a firm interpretation of NuMA function in mammalian cells difficult.

Obviously, the cleanest way of resolving the true NuMA phenotype lies in complete removal of the protein. In principle, this should be easily accomplished using contemporary RNAi approaches. Indeed, this strategy has been used to reduce NuMA levels multiple times (including in the original description of mammalian cell siRNA) (Chang et al., 2005; Du and Macara, 2004; Elbashir et al., 2001; Harborth et al., 2001; Quintyne et al., 2005). However, no data have been produced to date that identify the effect of siRNA mediated NuMA depletion on spindle structure, nor on the mitotic consequences of NuMA loss, and all attempts have failed to clarify earlier phenotypic discrepancies from antibody microinjection and ‘dominant’

overexpression experiments. As mentioned above, in one effort, reducing NuMA levels actually restored spindle bipolarity in a population of cells with a high incidence of multipolar spindles (Quintyne et al., 2005). In another study, an image of a perfectly bipolar spindle with tightly aligned metaphase chromosomes in a cell treated with siRNA against NuMA provided evidence of to the inability of this approach to produce a spindle phenotype (Chang et al., 2005). Efficient knockdown of the NuMA protein in mammalian cells has proven difficult, and convincing evidence for significant reduction of NuMA protein levels lacking. This may explain why siRNA directed against NuMA has not yet been demonstrated to result in a loss of bipolar spindle structure, spindle pole focusing defects, chromosome segregation, or in fact any severe mitotic defect whatsoever predicted to result from NuMA depletion

1.2.5 Additional features and functions of NuMA during mitosis

1.2.5.1 Modification by poly-ADP-ribosylation

Substantial investigation of the mitotic role of NuMA at spindle poles in a variety of systems has yet to provide a definitive clarification of its function, but has revealed several additional features of NuMA during mitosis. For example, the surprising recent description of a binding motif for tankyrase-1, a poly(ADP-ribose) polymerase, within the C-terminus of NuMA (Sbodio and Chi, 2002). NuMA appears to be required for tankyrase-1 localization to mitotic spindle poles and is also a substrate for the activity of this enzyme, which

catalyzes the addition to proteins of a long, branched, negatively charged polymer of ADP-ribose, a modification which is commonly found on histones (Karsenti, 2004) (Chang et al., 2005) (Chang et al., 2005). Interestingly, depletion of tankyrase-1 or inhibition of its activity during mitosis has no effect on NuMA localization, but dramatically worsens spindle morphology and causes an increase in multipolarity (Chang et al., 2004; Chang et al., 2005). These results suggest that NuMA function at spindle poles may depend on its recruitment of, and post-translational modification by, tankyrase-1. How poly-ADP ribose (PAR) modification of NuMA is involved in initiating and/or maintaining spindle bipolarity remains unknown.

1.2.5.2 Asymmetric cell division

In addition to its putative role in spindle pole focusing during normal mitotic divisions, recent work has implicated NuMA in the maintenance of spindle orientation in asymmetric divisions. The plane of cell division is often a key determinant of cell fate during development and in specifying stem cell self-renewal versus differentiation. Asymmetric division can result in the differential localization of fate-specifying proteins between daughter cells or the spatially directed birth of daughter cells into fate-defining niches, and requires that the spindle be oriented and fixed in a specific plane from metaphase to the initiation of telophase (Morrison and Kimble, 2006). Proper spindle orientation is likely maintained by anchoring astral microtubules to the

cell cortex, in a manner dependent on the asymmetric positioning of cortical factors.

Although the mitotic localization of NuMA is accepted to be primarily at spindle poles, some evidence exists to suggest that it may in fact also localize to the cortex. The cortical localization of NuMA is most obvious under conditions of overexpression of LGN or Gαi (cortically localized NuMA-interacting proteins) (Du and Macara, 2004) but is also seen in cultured primary human cells (Lechler and Fuchs, 2005). Interestingly, mutation of a single putative phosphorylation site (threonine 2040 to alanine) results in the obvious and dramatic localization of NuMA to the cell cortex and a reduction in levels at spindle poles (Compton and Luo, 1995), suggesting that phosphorylation may regulate cortical NuMA localization and therefore function. The *Drosophila* protein Mud shares a short region of high homology with NuMA, specifically in the LGN binding domain (Siller et al., 2006), and also localizes to the cortex, as seen in asymmetrically dividing *Drosophila* embryonic neuroblasts. There is a clear role for Mud in the asymmetric division of these neuroblasts, which is disrupted in Mud mutant flies (Siller et al., 2006) (Bowman et al., 2006). Notably, in addition to the cell cortex, Mud is localized to spindle poles, and while supernumerary centrosomes are observed in Mud mutants (Izumi et al., 2006) no pole focusing defects are seen and the protein does not seem to be nuclear in interphase cells,

suggesting that Mud may carry out some, but not all, functions of vertebrate NuMA.

A putative *C. elegans* NuMA homolog, Lin-5, is similar to Mud in that it shares high homology with NuMA only in the LGN binding region, and localizes to spindle poles and the cell cortex but not to interphase nuclei (Fisk Green et al., 2004; Lorson et al., 2000). Also like Mud, Lin-5 is thought to be required for spindle positioning; the stereotypic asymmetry of divisions in the early *C. elegans* embryo is lost after Lin-5 depletion. Although many of the conserved cortical proteins likely to be involved in positioning and maintaining spindle orientation during asymmetric divisions have been identified, it remains unclear exactly how these proteins (including Mud and Lin-5) are regulated to dictate the axis of division.

Based on mutant phenotypes and protein localization patterns, it is clear that neither Mud nor Lin-5 are true NuMA homologs in all functional capacities. However, it may be the case that with regards to spindle orientation, these proteins inform us on overlooked aspects of mitotic NuMA function. Indeed, good evidence exists to support the interaction of vertebrate NuMA with proteins that clearly localize to the cortex, even though no studies have as of yet directly tested the consequences of NuMA disruption in cells undergoing asymmetric divisions.

1.2.6 Organization of the interphase nucleus

In addition to remaining questions about the mitotic function of NuMA, the interphase localization of the protein to the nucleus suggests additional avenues of investigation: a potential, and as of yet undefined, non-mitotic role. The most reasonable aspect in which NuMA, as a large coiled-coil protein, might function during interphase is as a structural component of the nucleus. Such a function may have been previously overlooked considering that a broad appreciation for the high degree of nuclear complexity is only relatively recent. Essential nuclear structural proteins have not yet been described, but may well exist. An analogous set of functional elements is found in the cell body, in which it is well established that a structural framework of microtubules, actin and intermediate filaments organizes the cytoplasm of mammalian cells. These structural proteins, along with actin and microtubule based motors, are responsible for positioning and proper function of major sub-cellular organelles, including mitochondria, endoplasmic reticulum, the Golgi network, peroxisomes, vacuoles, etc.

It has becoming increasingly apparent that in parallel to the cytoplasm, the mammalian cell nucleus is also highly organized. Many nuclear proteins are found to be arranged in subcompartments, such as PML bodies, speckles, and nucleoli, which occupy distinct regions within the nucleus and dynamically exchange components with the nucleoplasm (Misteli, 2001). Although only partially characterized, these “nuclear organelles” seem to participate in non-

overlapping nuclear functions including RNA synthesis and processing (Spector, 2001). Chromatin, the major component of the nucleus, also seems to be organized. Chromosomes have been shown to exhibit localized movement in interphase, which is likely to reflect the existence of chromosome territories, regions within the nucleus to which specific chromosomes are confined (Gasser, 2002; Heun et al., 2001; Meaburn and Misteli, 2007).

Interphase chromosome movements may depend partly on telomere tethering to the nuclear lamina (Gasser, 2002), a protein network composed primarily of lamins (intermediate filament family proteins) which line the nuclear face of the inner nuclear membrane. Interestingly, mutations in *LMNA*, which encodes lamin A and lamin C, two major components of the nuclear lamina, give rise to a variety of recessively inherited neuropathies, lypodistrophies and myopathies. Whether these diseases are due to effects on chromatin organization, transcriptional regulation by proteins of the lamina, or loss of mechanical integrity of the nucleus is unknown (Burke and Stewart, 2002). Combinations of these factors may play distinct role in the differing pathologies of the multitude of laminopathies. Clearly, structural proteins of the nuclear lamina are important for normal cellular function; however, the existence of structural elements lining the nuclear envelope seems insufficient to explain the high degree of internal nuclear organization.

Few data exist which address the basic question of how, or even whether the nucleoplasm is structured. In stark contrast to the multitude of

structural elements responsible for organizing cytoplasmic bodies, no such functionally equivalent proteins have been demonstrated to reside within the internal space of the nucleus. More weight has been given recently to the likelihood that some cytoplasmic structural elements, including actin, are present and functional in the nucleus. The existence of actin within the nucleus has been suspected for many years, but remained highly controversial. the concept of nuclear actin and actin related proteins (ARPs) is now more generally accepted. Within the nucleus, actin has been implicated in such processes as transcription, RNA processing, and nuclear export of RNA and proteins (Chen and Shen, 2007; Olave et al., 2002). How actin carries out its functions within the nucleus is currently a topic of investigation. Recent studies have indicated that actin may be a component of various chromatin remodeling complexes (Chen and Shen, 2007).

Despite inroads into discovering and understanding new features of the nucleoplasm and major progress towards the identification and characterization of various organized nuclear subcompartments, the nature of the inter-chromatin space within which they reside remains largely undefined (Shopland and Lawrence, 2000). As complexities of nuclear organization and function are further identified, their dependence on structural elements in the nucleoplasm remains a distinct possibility, an emerging field of study, and a major unanswered question in cell biology.

1.2.7 NuMA is a candidate nuclear structural component

The Nuclear Mitotic Apparatus protein (NuMA) is an excellent candidate for a nuclear structural component. NuMA was first identified more than twenty five years ago as a large protein with a unique cell-cycle specific localization pattern (Lydersen and Pettijohn, 1980). In interphase, NuMA is localized exclusively to the nucleus, but translocates to spindle poles during mitosis where it is thought to play a scaffolding or crosslinking role as an essential component of the spindle assembly machinery by interacting with microtubules and the dynein/dynactin motor complex (described in greater detail above) (Compton et al., 1992; Lydersen and Pettijohn, 1980; Merdes et al., 1996). While the requirement for NuMA in proper progression through mitosis has been the subject of substantial study, a nuclear function is as of yet only inferred, partly from evidence that NuMA is retained in nuclei of post-mitotic cells (Ferhat et al., 1998).

Multiple lines of evidence suggest that NuMA functions in a structural capacity within the nucleus, including: i) NuMA contains an extremely long coiled-coil domain. Indeed, coiled-coils are motifs common to structural molecules, including the nuclear lamins and other members of the intermediate filament family (Hutchison, 2002); ii) visualization of isolated recombinant NuMA molecules by electron microscopy has demonstrated its ability to form extended dimers of 200 nm in length (Harborth et al., 1995) as well as higher order multi-armed structures (Harborth et al., 1999); iii)

overexpression of NuMA in HeLa cells results in the formation of a quasi-hexagonal nuclear lattice (Harborth et al., 1999). albeit whether such an array represents the real arrangement of nuclear substructure is unproven; iv) endogenous NuMA is highly abundant, present at 10^6 or greater copies per nucleus (Compton et al., 1992; Kempf et al., 1994) , a level which would be sufficient to allow the creation of some type of framework; v) a correlation between nuclear shape and NuMA levels has previously been suggested (Merdes and Cleveland, 1998), NuMA seems to be absent from the nuclei of cells which are non-spherical in shape; and finally vi) with regards to the putative dual function of NuMA at spindle poles and in nuclei, work in *Drosophila* has implicated a number of coiled-coil proteins as functioning both to maintain spindle structure during mitosis and contributing to nuclear architecture in interphase (Qi et al., 2005; Wasser and Chia, 2000). This may represent a conserved evolutionary strategy of co-opting structural proteins to function on mitotic spindles and as nuclear structural elements. These multiple lines of evidence suggest the likelihood of a nuclear function for NuMA, which should be taken into account when studying the mitotic role of NuMA at spindle poles.

The text of Chapter 1 in part, is a reprint of the material as it appears in *Cancer Cell*, 2007(11):25-36, Weaver BA, Silk AD, Montagna C, Verdier-Pinard P and Cleveland, DW. The dissertation author was a major contributing researcher and second author of this paper.

Chapter 2: Aneuploidy acts both oncogenically and as a tumor suppressor

2.1 Introduction

An abnormal chromosome number, a condition known as aneuploidy, is a common characteristic of tumor cells. Because of this correlation, Boveri proposed nearly 100 years ago that aneuploidy causes tumorigenesis, but this has remained untested due to the difficulty of selectively generating aneuploidy. The mitotic checkpoint acts during the process of chromosome segregation to prevent errors leading to the development of aneuploidy. Consequences of checkpoint failure have previously been reported to include tumor development (Dobles et al., 2000). However, the distinct possibility of additional cellular defects in these models has made the causative link between aneuploidy and tumorigenesis unproven.

In collaboration with Beth Weaver, I have exploited the property that cells and mice with reduced levels of the mitosis specific, kinesin-like motor protein CENP-E generate high rates of aneuploidy in the absence of other defects (Weaver et al., 2007) to test the hypotheses that aneuploidy either drives tumorigenesis, or is benign. We find that aneuploidy due to missegregation of whole chromosomes contributes to transformation *in vitro* and causes an increase in spontaneous spleen and lung tumors *in vivo*. Surprisingly, in examples of chemically or genetically-

induced tumor formation in mice, an increased rate of aneuploidy can be a more effective inhibitor than initiator of tumorigenesis.

2.2 Aneuploidy Contributes to Tumorigenicity *In Vivo*

To test if increased chromosomal loss or gain would affect tumorigenicity, primary MEFS, p19ARF null MEFs and SV40 large T immortalized MEFs with normal or reduced CENP-E levels were tested for the ability to form tumors when injected into nude mice. Animals injected with primary MEFs, and low passage immortalized MEFs did not form tumors at the injection site. Nor did animals injected with late passage p19/ARF cells with normal levels of CENP-E, even when observed for 3 months (n=6). However, 19 of 19 mice injected with p19/ARF CENP-$E^{+/-}$ cells formed tumors at the injection site with a latency of ~1-2 weeks (Figure 2.1). Similarly, 10 of 10 mice injected with high-passage (P ≥ 45) CENP-$E^{+/-}$ MEFs expressing SV40 large T formed tumors at the injection site with a latency of 1 to 6 weeks. None of the mice injected with CENP-$E^{+/+}$ MEFs immortalized with SV40 large T formed tumors at the injection site within the same time frame (Figure 2.1). One of 12 mice injected with late passage CENP-$E^{+/+}$ cells expressing SV40 large T did form a tumor at the injection site, but it took 12 weeks to form, twice the length of the longest latency of tumors formed by CENP-$E^{+/-}$ cells expressing SV40 large T.

Histological examination of each of the tumors revealed it to be a fibromyosarcoma, as expected if derived from the injected MEFs, a conclusion confirmed by genotyping. Cell lines were successfully isolated from a subset of the tumors and chromosome spreads from these lines were examined (Figure 2.1). The tumor cells exhibited a wide range of chromosome numbers, indicative of chromosomal instability. These results demonstrate that aneuploidy contributes to the transformation and tumorigenic potential of immortalized cells.

2.3 Aneuploidy Drives Tumorigenesis *In Vivo*

To determine if the elevated aneuploidy generated *in vivo* in mice with reduced CENP-E can drive tumorigenesis, cohorts of wild type and CENP-$E^{+/-}$ animals were aged to 19-21 months and examined for development of spontaneous tumors. Lymphomas of the spleen were detected in 10% of CENP-$E^{+/-}$ mice, while none of the wild type mice had similar tumors (Figure 2.2). Additionally, a 3-fold increase in lung tumors in the aged CENP-$E^{+/-}$ versus normal littermates was observed (Figure 2.2). Histological examination identified these as pulmonary adenomas (Figure 2.2). Thus, aneuploidy caused by elevated rates of whole chromosome missegregation validates Boveri's initial hypothesis: aneuploidy can indeed promote tumorigenesis in the absence of other defects.

2.4 Aneuploidy Inhibits Tumorigenesis in Tissues Prone to Tumor Formation

Liver tumors were the most common neoplasms observed in our wild type mice, with 14% of wild type animals having one or more. Despite increases in adenomas and lymphomas, widespread aneuploidy was accompanied by a 50% decrease of spontaneous liver tumors in aged CENP-$E^{+/-}$ animals (to 7%). None of these animals had more than one tumor in the liver, while wild type animals with liver tumors often did (Figure 2.3). Additionally, the tumors in the wild type livers were significantly larger than the tumors observed in the CENP-$E^{+/-}$ animals (Figure 2.3). Interestingly, in addition to the polyploidy commonly found in hepatocytes, previous analysis performed in our lab indicated that ~20% of wild type liver cells missegregate one or more chromosomes during mitosis (Putkey et al., 2002). Thus, increasing aneuploidy further by reduction in CENP-E actually inhibits spontaneous tumorigenesis and possibly tumor progression in the liver.

To determine whether aneuploidy due to single chromosome loss or gain affected tumor initiation or progression in tumors provoked by exposure to a well characterized carcinogen, 7,12-dimethylbenz[a]anthracene (DMBA), thirty-eight animals were given a single dose of DMBA at postnatal day 3-5. The animals were sacrificed at 8 months of age and examined for tumors. Forty percent of the wild type animals harbored a single lung tumor (Figure 2.3). An additional wild type animal that did not develop a lung tumor

contained one ovarian and two mammary tumors. Surprisingly, lung tumors were identified in a smaller portion of the CENP-$E^{+/-}$ animals (Figure 2.3). No tumors were identified in any other organs in the CENP-$E^{+/-}$ mice. The size of the lung tumors was indistinguishable between CENP-$E^{+/-}$ and CENP-$E^{+/+}$ animals (0.30 +/- 0.06 mm^3 in wild type versus 0.20 +/- 0.11 mm^3 in CENP-$E^{+/+}$). Thus, aneuploidy due to CENP-E heterozygosity did not accelerate tumor initiation or progression after treatment with this carcinogen.

Loss of heterozygosity (LOH) at individual gene loci, especially tumor suppressors, is a well accepted mechanism for promoting tumorigenesis (Wijnhoven et al., 2001). LOH of a tumor suppressor driven by single chromosomal loss due to CENP-E heterozygosity would be expected to accelerate tumorigenesis, especially in animals with a germline deletion of one allele. Therefore, the effect of aneuploidy on tumors initiated by the complete absence of a tumor suppressor was tested. Two rounds of mating produced CENP-$E^{+/-}$ animals that were also deficient for the p19/ARF tumor suppressor gene, as well as p19/$ARF^{-/-}$, CENP-$E^{+/+}$ littermates. p19/$ARF^{-/-}$ animals develop malignant cancers, predominantly sarcomas and lymphomas, and ~80% of these animals die within one year. Adding elevated rates of single chromosomal loss to tumors initiated by absence of the p19/ARF tumor suppressor had a striking and unexpected effect on survival. Elevated aneuploidy increased the average tumor-free survival of these animals by 93 days (Figure 2.3). Thus, aneuploidy from whole chromosome loss (or gain)

can act as a strong inhibitor of tumorigenesis after loss of the p19/ARF tumor suppressor gene.

2.5 Discussion

By reduction in a mitotic motor that is also a component of mitotic checkpoint signaling, we have demonstrated that increased rates of whole chromosome gain or loss, and resultant aneuploidy, can enhance transformation in culture and spontaneous tumorigenesis during aging, while diminishing tumor formation initiated by a chemical carcinogen or by loss of the p19/ARF tumor suppressor. These outcomes provide a direct test of the 100 year old hypothesis that aneuploidy, a salient characteristic of solid tumors, drives tumorigenesis. The unambiguous answer is that it can do so, but the cellular context is crucial. Both answers have important implications for human tumors.

Consistent with human cancers, aneuploidy-induced cellular transformation is a slow process with a long latency, requiring ≥ 30 passages in culture. Even then it is not completely penetrant. Only a proportion of p19/ARF$^{-/-}$, CENP-E$^{+/-}$ cell lines acquired the ability to grow in soft agar and to form tumors in nude mice, even after ≥40 passages in culture. This apparently required the complex aneuploidy of the type routinely seen in solid human tumors. In animals, tumorigenesis was a late event, identified only in aged animals (19-21 months) and not in all tissues.

Aneuploidy has been argued to drive tumorigenesis (Li et al., 1997), to promote tumor progression but not initiation (Marx, 2002), and to be completely benign (Hahn et al., 1999). Since, to our knowledge, aneuploidy has never been proposed to inhibit tumorigenesis, this was our most surprising finding. Previous experiments with animals with reduced levels of other proteins (MAD2, BUB3 and BUBR1) that participate in the mitotic checkpoint did not uncover a role of aneuploidy in inhibiting tumorigenesis. However, as detailed earlier, unlike CENP-E, these proteins are expressed throughout the cell cycle and have been implicated in apoptosis (BUBR1), transcriptional repression (BUB3), the DNA replication checkpoint (MAD2), and gross chromosomal rearrangements (MAD2, BUB3, BUBR1). Therefore, reduction of MAD2, BUB3 or BUBR1 would be anticipated to produce defects in addition to simple increases in single chromosome aneuploidy that might affect their tumor suppressing potential.

How, then, can whole chromosomal aneuploidy drive tumor suppression? Several factors probably converge to produce aneuploidy-mediated tumor prevention. High levels of chromosomal instability can prevent clonal expansion since cells that have acquired a rare transformative karyotype through multiple chromosome missegregation events are likely to lose that karyotype in the next round of cell division. The situation is analogous to what has been shown for genetic instability in bacteria. While low

levels of instability provide a growth advantage, higher levels of instability generate a so-called “mutational meltdown” in which the population of highly genetically unstable bacteria loses viability. Such sensitivity is also analogous to genetic instability due to DNA damage. Cells sustain DNA damage on a regular basis but this is normally countered by repair mechanisms. Higher levels of DNA damage due to mutations in mismatch repair enzymes result in viable cells, but are associated with cancers, particularly hereditary nonpolyposis colorectal cancer (HNPCC) (Strate and Syngal, 2005). Chemotherapeutic drugs (e.g., cisplatin) produce even higher levels of DNA damage, provoking cellular death and tumor regression. Our evidence now demonstrates that aneuploidy behaves similarly: it both drives tumorigenesis as Boveri had initially proposed and inhibits tumorigenesis, depending on the total level of genomic damage that is sustained.

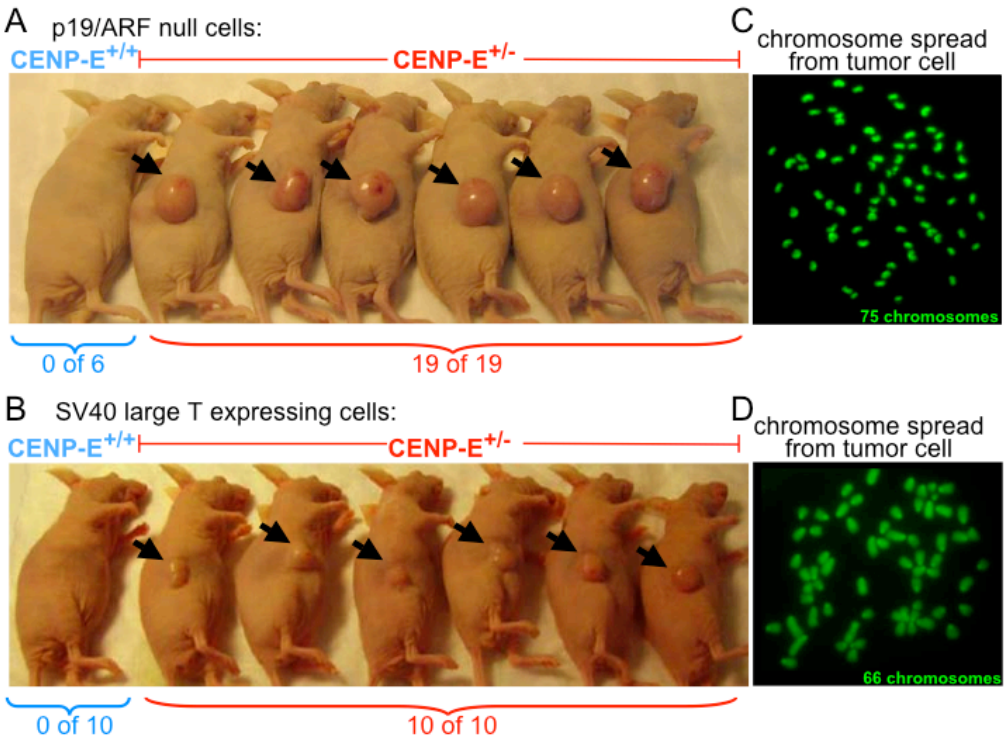

Figure 2.1 Aneuploidy Due to CENP-E Heterozygosity Contributes to Tumorigenicity

(A) Nude mice injected with p19/ARF-/- cells that are heterozygous for CENP-E form tumors at the injection site (arrows) but mice injected with p19/ARF null cells that are wild type for CENP-E do not form tumors. (B) Nude mice injected with CENP-E+/- cells expressing SV40 large T form tumors at the injection site (arrows), but mice injected with wild type cells expressing SV40 large T do not. (C-D) Chromosome spreads prepared from (C) CENP-E+/- p19/ARF-/- null tumor cells (n = 30) and (D) CENP-E+/- SV40T expressing cells (n = 100). The number of chromosomes in the spread shown is listed in the bottom left hand corner.

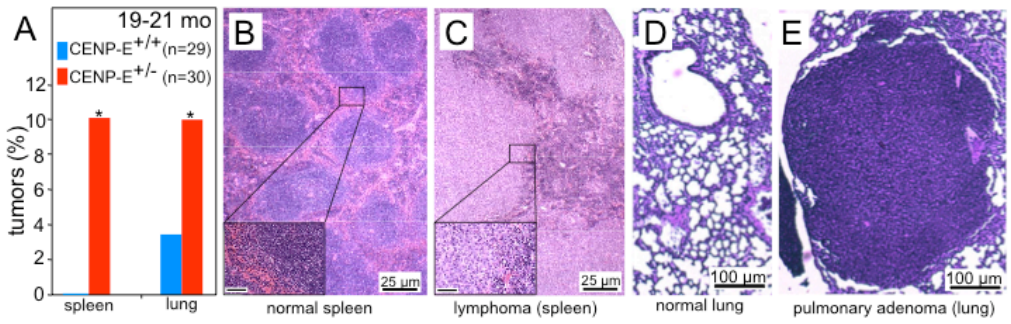

Figure 2.2 Aneuploidy promotes tumorigenesis.
(A) Aged CENP-E$^{+/-}$ animals develop elevated levels of spontaneous spleen and lung tumors. (B) H&E stained section of a normal spleen showing purplish circular follicles of B and T cells. Box indicates the region enlarged in B. Scale bar = 50 µm. (B') Magnified view of the edge of a follicle in normal spleen. Scale bar = 100 µm. (C) H&E stained tissue section of a lymphoma showing monotonous appearance and loss of normal follicles. Box indicates the region shown in C'. Scale bar = 50 µm. (C') Enlarged view of the border between the lymphoma on the left (with enlarged, light colored nuclei) and normal spleen cells on the right (with small, dark purple nuclei). Scale bar = 100 µm. (D) H&E stained section of a lung tumor, identified as a pulmonary adenoma, which appears as densely packed nodule. Scale bar = 100 µm. (E) Normal lung tissue showing a lacy appearance. Scale bar = 100 µm.

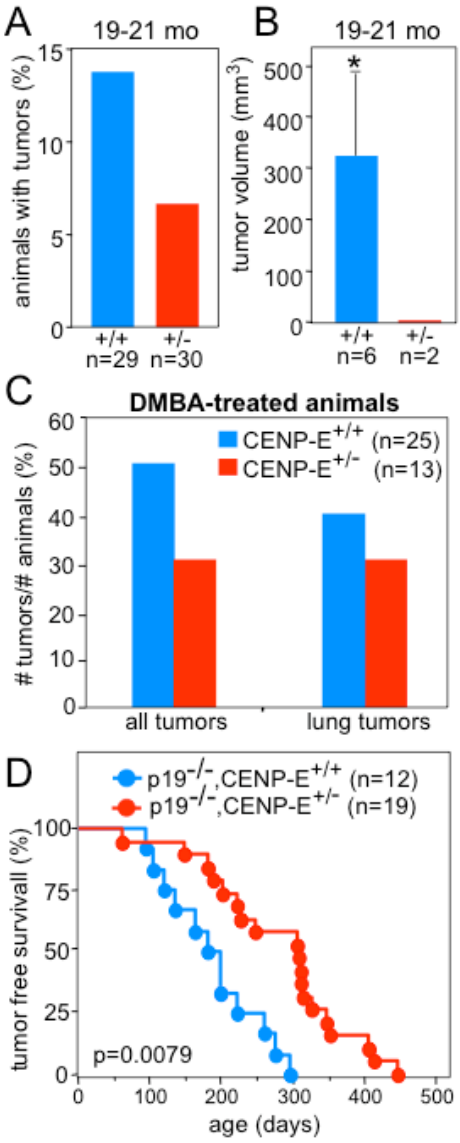

Figure 2.3 Aneuploidy inhibits tumorigenesis
(A) Aged CENP-E$^{+/-}$ animals have a decreased rate of spontaneous liver tumorigenesis. (B) Liver tumors in CENP-E$^{+/-}$ animals are significantly smaller than those found in wild type animals. (C) CENP-E heterozygosity inhibits tumorigenesis in animals treated with the carcinogen DMBA. (D) Aneuploidy due to CENP-E heterozygosity delays tumorigenesis in p19/ARF null mice.

Chapter 2 in part, is a reprint of the material as it appears in *Cancer Cell*, 2007(11):25-36, Weaver BA, Silk AD, Montagna C, Verdier-Pinard P and Cleveland, DW. The dissertation author was a major contributing researcher and second author of this paper.

Chapter 3: Distinct requirements for NuMA in the establishment and maintenance of mammalian spindle poles demonstrated with inducible gene inactivation

3.1 Introduction

The mitotic spindle is a bipolar array of microtubules that is required for the alignment and segregation of chromosomes during mitosis. The poles of the spindle are major focal points for the minus ends of spindle microtubules, and serve as the final destination for chromosomes segregated in anaphase (Compton, 1998). In normal animal somatic cell mitosis, spindle poles are always coincident with centrosomes, the major cellular microtubule organizing structures. However, centrosomes are not absolutely required for spindle, or pole, formation. *In vitro*, DNA coated beads catalyze the formation of bipolar microtubule spindles in *Xenopus* egg extracts (Heald et al., 1996). This process requires NuMA, a large (>200 kD), abundant, spindle pole localized protein that interacts with tubulin (Haren and Merdes, 2002) and the dynein/dynactin complex (Merdes et al., 1996) to direct microtubule focusing towards spindle poles. Additionally, bipolar spindles also form in somatic mitotic cells in which one or both centrosomes have been destroyed by laser ablation (Khodjakov et al., 2000), or prevented from forming normally by depletion of essential centrosomal components (Mahoney et al., 2006).

Kinetochore fibers are comprised of bundles of microtubules that link spindle poles to the kinetochores of each chromosome. A long standing controversy has been settled on the potential contribution to kinetochore fiber formation by centrosome independent microtubule assembly. In a process likely to be dependent on a gradient of Ran-GTP (Dasso, 2001), kinetochore-fibers can form in a kinetochore driven process even in cells that have completely functional centrosomes (Khodjakov et al., 2003; Maiato et al., 2005). Multiple microtubules are nucleated in the vicinity of kinetochores, near-simultaneously elongated and captured by centrosomal microtubules (O'Connell and Khodjakov, 2007). How these kinetochore bundles are captured and focused towards centrosomes, the means for sustained anchoring of kinetochore fibers at spindle poles, and the role of centrosomes in both active focusing and the maintenance of spindle pole integrity are not established.

NuMA, along with the activity of cytoplasmic dynein, has been proposed to participate in actively focusing microtubules toward the poles of the mitotic spindle (Khodjakov et al., 2003; Merdes et al., 1996). The foundation for our current mechanistic understanding of the role for NuMA during mitosis was established by work in cell free extracts. Relative to typical mammalian spindles, those formed in *X. laevis* egg extracts are much larger, undergo substantially greater microtubule flux, have limited astral microtubules and no cortical attachments, seem to rely significantly more on a gradient of Ran-GTP emanating from chromosomes to contribute to spindle assembly (Kalab et al.,

2006; Kalab et al., 2002), and have relatively few bundled microtubules comprising kinetochore fibers.

Examinations of NuMA function in mammalian mitosis have previously used antibody microinjection approaches that yielded contradictory outcomes. An early study reported spindle collapse to monopolarity (Yang and Snyder, 1992) and subsequent efforts demonstrated unfocused spindle poles and an extended mitotic delay (Gaglio et al., 1995). The difficulty in removing NuMA protein has confounded mammalian siRNA approaches [e.g., (Chang et al., 2005; Elbashir et al., 2001)]. To test the principles of mammalian spindle assembly, especially the mechanisms of spindle pole focusing and the maintenance of pole integrity, I have now used gene replacement to engineer mice and cells in which NuMA expression can be selectively disrupted by administration of a small molecule drug (4-hydroxy tamoxifen). I show during the first mitosis following inhibition of spindle pole association of NuMA, that spindles initially form with poles well focused at centrosomes. However, subsequent to this initial spindle assembly and upon generation of spindles forces, centrosome-spindle attachment is uncoupled, kinetochore fibers become de-focused, and centrosomes fail to maintain and re-establish connection with the spindle. Additionally, I show that the initial formation of focused spindle poles when NuMA is disrupted is dependent on the presence of centrosomes. Chromosome segregation is largely intact even without NuMA anchoring of kinetochore fibers to centrosomes. From these findings, I

propose that NuMA and centrosomes function redundantly to focus microtubules at spindle poles, but that NuMA is absolutely required to maintain centrosome attachments to kinetochore fibers throughout mitosis.

3.1 NuMA expression pattern indicates a potential interphase function

Immunoblotting a panel of mouse tissues revealed that NuMA was expressed at similar levels in most tissues examined, with the exception of heart and skeletal muscle (Figure 3.1). The appearance of NuMA immunoreactive bands smaller than two hundred kilodaltons in size in some tissues may be indicative of isoforms or indicate post-translational processing of the mature NuMA protein. The absence of NuMA from these two tissues is consistent with a previous report that cultured myoblasts lose NuMA during differentiation into myotubes (Merdes and Cleveland, 1998) and with the inability to detect NuMA by immunofluorescence in cultured primary mouse myocytes (data not shown). The near-ubiquitous expression pattern of NuMA was in sharp contrast with proteins thought to function primarily or exclusively during mitosis, including CENP-E, BubR1 and Mad2, which were only detected in testes and spleen (tissues with large populations of actively dividing cells). Lamins A and C, proteins known to be required during interphase for multiple cell types, were found in all tissues examined, and much more closely mirrored that of NuMA (Figure 3.1).

To examine NuMA expression in permanently post-mitotic cells more directly, I carried out indirect immunofluorescence staining of frozen tissue sections to examine NuMA localization in terminally differentiated neurons in the spinal cord and cerebellum of adult mice. As expected, NuMA was found diffusely within the nucleus and excluded from nucleoli in motor neurons and Purkinje cells (Figure 3.1). Expression in these cells is consistent with *in situ* hybridization data demonstrating high levels of NuMA transcripts in both of these cell types (www.brainatlas.org/aba/) (Lein et al., 2007). The ubiquitous expression pattern and accumulation in nuclei of terminally differentiated, post-mitotic cells strongly supports a post-mitotic, interphase function of NuMA.

3.2 Exon mapping functional domains of murine NuMA

To test a mitotic role for NuMA without disrupting the putative nuclear function(s), we used gene targeting in mouse embryonic stem cells to create a conditional loss-of-mitotic function allele of NuMA. To do this, I identified an in-frame deletion that prevented efficient spindle pole localization of NuMA without effecting nuclear accumulation in interphase. This was accomplished by further characterizing the tubulin-binding domain of NuMA, which had been narrowed down to one hundred amino acids in the C-terminal globular tail that mediate both direct interaction with tubulin *in vitro* and localization of NuMA to spindle poles *in vivo* (Haren and Merdes, 2002). Mouse and human NuMA share 88% amino acid identity in this domain, which is partially encoded by

nucleotides comprising the 22nd exon of the mouse NuMA gene. I reasoned that an allele of NuMA deleted of the minimal tubulin binding domain might be expected to have a severe effect on NuMA function during mitosis, and be unlikely to impact the role of the protein in the nucleus. Therefore I expressed GFP-tagged versions of the 410 amino acid globular tail of the mouse NuMA protein that were either wild-type, or deleted of residues encoded by exons 22. Only the C-terminal tail was used in order to avoid association of tagged and endogenous proteins mediated by the central coiled-coil dimerization domain (Harborth et al., 1995). The wild-type tail fragment localized appropriately to nuclei in interphase and was present in the crescent-shaped pattern typical of endogenous NuMA at spindle poles during mitosis. The GFP-tail fragment lacking the amino acids provided by exon 22 was also nuclear during interphase, but failed to efficiently concentrate at spindle poles in mitosis (Figure 3.2). These results demonstrated that residues encoded by exon 22 of the mouse NuMA gene are required for efficient localization of the protein to spindle poles, but not necessary for interphase nuclear accumulation.

3.3 Creation of conditional and deletion alleles of NuMA

To develop a system for investigating NuMA function in mammalian cells, I took advantage of the exon-restricted spindle pole localization determinants within the C-terminal tail of NuMA to create a conditional, separation of function allele of NuMA in the mouse. Homologous

recombination in mouse ES cells was used to flank exon22 with *loxP* sites and introduce a downstream *FRT*-flanked Neomycin cassette (Figure 3.3). ES clones were screened for homologous recombination at 5' and 3' ends of the exon22 targeting construct by PCR and DNA blotting, and multiple targeted clones were identified (Figure 3.3). Two independently targeted ES cell lines were used to generate mice with this $NuMA^{Neo}$ allele. These animals were crossed to a FLPe deleter strain (Rodriguez et al., 2000) to remove the neomycin gene, thereby generating a conditional allele, $NuMA^{flox}$. Subsequent mating to a mouse expressing Cre in the female germ line (Lewandoski et al., 1997) produced animals heterozygous for the NuMA deletion allele, $NuMA^{\Delta 22}$ (Figure 3.3). Genotypes were confirmed and followed in mice using a three-primer PCR reaction capable of distinguishing wild-type and all engineered NuMA alleles (Figure 3.3).

Analysis of NuMA levels in ES cells and multiple tissues from mice heterozygous for $NuMA^{Neo}$, demonstrated a reduction in NuMA protein levels relative to wild-type cells and animals (Figure 3.3), most likely the result of aberrant splicing caused by the presence of the intronic neomycin cassette (Figure 3.4). Taking advantage of this hypomorphic expression from $NuMA^{Neo}$, I tested the requirement for NuMA in embryonic development and viability. Using mice created from each of two independently targeted ES cell lines, the $NuMA^{Neo}$ allele could not be bred to homozygosity. No $NuMA^{Neo/Neo}$ live pups or early embryos were ever recovered (0/88 pups and 0/50 embryos, see

Table1). In contrast, $NuMA^{flox}$ (produced by FLPeR mediated removal of the Neomycin cassette) could be readily made homozygous, as expected (Table 1). Like $NuMA^{Neo}$, $NuMA^{\Delta 22}$ (a 59 amino acid internal deletion) was embryonic lethal when present homozygously (Table 1). There was no evidence for NuMA haploinsufficiency or dominant effects that might be produced from either $NuMA^{Neo}$ or $NuMA^{\Delta 22}$: in crosses of mice heterozygous for either of these alleles, heterozygous and wild-type pups were produced in expected Mendelian ratios (Table 1). Additionally, I aged cohorts of $NuMA^{Neo/+}$ and $NuMA^{\Delta 22/+}$ mice for up to 18 months, and in neither case were any overt phenotypes observed. These observations demonstrate that NuMA is essential for one or more aspects of embryonic development and viability, that $NuMA^{flox}$ encodes a fully functional protein, and that $NuMA^{Neo}$ and $NuMA^{\Delta 22}$ are loss of function alleles.

3.4 Efficient tamoxifen-regulated Cre-mediated deletion of NuMA

In order to examine cellular phenotypes resulting from loss of mitotic NuMA function, which might explain the requirement for NuMA in embryonic viability, I generated cell lines in which efficient spindle pole accumulation of NuMA could be prevented by the addition of a membrane permeant drug. This was accomplished by crossing the $NuMA^{flox}$ allele into mice carrying the Cre-ER^{TM} transgene (Hayashi and McMahon, 2002), which ubiquitously expresses

the Cre recombinase fused to a mutated form of the estrogen receptor. This receptor is insensitive to estrogen, but binds with high affinity to the synthetic ligand 4-hydroxy-tamoxifen (4-OHT). Binding of 4-OHT allows translocation of the receptor-Cre fusion protein, which is otherwise sequestered in the cytoplasm, into the nucleus where it causes recombination between *loxP* sites. We confirmed that nuclear localization of the Cre-fusion is dependent on the continued presence of 4-OHT, and that Cre is relocalized to the cytoplasm when the drug is removed.

From matings between NuMA$^{flox/wt}$,Cre-ER^{TM} and NuMA$^{flox/wt}$ mice, I derived mouse embryo fibroblasts (MEFs) from E14.5 embryos that were either wild-type, heterozygous or homozygous for the conditional NuMA allele, and also carried the Cre-ER^{TM} transgene. To confirm that addition of 4-OHT would result in efficient recognition and recombination of *loxP* sites within the NuMA gene, contact inhibited cells were treated with 0.1μM 4-OHT for 48h in low serum, followed by drug wash-out and maintenance under growth arrest conditions for an additional 48h to allow turnover of endogenous NuMA (Figure 3.5). Multiple independent NuMA$^{flox/flox}$,Cre-ER^{TM} cell lines showed highly efficient deletion of exon 22 within 48h of 4-OHT treatment (Figure 3.5). Quantification of Cre-ER^{TM} activity by qPCR showed a time and 4-OHT dose dependence to excision efficiency, with a maximum effect observed after 48h of treatment with 0.1μM 4-OHT (data not shown). This resulted in a fibroblast population with 90% conversion of NuMA^{flox} to NuMA$^{\Delta 22}$ at day 4 (Figure 3.5).

[This protocol was used to achieve NuMA deletion in every subsequent experiment described using primary fibroblasts.]

NuMA protein lacking residues encoded by exon 22 accumulated to less than the initial level of wild-type NuMA, as revealed by immunoblotting (Figure 3.5). It is highly unlikely that remaining NuMA protein in cells deleted of exon 22 represented wild-type protein that had not yet turned over, because doubling the incubation time of cells in low serum media after 4-OHT wash out did not result in further reduction of NuMA levels (data not shown). As anticipated, exon 22 deleted NuMA still accumulated appreciably in nuclei, but was nearly quantitatively lost from spindle poles during mitosis (data not shown). From these results, we conclude that wild-type NuMA protein is completely absent from $NuMA^{\Delta 22/\Delta 22}$ MEFs within 4 days of exon 22 deletion, sub-endogenous levels of mutant protein are produced from the $NuMA^{\Delta 22}$ allele, and that amino acids encoded by exon 22 are dispensable for the nuclear accumulation of NuMA, but necessary for efficient spindle-pole localization.

3.5 NuMA is required for the proliferation of primary embryo fibroblasts

To directly assess the consequence of preventing NuMA accumulation at spindle poles, population growth curves were generated for, $NuMA^{wt/wt}$, $NuMA^{flox/wt}$ and $NuMA^{flox/flox}$ MEFs, each carrying the Cre-ER^{TM} transgene.

Following treatment with 4-OHT to convert these cells to NuMA$^{+/+}$, NuMA$^{+/\Delta 22}$ and NuMA$^{\Delta 22/\Delta 22}$ as described above, NuMA$^{+/+}$ and NuMA$^{+/\Delta 22}$ cells grew normally after release from low-serum arrest demonstrating that there are no dominant effects on cell cycle progression of mutant protein produced from the NuMA$^{\Delta 22}$ allele. NuMA$^{\Delta 22/\Delta 22}$ MEFs failed to increase in number (Figure 3.5), demonstrating that this NuMA deletion results in cell-autonomous growth defects. These conclusions are consistent with cell-intrinsic defects causing early embryonic lethality in NuMA$^{\Delta 22/\Delta 22}$ mice and the lack of dominant effects or haploinsufficiency we observed in NuMA$^{+/\Delta 22}$ animals, which develop and age normally.

To determine if loss of NuMA function at spindle poles in mitosis provoked an extended mitotic delay, as has been previously reported from antibody microinjection mediated disruption of NuMA (Gaglio et al., 1995), the mitotic index of NuMA$^{\Delta 22/\Delta 22}$, NuMA$^{+/\Delta 22}$ and wild-type MEFs was determined. Using histone H3 phosphorylation as a marker for cells in M-phase, I observed no increase in the percentage of cells in mitosis caused by NuMA exon 22 deletion (Figure 3.5). To look more directly at mitotic timing, I immortalized Cre-ER^{TM}, NuMA$^{+/+}$ and Cre-ER^{TM}, NuMA$^{flox/flox}$ fibroblasts with the SV40T antigen, treated these cells with 4-OHT as described above, filmed them by phase-contrast microscopy, and measured the duration of mitosis. [Immortalized cells were prepared for this experiment because the substantially longer cell cycle time and very low mitotic index of primary cells

precluded their efficient use in this assay.] Following 4-OHT treatment, $NuMA^{flox}$ was converted to $NuMA^{\Delta 22}$ with the same efficiency as seen in primary cells (not shown). Mitosis was defined as the period between the first discernable stage of cell rounding and the time at which rounded cells were seen to completely flatten back onto the substrate. Consistent with the failure of NuMA disruption to affect mitotic index, no significant increase in the duration of mitosis was observed between NuMA deleted versus control cells (Figure 3.5).

3.6 Spindle defects caused by loss of mitotic NuMA function

Despite normal timing of progression through mitosis, $NuMA^{\Delta 22/\Delta 22}$ deleted primary cells displayed obvious spindle defects, most striking of which was the loss of centrosomes from the ends of mitotic spindles. In some cells, spindles retained focused arrays of microtubule ends despite having no closely associated centrosome, while in others, even those poles with associated centrosomes lacked a discernable microtubule focus (Figure 3.6). Greater than 50% of metaphase-like cells in the $NuMA^{\Delta 22/\Delta 22}$ population had at least one centrosome which was clearly not associated with a spindle pole (apolar centrosome), and a similar frequency had at least one pole in which microtubules did not converge to a single focal point (unfocused K-fibers) (Figure 3.6). These phenotypes contrasted sharply with metaphases observed in wild-type and $NuMA^{+/\Delta 22}$ cells, which consistently showed typical spindle

architecture and had well-focused microtubules terminating near centrosomes (Figure 3.6). Co-staining metaphase spindles with a γ-tubulin antibody confirmed that dissociated microtubule nucleating structures were *bona fide* centrosomes (Figure 3.7). Immunostaining of unperturbed fibroblasts with a cyclin B1 antibody confirmed that spindle defects caused by loss of NuMA were occurring prior to anaphase onset (Figure S4). Cells arrested in metaphase by blocking cyclin B and securing degradation by treatment with the proteasome inhibitor MG132 showed the same defects at high frequency, corroborating this interpretation (Figure 3.7).

In addition to centrosome-spindle coupling and microtubule focusing defects, metaphase spindle lengths in MG132 arrested cells with spindle-pole localization deficient NuMA were on average 30% longer than either wild-type or $NuMA^{+/\Delta 22}$ controls (Figure 3.6). Spindle abnormalities were not due to a failure of the dynein/dynactin complex, the major mitotic binding partner of NuMA, to localize appropriately. By examining the localization of the p150 component of dynactin; I found that this subunit localized to centrosomes independent of spindle attachment, suggesting that failure of centrosome-spindle coupling and loss of K-fiber focusing did not result from dynein mislocalization (Figure 3.8). Cold treatment to preferentially depolymerize dynamic microtubules confirmed that K-fibers remained stable and attached to kinetochores in NuMA-disrupted cells, even when completely defocused at poles and detached from centrosomes (Figure 3.8).

Consistent with the absence of a mitotic delay (Figure 3.5), anaphases in MEFs with defective mitotic-NuMA appeared at a frequency comparable to wild-type fibroblasts. Like metaphases figures, anaphases also showed defects in centrosome positioning and K-fiber focusing, although chromosome segregation clearly initiated even in the presence of these abnormalities (Figure 3.6). NuMA-deficient anaphases frequently displayed lagging chromosomes and/or bridges of chromatin connecting the two separated chromosomes masses (Figure 3.6). From these results, I conclude that general mammalian spindle pole integrity is defective in the absence of functional NuMA, and more specifically that NuMA is required at spindle poles to couple centrosomes to kinetochore-fibers. I also note that kinetochore-microtubule attachments appear to be intact, and that despite an increase in minor segregation errors, major anaphase chromosome movements (segregation of most chromosomes) proceed largely as normal.

3.7 Spindle bipolarization precedes centrosome detachment in the absence of NuMA

As noted above, the most striking defect in spindles of primary cells undergoing mitosis in the absence of functional NuMA was the displacement of centrosomes from spindle kinetochore-fibers in metaphase. This could arise either from a failure of initial spindle microtubule focusing during formation of spindle poles, or an inability to maintain centrosome at poles of a fully formed

spindle. To distinguish these possibilities, I followed, by direct observation, spindle formation in NuMA-deficient cells. Primary MEFS were transduced with a retrovirus encoding tubulin-YFP two days prior to the initiation of Cre recombinase activity with the 4-OHT treatment protocol, and then cells were filmed following eventual release from low-serum arrest. NuMA$^{+/\Delta 22}$ MEFs that progressed through mitosis with both spindle poles visible (in focus, in the field of view) always formed bipolar spindles and maintained centrosomes at spindle poles throughout mitosis, even in examples that experience the most prolonged metaphases (6/6 morphologically normal spindles) (Figure 3.9). In contrast, NuMA-deleted fibroblasts exhibited a high frequency of pole-defocusing and centrosome detachment phenotypes (9/13 spindles aberrant) (Figure 3.9). Live cell imaging showed clearly that in the absence of wild-type NuMA, microtubules can establish focusing towards centrosomes during the initial stages of spindle assembly, but that as cells progress through mitosis, maintenance of centrosome-spindle coupling is lost and poles subsequently defocus. Despite these defects, completion of mitosis was not atypical: daughter cells formed morphologically normal nuclei, and cytokinesis, including abscission, also occurred. In tubulin-YFP expressing MEFs in which I could clearly observe spindle structure in cells entering and exiting mitosis, I also measured the duration of mitosis as defined by the length of time between nuclear envelope breakdown (NEBD) and the first observable stage of midbody formation. I found mitotic timing to be similar for heterozygous

(33min ± 9min, n=6) and NuMA-deficient cells that experienced spindle defects (27min ± 5min, n=5). Additionally, the kinetics of spindle bipolarization, the first time point following NEBD at which microtubules were seen to be organized into a typical football-shaped spindle was similar in control (12±4min, n=6) and subsequently phenotypic NuMA$^{\Delta 22/\Delta 22}$ cells (13±3min, n=5). These observations indicate that loss of NuMA function during mitosis does not interfere with the initial establishment of focused bipolar spindles, but results in the loss of centrosome maintenance at poles, followed by microtubule defocusing.

3.8 Reduced levels of nuclear NuMA support all essential interphase functions

Mitotic phenotypes we observed in NuMA$^{\Delta 22/\Delta 22}$ fibroblasts were consistent with specific defects in spindle pole integrity, and are unlikely to reflect indirect effects from disrupted nuclear function. The ability of NuMA$^{\Delta 22/\Delta 22}$ cells to enter mitosis further indicated the absence of cell-cycle disruption from NuMA exon 22 deletion. To confirm the absence of nuclear defects in NuMA$^{\Delta 22/\Delta 22}$ cells, I designed a sensitive and specific *in vivo* test for nuclear function of the exon 22 deleted NuMA protein. This was accomplished by replacement of wild-type NuMA with the NuMA$^{\Delta 22}$ protein in adult spinal cord motor neurons, a cell type in which NuMA is known to be present in nuclei. These cells were chosen for a variety of considerations, including: i)

defects in motor neuron function give rise to characteristic and easily scorable motor-deficits including gait alterations and paralysis; ii) they are extraordinarily long-lived, allowing access to any age-dependent features of loss of interphase NuMA function; and iii) existing motor-neuron specific Cre transgenes were available to direct Cre expression specifically in post-mitotic motor neurons.

NuMA was deleted specifically from motor neurons by crossing the $NuMA^{flox}$ allele with animals carrying the VAchT-Cre transgene. This transgene has previously been demonstrated to direct Cre recombinase expression exclusively in motor neurons, and only after the final division of motor neuron progenitors (Misawa et al., 2003), ensuring that any phenotypes would arise exclusively from post-mitotic loss of NuMA. $NuMA^{flox/flox}$,VAchT-Cre; $NuMA^{+/flox}$,VAchT-Cre; and $NuMA^{flox/flox}$ littermate controls were obtained. Animals of all genotypes and genders were produced in expected Mendelian ratios, followed by regular visual inspection, weighed, and tested on the rotorod (a standard test of motor function) at 100 and 200 days of age. Activity of Cre and restriction of expression to motor neurons in VAchT-Cre mice was confirmed by mating to the ROSA26R reporter strain (Soriano, 1999), which carries a transgene that expresses β-galactosidase only in Cre expressing cells and their daughters. Examination of spinal cord and sagital brain sections from VAchT-Cre,ROSA26R mice for β-galactosidase expression (Figure 3.10) confirmed that Cre expression was restricted to motor neurons.

Extensive visual observation demonstrated that NuMA$^{flox/flox}$,VAchT-Cre animals showed no obvious behavioral defects, including gait alterations, paralysis, hind-limb clasping behavior or weakness, seizures, or signs of muscle atrophy indicative of motor neuron dysfunction, even at up to two years of age. In addition, quantitative data from rotorod testing showed no significant differences in performance between wild-type, heterozygous and animals homozygously deleted for exon 22 of NuMA specifically in motor neurons (data not shown). Weight gain, an early indicator of motor neuron dysfunction, in control and motor-neuron NuMA-deleted animals was also similar (Figure 3.10). Finally, counting of Cresyl-violet stained motor neuron cell bodies in spinal cord sections of 200-day-old animals revealed indistinguishable motor neuron numbers in animals of experimental and control genotypes (Figure 3.10). These data lead me to conclude that although reduced levels of protein are ultimately produced from the NuMA$^{\Delta 22}$ allele, the exon 22 deleted mutant complements all potential nuclear functions of NuMA throughout the post-mitotic life of these motor neurons.

3.9 NuMA is required for the maintenance of centrosome-spindle coupling in bipolar spindles under tension

Live imaging of tubulin-YFP marked spindles in unperturbed fibroblasts strongly supported a maintenance, rather than establishment role for NuMA in the attachment of centrosome to kinetochore-fibers, since initial focusing

appeared normal. To confirm this interpretation, I arrested NuMA wild-type, $NuMA^{\Delta 22/+}$ and $NuMA^{\Delta 22/\Delta 22}$ cells in mitosis with the Eg5 inhibitor S-trityl-L-cysteine (STLC) (Skoufias et al., 2006). Eg5 is a bipolar, homotetrameric, kinesin-related motor protein that is required during mitosis to maintain separation of centrosomes. It is thought to function by cross-linking and sliding anti-parallel microtubules from opposing centrosomes, thereby pushing centrosomes apart (Kapitein et al., 2005). STLC prevents activity of Eg5, causing collapse of bipolar spindles. In all MEF cell lines regardless of genotype, STLC treatment produced a high frequency of monopolar spindles that appeared almost exclusively as chromosome “rosettes” surrounding a central gamma tubulin positive pole (Figure 3.11). This indicates that centrosomes continue to dictate the location of spindle pole formation when normal NuMA function is disrupted, and that kinetochore fibers do not require NuMA for active focusing towards centrosomes.

Interestingly, in the absence of pole-localized NuMA, centrosomes persisted at the center of monopolar spindles despite the extended mitotic delay produced by treatment with STLC. How can this observation be reconciled with a maintenance role of NuMA in centrosome-spindle coupling? Relative to bipolar metaphase spindles, monopolar mitoses produced by Eg5 inhibition are likely to have reduced tension forces acting between centrosomes and kinetochores. The maintenance of centrosomes at microtubule minus ends in monopolar spindles in the absence of efficiently

localized NuMA suggests that the spindle phenotypes I observed in unperturbed cells might reflect a requirement for NuMA in maintaining centrosomes at poles of spindles under normal tension.

Therefore, STLC was washed out from monopolar-arrested cells to test the effect of reintroducing tension into spindles with kinetochore-fibers focused towards a monopole. One hour after release, cells were fixed for immunofluorescence. Specifically in NuMA$^{\Delta 22/\Delta 22}$ cells, anaphase figures were apparent in which chromosomes had segregated apparently normally, but centrosomes had failed to separate. Control anaphases always had one centrosome at each pole (Figure 3.11). Using live imaging to follow recovery of spindle bipolarity in retrovirally-transduced, tubulin-YFP expressing fibroblasts released from STLC arrest, I observed similar phenotypes. Of those spindles that formed and oriented parallel to the surface, and were therefore amenable to imaging, control cells were uniformly observed to recover from monopolarity by separating centrosomes and forming bipolar spindles with well-focused poles (7/7 cells) (Figure 3.11). NuMA$^{\Delta 22/\Delta 22}$ fibroblasts, in contrast, often formed spindles with one well-focused and one splayed spindle pole (8/13 cells) (Figure 3.11). The juxtaposed centrosomes were always observed at the spindle end with focused microtubules, although as cells progressed through mitosis, the paired centrosomes were often seen to dissociate from this pole. These “cone-shaped” spindles were not simply arrested monopolar spindles seen in profile, because they uniformly proceeded into anaphase, indicating

that mitotic checkpoint signaling resulting from kinetochores without proper microtubule attachment had been relieved. From these data, I conclude that in the absence of normally localized NuMA, only when spindle forces are low do centrosomes continue to associate with kinetochore-fiber minus-ends. Further, normal NuMA function is required for centrosome separation following recovery from a monopolar state. Additionally, I conclude that in the absence of centrosomes (as seen in the centrosome-distal half of each NuMA-deficient spindle following release from STLC) NuMA is required for the establishment of microtubule focusing.

3.10 Stable kinetochore-microtubule interactions are required for centrosome separation during prometaphase

My observations of failure of centrosome separation during recovery from monopolarity in the absence of functional NuMA raised the possibility that centrosomes require physical tethering to kinetochore-fibers in order to be moved apart by Eg5, rather than being pushed away from each other through the sliding apart of antiparallel, overlapping microtubules nucleated directly by centrosomes. This interpretation gives rise to the prediction that stable attachment of microtubules to kinetochores is also required for centrosome separation following nuclear envelope breakdown. The Ndc80 complex, a heterotetramer composed of the Ndc80, Nuf2, Spc24 and Spc25 proteins, is a key component involved in the stable attachment of microtubule bundles at

kinetochores. Overall stability and microtubule-binding capacity of the complex relies on the presence of all four subunits (Cheeseman and Desai, 2005). Therefore, to directly test the requirement for kinetochore-microtubule attachment in centrosome separation, I, along with Dr. Andrew Holland, used siRNA to deplete Nuf2 in HeLa cells stably expressing fluorescently tagged tubulin and histone H2B. We arrested these cells in a monopolar state using STLC, and then washed out the drug and used time-lapse fluorescence microscopy to observe, in real time, recovery of spindle bipolarity. In control siRNA treated cells, 90 minutes following STLC wash-out, all but 3% of cells had effectively separated their centrosomes and formed bipolar spindles. In a similar amount of time, 35% of Nuf2 depleted spindles failed to resolve their centrosomes and form bipolar spindles (Figure 3.15). Prophase mechanisms (functioning prior to kinetochore fiber formation) of centrosome separation were not affected by Nuf2 depletion; Nuf2 siRNA alone did not result in spindle monopolarity. From these results I conclude that Eg5 acts to separate centrosomes by pushing apart parallel kinetochore-fibers, and that the mechanism of prometaphase centrosome separation relies on the two-point attachment of kinetochore-fibers at centrosomes and kinetochores.

3.11 Kinetochore fibers are not required for NuMA accumulation at spindle poles

To further investigate the relationship between spindle formation and NuMA localization, I analyzed the kinetics of NuMA accumulation at centrosomes as cells entered mitosis and formed spindles. This was carried out in cell lines expressing GFP-tagged NuMA, and co-expressing mRFP-tagged histone H2B to mark chromatin. Stable cell lines were derived which expressed fluorescently tagged NuMA at approximately 5-10% of endogenous levels (Figure 3.12). HeLa cells expressing fluorescent tubulin and H2B were imaged in parallel to identify the stages of spindle formation. Within five minutes of NEBD, a time point at which spindles were observed as two pronounced centrosomal asters, wild-type NuMA-GFP was already seen to accumulate at centrosomes. Ten minutes after nuclear envelope breakdown, when bipolar spindles appeared fully formed, but at least 30 minutes before HeLa cell anaphase initiation (Yang et al., 2008), almost all NuMA was completely incorporated into spindle poles (Figure 3.13). Although the accumulation of the majority of NuMA at centrosomes early during bipolar spindle formation suggested that transport of NuMA to spindle poles is kinetochore-fiber independent; to test directly whether NuMA could localize to centrosomes in the absence of kinetochore-fibers, I generated stable cell lines expressing a GFP-tagged nuclear-excluded version of NuMA. This mutant was generated by replacing the 5 amino acid putative nuclear localization

sequence (NLS) with a well characterized nuclear export sequence (NES) from the PKC inhibitor PKI (Wen et al., 1995) This mutant, “NuMA(NES)-GFP” did not accumulate in the nucleus during interphase, but localized appropriately to spindle poles during mitosis (Figure 3.12). No effects on the interphase tubulin cytoskeleton from stable expression of NuMA(NES)-GFP were observed (data not shown). As cells expressing this cytoplasmic NuMA entered mitosis, NuMA(NES)-GFP could clearly be seen to accumulate at centrosomes prior to NEBD, and coincident with rearrangement of the tubulin cytoskeleton and formation of prophase centrosomal asters (3.13). These observations indicate that wild-type NuMA localization to spindle poles begins immediately following NEBD, and that NuMA recruitment initiates prior to kinetochore fiber formation. I suspect that accumulation of NuMA at the spindle pole is only rate limited by kinetics of its interaction with the poleward transport machinery dynein (Merdes et al., 2000).

3.12 Discussion

I have described here the creation of a deletion within the mouse NuMA gene, the removal of exon 22 ($NuMA^{\Delta 22}$), which produces a mutant protein unable to efficiently localize to spindle poles during mitosis. When homozygous, this allele results in the detachment of centrosomes from the ends of kinetochore-fibers and the subsequent de-focusing of microtubules at spindle poles following the initial formation of bipolar spindles during mitosis in

primary somatic cells. It is clear that these defects are not due to dominant effects because NuMA$^{\Delta 22/+}$ cells have spindles that are completely indistinguishable from wild-type cells in every aspect examined. I exploited the strong and highly penetrant mitotic phenotype of NuMA$^{\Delta 22/\Delta 22}$ cells to investigate mechanisms of spindle pole establishment and maintenance in mammalian mitosis.

3.12.1 Mechanisms of microtubule focusing

It is now clear that in mammalian somatic spindles, some kinetochore fibers are derived from non-centrosomal sources (Rieder, 2005). This presents the problem of how these microtubule bundles have their minus-ends drawn towards the spindle pole. Models for kinetochore fiber focusing have suggested that NuMA functions as an active participant in microtubule coalescence towards poles. This has been proposed to occur through capture of kinetochore-fibers by NuMA, which itself is transported towards spindle poles on centrosomal/astral microtubules by dynein (Khodjakov et al., 2003). However, it cannot be the case that microtubules growing from centrosomes are required for the transport of NuMA toward poles, nor that kinetochore-fibers require centrosomes to become focused. This is clear because when centrosomes are destroyed by laser ablation prior to mitotic entry, bipolar spindles still form, and these have well-focused poles to which NuMA is localized (Khodjakov et al., 2000). Therefore, even in mammalian cells with

centrosomes, just as there is a centrosome independent mechanism for spindle formation, there must be a mechanism for centrosome independent spindle pole focusing. The specific requirement for NuMA in this process has been proposed (Khodjakov et al., 2000), and is also suggested by spindle defects observed in acentrosomal spindles formed around DNA coated beads in *Xenopus* extracts depleted of NuMA (Merdes et al., 2000). I have now tested this proposal. My observations during live cell imaging of spindle formation after release from STLC arrest demonstrate of a critical function for NuMA in this process. In cells from monopolarity, I frequently saw that microtubules in NuMA$^{\Delta 22/\Delta 22}$ fibroblasts remained focused around an unseparated centrosome pair, but were severely defocused in the acentrosomal spindle half (Figure 5D). These NuMA-deficient spindles were truly bipolar because they exited mitosis once released from STLC, and despite centrosome separation failure, they segregated chromosomes into two distinct masses (Figure 5C). The formation of these monoastral, bipolar, “cone-shaped” spindles indicates that NuMA is required for spindle pole focusing in the absence of centrosomes. The NuMA-dependent process of acentrosomal spindle pole focusing is likely to rely on dynein-dependent transport and self-assembly properties of NuMA (Harborth et al., 1999) (Figure 3.15). To be able to use primary fibroblasts able to test the role of NuMA in acentrosomal spindle pole focusing was an added unanticipated bonus of building the NuMA$^{flox/flox}$ mice. Indeed the failure of centrosome separation I

observed during STLC recovery in the absence of NuMA was highly surprising. I suspect that mammalian acentrosomal-spindle systems, including mouse oocytes, rely heavily on NuMA for the establishment of spindle poles, and it will be interesting to determine whether this is the case by examining spindle formation in oocytes homozygous for the $NuMA^{\Delta 22}$ allele.

In addition to the identification of additional components involved in spindle pole focusing remains the question of whether the pathway of acentrosomal spindle pole focusing co-operates or acts as an independent back-up system to the centrosomal pathway in normal bipolar spindles when centrosomes are present. It could be that acentrosomal spindle focusing mechanisms are only invoked in the absence of centrosomes. The idea of parallel mechanisms functioning exclusively as “back-up” or “failsafe” systems does not seem to be the case with the formation of kinetochore fibers, which develop in a centrosome-independent manner even when centrosomes are present (Khodjakov et al., 2003; Maiato et al., 2004; Tulu et al., 2006), although the degree to which non-centrosomally derived K-fibers are required during normal spindle formation is not established. With regards to microtubule focusing, based on the apparently unaltered duration of mitosis, and more specifically the normal kinetics of initial spindle pole focusing in primary fibroblasts in the absence of functional NuMA, I suspect that sufficient centrosome-dependent forces exist to power kinetochore fiber coalescence in the absence of a functioning co-operative pathway. Alternatively, this could

reflect, in a normal mitosis when centrosomes are present, a relatively low involvement in kinetochore fiber formation from non-polar sources. New methodologies will have to be developed in order to determine the relative contribution of centrosomal and non-centrosomal routes to kinetochore-fiber formation during normal mitosis in mammalian cells, which will help to address this point.

Given that bipolar spindle formation initiates normally in cells with separated centrosomes that enter mitosis in the absence of functional NuMA, there are likely to be alternative processes involved in microtubule focusing, as has been previously proposed (Gordon et al., 2001). These are likely to be heavily dependent on the presence of centrosomes, which serve as strong attractive forces for spindle microtubules, and involve components such as HSET in mammals (Gordon et al., 2001) and Ncd in Drosophila (Goshima et al., 2005). The minimal role I documented for NuMA in active microtubule focusing brings me to re-interpret the proposed mitotic function of the major binding partner of NuMA, the dynein-dynactin complex (Merdes et al., 1996). It is intriguing that similar to the defects we observed in NuMA deleted MEFs, dynein disruption also gives rise primarily to centrosome-spindle uncoupling and to a lesser extent a mild degree of K-fiber unfocusing during metaphase (Goshima et al., 2005; Heald et al., 1997). In multiple contexts, dynein inhibition causes NuMA to redistribute from spindle poles to the length of spindle microtubules (Gaglio et al., 1997; Merdes et al., 2000), suggesting that

the major function of spindle-localized dynein in mitosis may be to transport NuMA, as a cargo, to microtubule minus ends. The rapid kinetics of NuMA localization to spindle poles and the kinetochore-fiber independent nature of NuMA accumulation at poles is consistent with this interpretation. If this is true, then dynein spindle phenotypes result directly from the failure to properly localize NuMA.

3.12.2 Function of Eg5 in prometaphase centrosome separation

In mitotic prophase, prior to nuclear envelope breakdown, two duplicated centrosomes can crawl across the nuclear envelope in a dynein-dependent manner to diametrically oppose each other in anticipation of bipolar spindle formation (Gonczy et al., 1999). Maintenance of centrosome separation following nuclear envelope breakdown requires the plus end directed motor Eg5, and centrosomes collapse together when this activity is inhibited, triggering an extended mitotic delay (Skoufias et al., 2006). As mentioned above, based on the view that Eg5 acts to establish bipolarity by sliding apart antiparallel microtubules (Kapitein et al., 2005), centrosome separation failure would not be predicted to result from NuMA deficiency during restoration of Eg5 activity after induction of monopolarity (Figure 3.16). This indicates that a more likely mechanism of Eg5 activity is, as initially proposed, provision of a force normal to the direction of the spindle axis that maintains spacing between parallel microtubules (Kapoor et al., 2000). To

separate centrosomes in recovering monopolar spindles in prometaphase, Eg5 tetramers might function by walking anti-poleward along parallel microtubules emanating from juxtaposed centromeres (Loncarek et al., 2007). As the motor approaches the closely spaced kinetochores, it could serve as a wedge, forcing itself into the diminishing space between kinetochore fibers and prying them apart (Figure 3.16). Connections between K-fiber minus ends and the centrosome would drag centrosomes along, like a balloon on a stick, as microtubules were pivoted around sister kinetochore pairs. The function of kinetochores as a pivot point in the process of Eg5 mediated prometaphase centrosome separation is supported by our observations that in the absence of stable kinetochore microtubule interactions, centrosome separation during prophase is inhibited.

Different cell types seem to rely differentially on mechanisms operating during prophase or prometaphase to separate their centrosomes. This is apparent from the degree of centrosome separation observed in HeLa vs. DLD-1 cells, a human cancer cell line in which nuclear envelope breakdown occurs early, while duplicated centrosomes remain juxtaposed. If this difference also exists between cancer cells and normal bystander cells affected during anti-mitotic chemotherapy, then the prometaphase pathway of centrosome separation might be an attractive target for inhibition as a cancer treatment. Prevention of centrosome-spindle coupling could inhibit susceptible cancer cells from efficiently forming bipolar spindles; leading to cell death after

extended monopolar mitotic delay as has been seen for KSP inhibitors (Shi et al., 2008).

3.12.3 Centromere reorientation and chromosome segregation in the absence of focused poles

The ability of sister chromatids in NuMA$^{\Delta 22/\Delta 22}$ primary fibroblasts to segregate despite centrosome separation failure after release from extended monopolar arrest indicates kinetochores are able to bi-orient without centrosome separation. Kinetochore bi-orientation is the state in which microtubule-bound sister kinetochores face in opposite directions. Recent evidence indicates that in monopolar spindles, chromosomes become deformed at the centromeric region, and both kinetochores from the same chromosome face in the same direction, towards the monopole (Loncarek et al., 2007). Restoration of normal centromere geometry, and resultant kinetochore bi-orientation, during recovery from a monopolar state was suggested to require centrosome separation (Loncarek et al., 2007). This is at odds with our observations that kinetochore fibers, rather than centrosomes, are the crucial component in dictating a return to kinetochore bi-orientation. In the NuMA deleted MEFs, weak connections between the paired centrosomes, which remain at the focused spindle pole, and kinetochore-fibers, might be sufficient to serve as an anchor point and provide resistance against which force can be applied to return deformed centromeres/kinetochores to the

native state. This suggests that centrosomes and stable kinetochore-microtubule interactions co-operate to restore bipolarity during recovery from monopole inducing drugs.

In addition to the production of centromere re-orienting forces in the absence of centrosome separation in NuMA$^{\Delta 22/\Delta 22}$ fibroblasts recovering from monopolarity, the capability of chromosomes to segregate almost completely normally in otherwise unperturbed NuMA$^{\Delta 22/\Delta 22}$ cells was also surprising. Previous reports have suggested that microtubule anchoring at spindle poles is required for chromosome movement during mitosis (Gordon et al., 2001). However, based on the almost normal segregation of chromatids on spindles with defocused poles and non-polar centrosomes, this does not seem to be true. Our results are more consistent with previous findings that mechanical severing of kinetochore fibers between spindle poles and kinetochores does not prevent continued poleward chromosome movements (Nicklas, 1989), and revive the question of why, during anaphase do “the chromosomes move toward the poles rather than the poles toward the chromosome” (Nicklas, 1989).

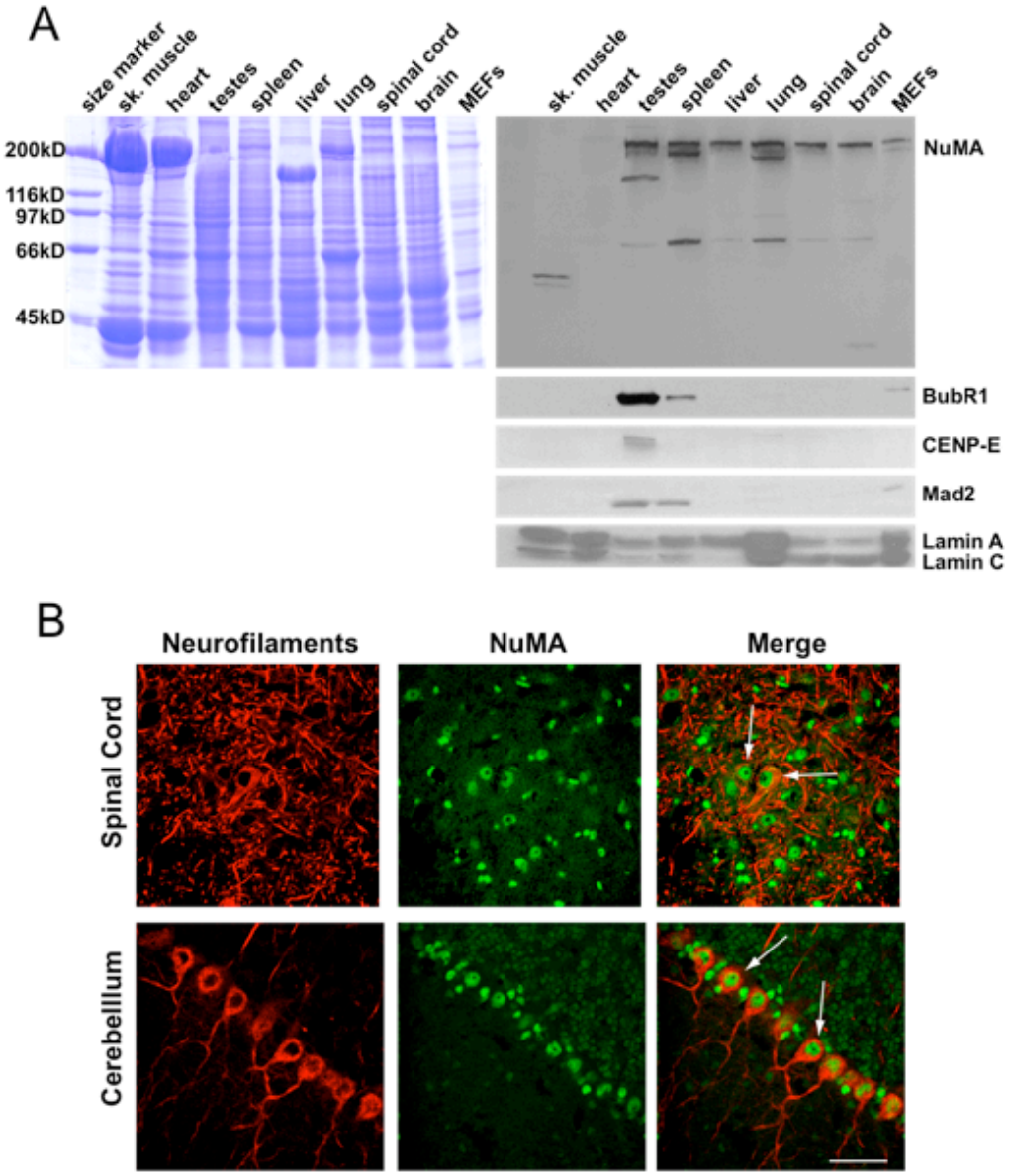

Figure 3.1 NuMA is broadly expressed in mouse tissues and present in nuclei of post-mitotic neurons

(A) Coomassie stained gel of tissue lysates from an adult C57/B6 mouse, and corresponding immunoblot of these tissues with antibodies to NuMA, BubR1, CENP-E, Mad2, and Lamins A and C.

(B) Immunofluorescence staining of frozen spinal cord and cerebellar sections from an adult C57/B6 mouse, with antibodies to NuMA (green) and unphosphorylated neurofilaments (red). Arrows indicate examples of NuMA-positive motor neurons in the spinal cord and Purkinje cells in the cerebellum. Scale bar represents 50 µm.

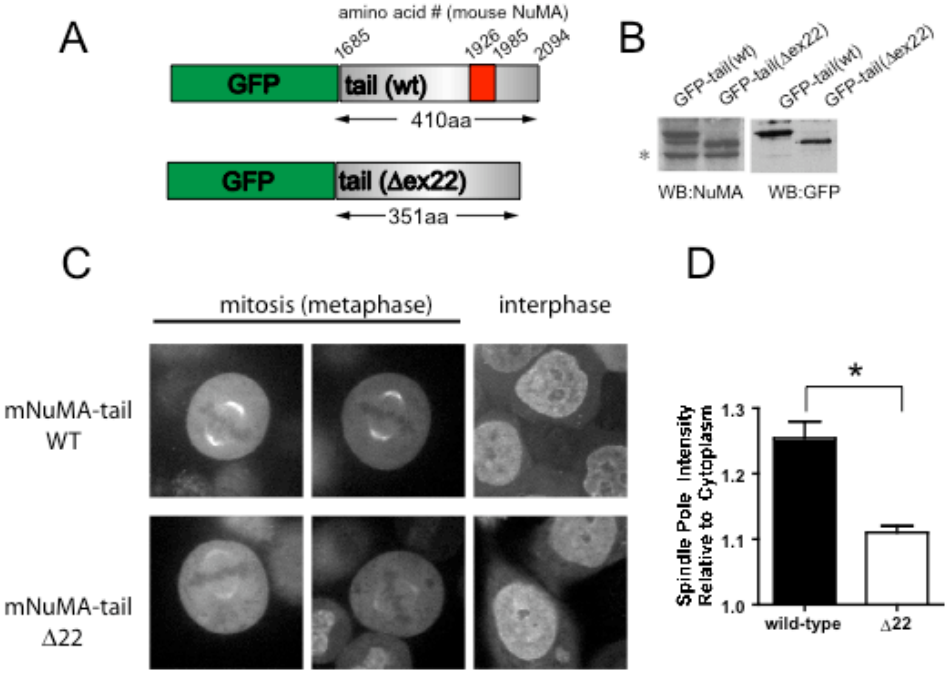

Figure 3.2 Efficient spindle-pole localization of NuMA requires exon 22

(A) Schematic of protein products expressed from constructs encoding either wild-type, "tail(wt)", or exon 22 deleted, "tail(Δex22)", C-terminal fragments of mouse NuMA. Amino acid numbers corresponding to mouse NuMA protein are indicated. Red box, residues encoded by exon 22.

(B) Immunoblot of cells expressing wild-type or Δex22 tail fragments, probed with antibodies to GFP and NuMA. *, non-specific band recognized by NuMA antibody.

(C) Localization of proteins depicted in (A) in HeLa cells during mitosis (metaphase) or interphase. Stage of mitosis was determined by chromosome positioning observed using phase-contrast microscopy. Images represent single confocal Z-sections taken through the center of each cell and were acquired using identical settings and exposure times and processed and scaled identically.

(D) Quantification of spindle pole fluorescence from images taken as in (C) of metaphase cells expressing GFP-tagged wild-type or exon22 deleted NuMA tail. Integrated pixel intensity was measured in a 100 square pixel box at the apex of each spindle pole, and normalized to an identically sized region in the cytosol behind that pole. n≥14 spindle poles per construct; *, p<.0001, t-test.

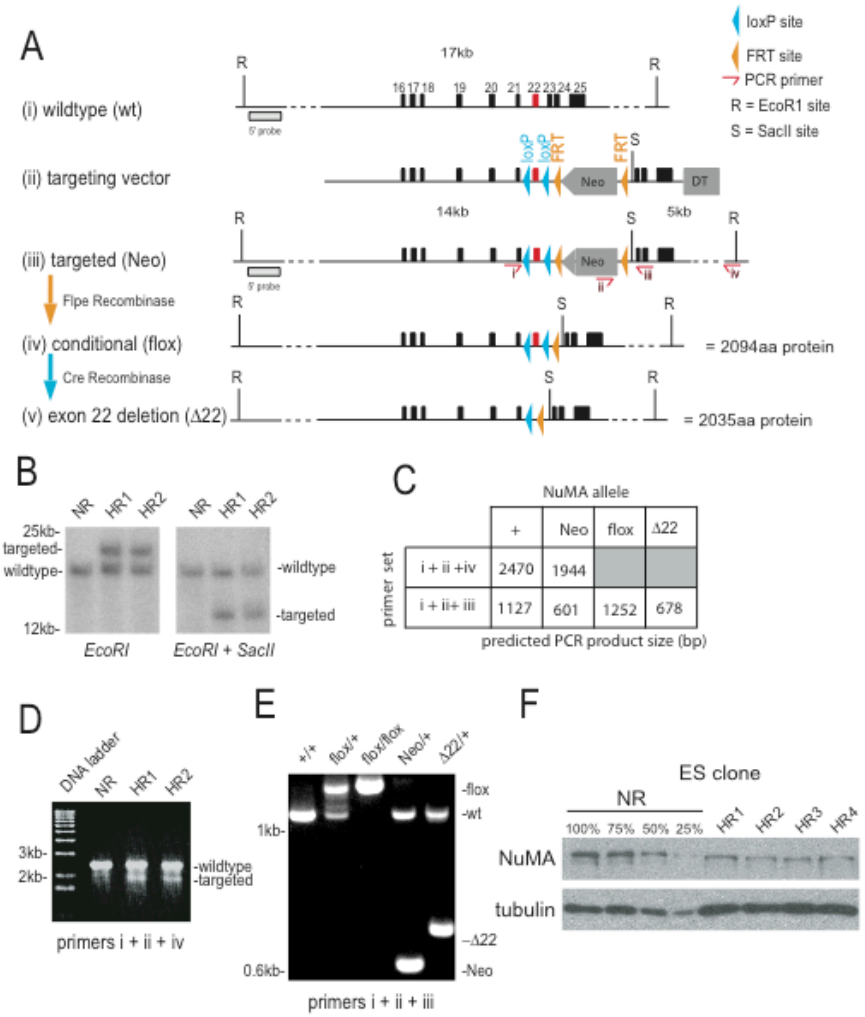

Figure 3.3 Creation of Conditional and Disrupted NuMA alleles

(A) Schematic representations of (i) a portion of the mouse NuMA gene including exons 16-25 and EcoR1 restriction sites, (ii) the exon 22 targeting vector showing the Neo (neomycin resistance) and DT (diphtheria toxin) cassettes and placement of loxP and FRT sites, (iii) the structure of the correctly targeted allele with the introduced SacII restriction site and locations of genotyping primers, (iv) the conditional allele (flox) produced by FLPeR mediated recombination of FRT sites flanking Neo, and (v) the deletion allele (Δ) produced by Cre recombination of loxP sites surrounding exon 22.

(B) Genomic DNA blotting from neomycin resistant ES clones after digestion with either EcoRI alone, or EcoRI and SacII in combination, and hybridization with the 5' probe shown in (A). NR, non-recombined; HR, homologously recombined.

(C) Predicted PCR fragment sizes for wt, Neo, flox and Δ alleles of NuMA using primer sets shown in (A).

(D) PCR products from neomycin resistant ES clones using primers i, ii and iv.

(E) PCR products from mouse tail DNA using primers i, ii and iii.

(F) Four independently targeted ES clones (HR1-HR4) and a dilution series of a non-recombined clone (NR) blotted with antibodies to NuMA and tubulin.

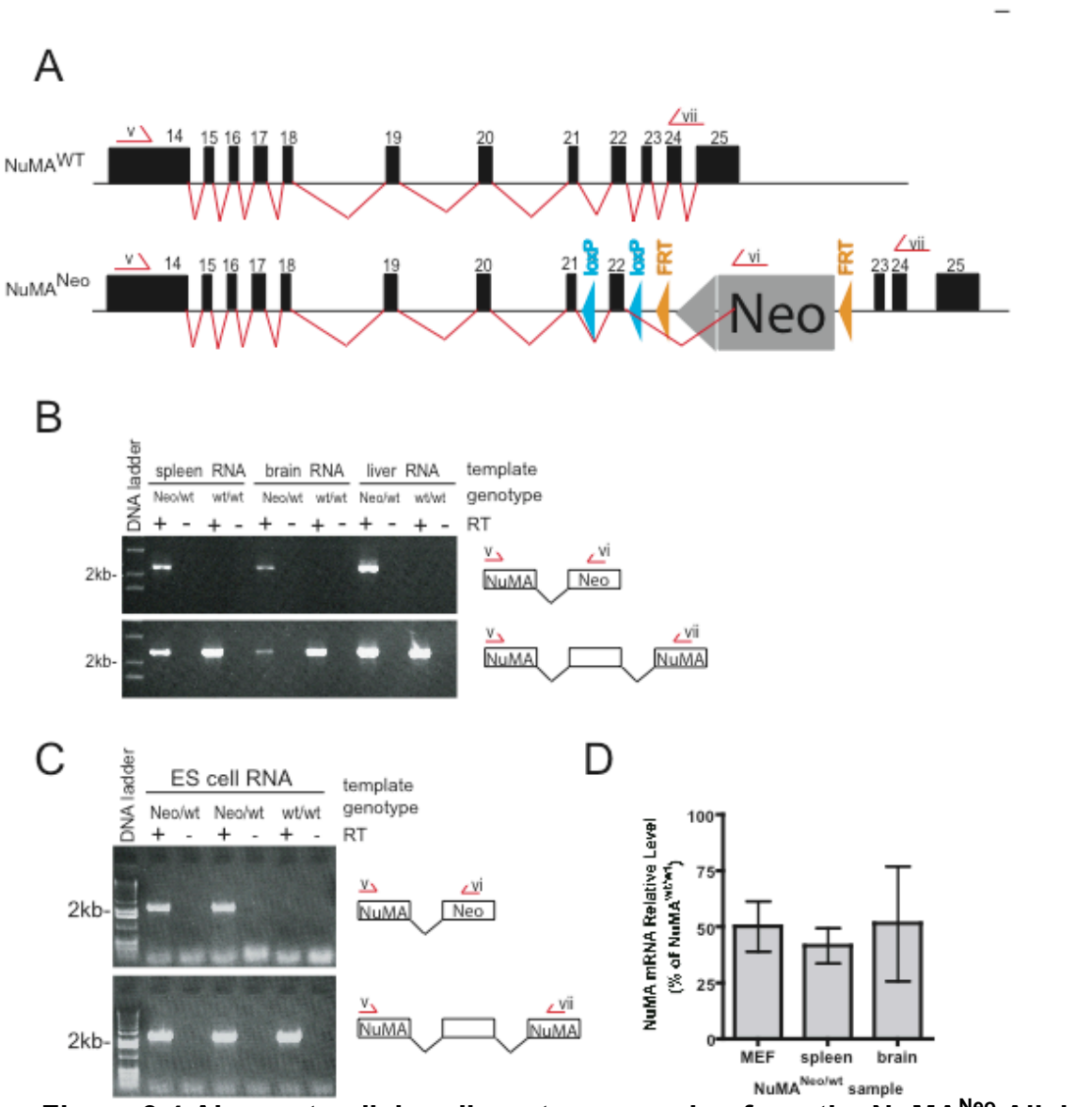

Figure 3.4 Aberrant splicing disrupts expression from the NuMA^{Neo} Allele

(A) Schematic of the wild-type (NuMA^{wt}) and targeted (NuMA^{Neo}) NuMA alleles, shown from exons 14-25. Splicing is indicated with red connecting lines below exons, and aberrant splicing into the *neo* cassette is indicated. Locations of PCR primers used to identify aberrant splice products (primers v, vi and vii) are shown.

(B) PCR from cDNA prepared with (+) or without (-) reverse transcription (RT) from total RNA extracted from tissues of wild-type (wt/wt) or NuMA^{Neo} heterozygous (Neo/wt) mice, to detect normal NuMA splicing (primers v and vii) or aberrant splicing into the *neo* cassette (primers v and vi). The aberrant splice product is detected only in Neo/wt, +RT samples.

(C) PCR as in (B) using total RNA prepared from homologously recombined (Neo/wt) or non-recombinant (wt/wt) neomycin resistant ES cell lines.

(D) Quantitative PCR to determine expression of normal NuMA message in mouse embryo fibroblasts (MEF) or tissues heterozygous for the NuMA^{Neo} allele, relative to wild-type samples. Bars represent mean of three experiments +/- SEM.

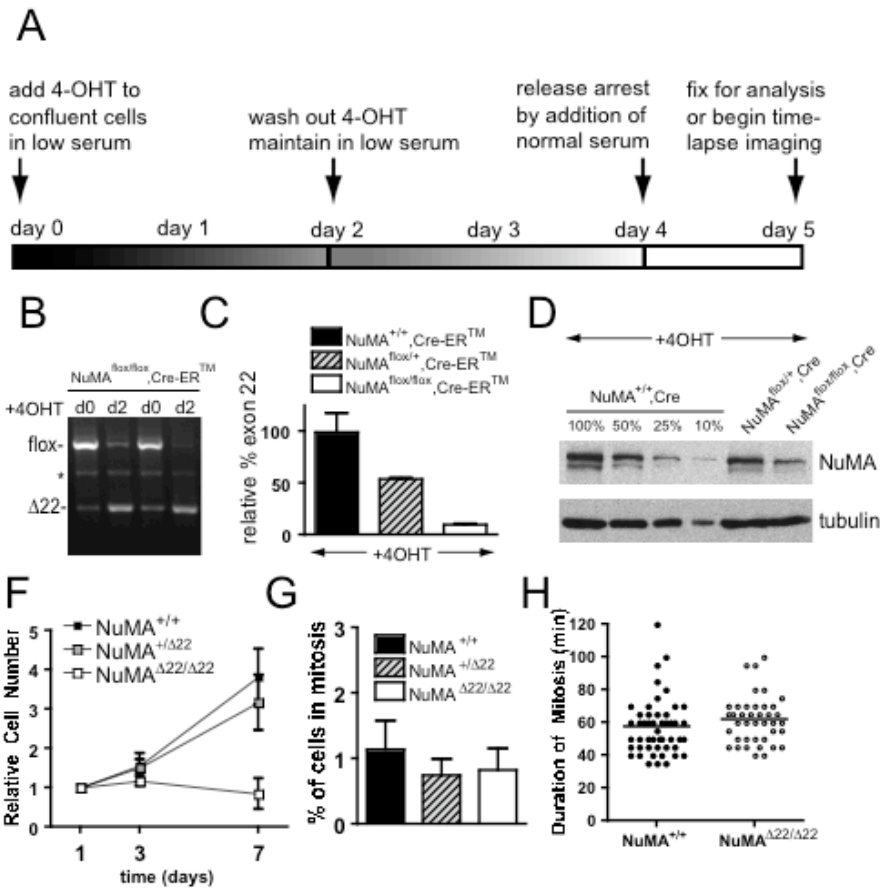

Figure 3.5 Tamoxifen induced disruption of NuMA inhibits proliferation of primary embryo fibroblasts

(A) Timeline showing experimental design, in which confluent primary cells are treated with 0.1μM 4-OHT in 2% serum for 48h, then washed and maintained in 2% serum for 48h before passaging into normal serum media for subsequent analysis. (B) Conversion of $NuMA^{flox}$ to $NuMA^{\Delta}$ in two independent primary $NuMA^{flox/flox}$ cell lines carrying the $Cre\text{-}ER^{TM}$ transgene was monitored by PCR, 48 hours after treatment with 0.1 μM 4-OHT. *, heteroduplex formed by annealing of "flox" and "Δ" PCR products. (C) Quantitative PCR using primers within the floxed region of NuMA was used to measure the efficiency of Cre mediated NuMA recombination in genomic DNA from fibroblasts treated with 0.1 μM 4OHT. Results represent the average of two separate experiments. (D) $NuMA^{flox/flox}$:Cre and a dilution series of $NuMA^{+/+}$:Cre fibroblasts, lysed in sample buffer and blotted with antibodies to NuMA and tubulin. (F) Growth curves of primary fibroblasts following 4-OHT mediated NuMA deletion, n=3 or 4 independent experiments per genotype. 1 day after release corresponds to day 5 of the experimental timeline (G) Mitotic index of primary MEFs treated with 4-OHT, n=2 cell lines per genotype, >2000 cells per genotype counted. (H) Duration of mitosis in wild-type (+/+:Cre) and NuMA-disrupted (flox/flox:Cre) immortalized embryo fibroblasts

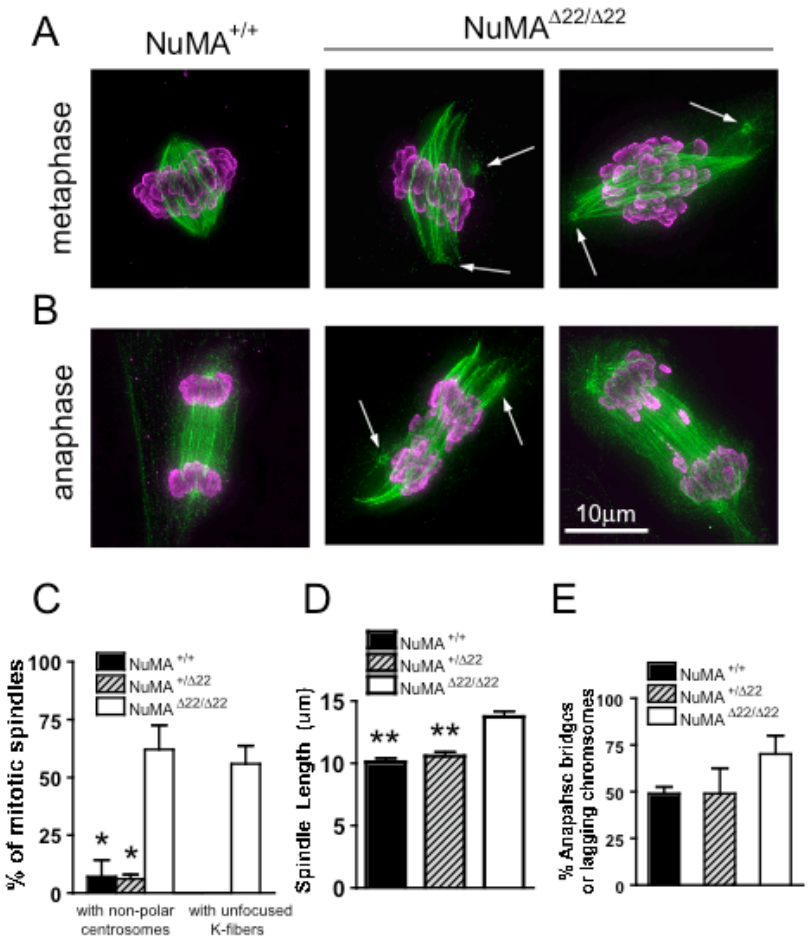

Figure 3.6 Spindle defects result from homozygous NuMA disruption

Primary fibroblasts were processed for immunofluorescence on experimental day 5 as shown in Figure 2A. (A) Metaphase in a control cell (NuMA$^{+/+}$) and spindles of two exon-22 deleted (NuMA$^{\Delta22/\Delta22}$) primary fibroblasts. (B) Anaphase in a wild-type and two NuMA$^{\Delta22/\Delta22}$ primary cells. Each image represents a maximum intensity projection of a deconvolved series of Z-sections spanning the entire cell in 0.2μm intervals. Arrows indicate centrosomes; tubulin, green; phosphorylated histone H3, purple. Scale bar = 10μm.

(C) Quantification of the frequencies of spindle-centrosome dissociation (non-polar centrosome) and pole splaying defects (unfocused K-fibers) seen in control and NuMA depleted cells. Cells were scored as phenotypic if at least one centrosome was non-polar, or at least one pole displayed an obvious lack of microtubule focusing. n=2 independent cell lines examined per genotype, >50 cells counted for NuMA$^{+/+}$, >130 cells counted for each of NuMA$^{+/\Delta22}$ and NuMA$^{\Delta22/\Delta22}$ fibroblasts. *, $p<0.01$, Bonferroni's Multiple Comparison Test, compared to NuMA$^{\Delta22/\Delta22}$.

(D) Spindle length in MG132 arrested primary fibroblasts, measured as the linear distance between spindle poles, or the approximate position of most spindle microtubule ends in defocused poles, n≥20 spindles per genotype. **, $p<0.001$, Bonferroni's Multiple Comparison Test, compared to NuMA$^{\Delta22/\Delta22}$.

(E) Frequencies of anaphase bridges and lagging chromosomes observed in cells stained to visualize mitotic chromatin using an antibody to phosphorylated histone H3. n>90 total anaphases pooled from 3 independent cell lines for each of NuMA$^{+/\Delta22}$ and NuMA$^{\Delta22/\Delta22}$ fibroblasts, n>30 anaphases for NuMA$^{+/+}$ cells.

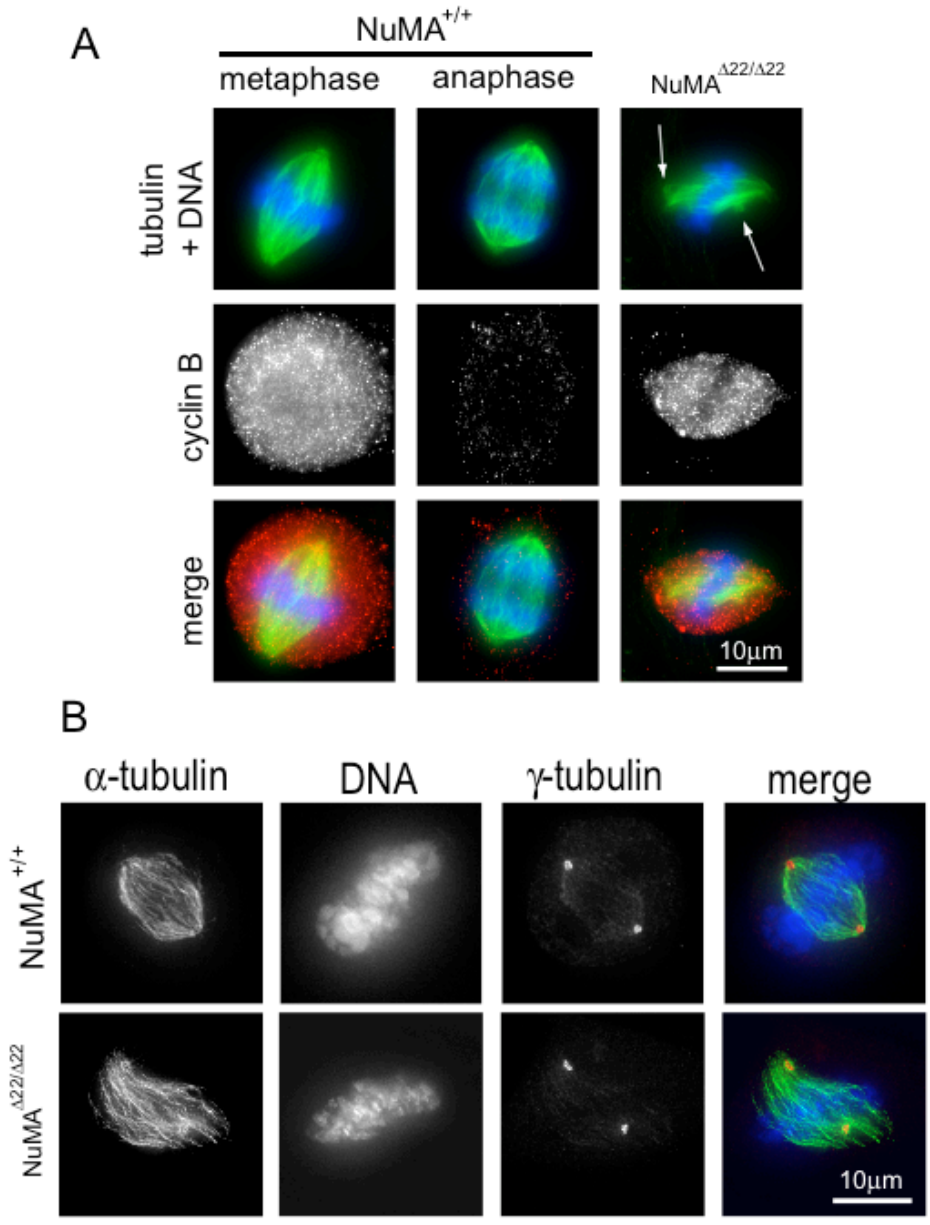

Figure 3.7 Spindle phenotypes in NuMA-deleted cells are apparent in metaphase

(A) Unperturbed primary fibroblasts stained for DNA (blue) and cyclin B1 (red) to identify metaphase cells, and tubulin (green) to mark spindles and centrosomes. Arrows indicate centrosomes, scale bar = 10 µm. Each image represents a maximum intensity projection of a series of Z-sections spanning the entire cell in 0.2 µm intervals.

(B) Primary fibroblasts arrested in metaphase with aligned chromosomes using MG132. In merged image, DNA, blue; α-tubulin, green; γ-tubulin, red. Scale bar = 10 µm. Each image represents a maximum intensity projection of a denconvolved series of Z-sections spanning the entire cell in 0.2 µm intervals.

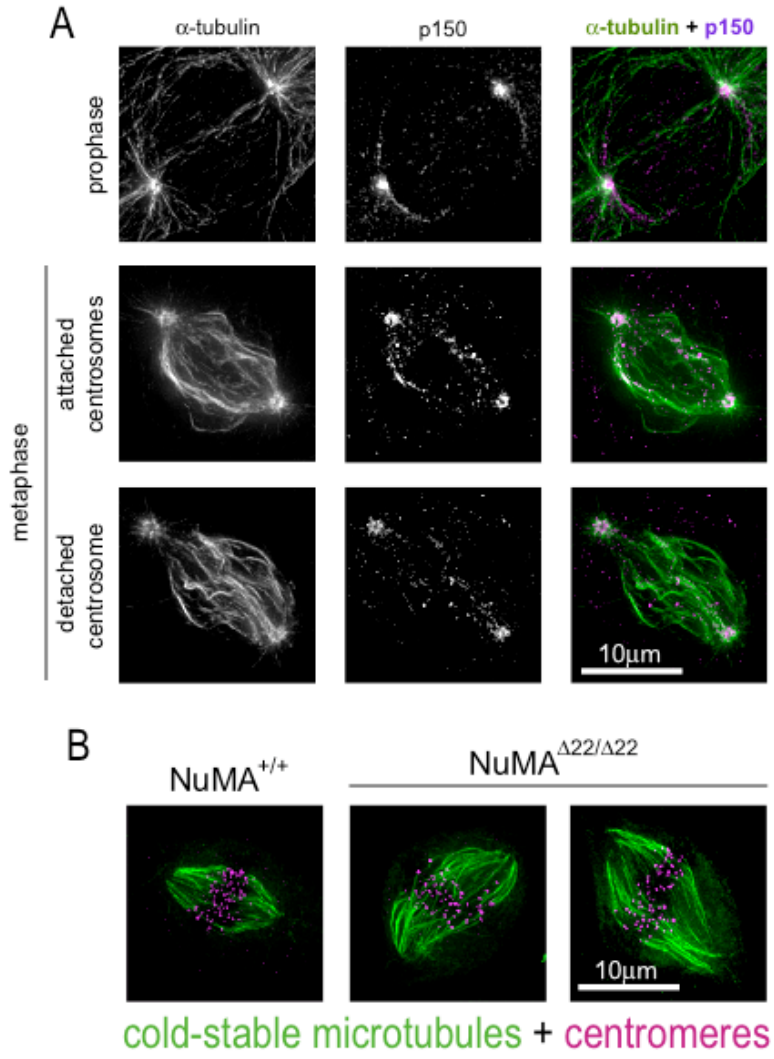

Figure 3.8 Normal dynein localization and K-fiber stability in aberrant spindles following NuMA disruption

(A) Examples of dynein localization in primary fibroblasts in prophase, a normal metaphase, and a metaphase figure with defocused poles and a centrosome clearly detached from the body of the spindle. In merged image, p150, purple; α-tubulin, green. Scale bar = 10 µm.

(B) Kinetochore-fibers in wild-type and NuMA$^{\Delta 22/\Delta 22}$ cells, selectively visualized by depolymerization of unstable microtubules with a 10 minutes incubation at 0°C prior to fixation. Centromeres marked with human ACA autoimmune antiserum, purple; α-tubulin, green. Scale bar = 10 µm.

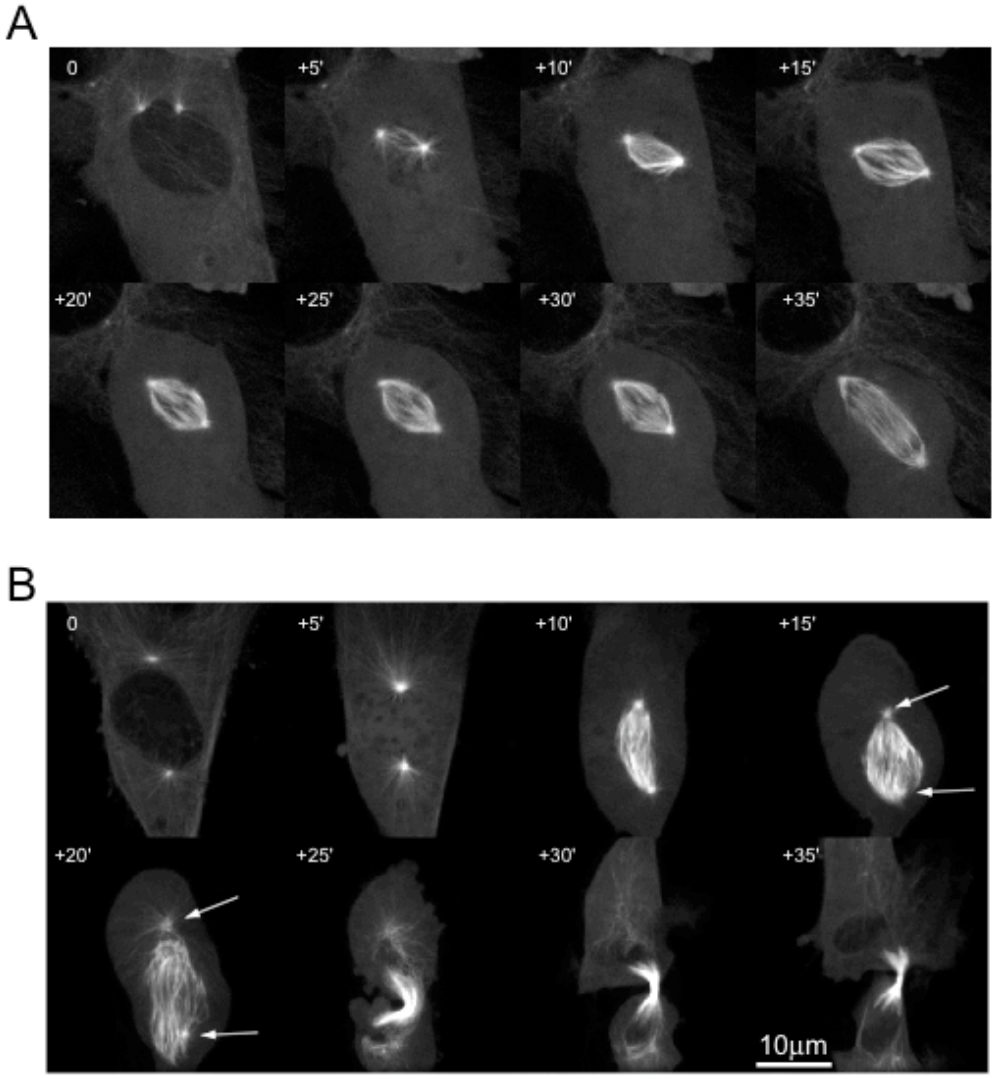

Figure 3.9 Bipolar spindle formation precedes centrosome detachment in the absence of NuMA

Selected images from movies of primary embryo fibroblasts transduced with retrovirus encoding tubulin-YFP, either (A) wild-type or (B) homozygous for NuMA$^{\Delta 22}$, undergoing mitosis following 4-OHT treatment and release from growth arrest. Arrows indicate centrosomes, each time point shows a maximum intensity projection of 5 confocal fluorescence Z-sections acquired in 2 µm intervals. Scale bar = 10 µm.

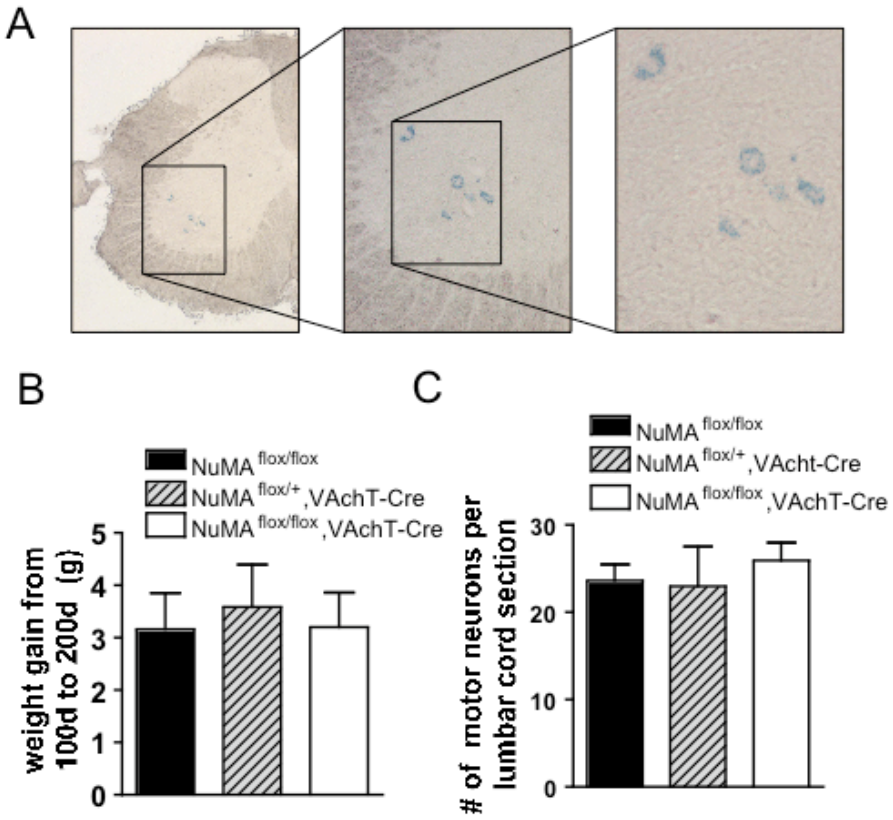

Figure 3.10 Normal cellular function and viability following *in vivo* motor neuron specific NuMA exon22 deletion

(A) X-gal staining of a spinal cord section, shown at increasing magnification, from mice expressing the VAchT-Cre transgene and carrying the ROSA26R B-gal reporter for Cre expression.

(B) Weight gain between 100 and 200 days of age in animals deleted of NuMA exon 22 in motor neurons, and littermate controls. n≥7 animals per genotype.

(C) Quantification of motor neuron numbers per 30 µm thick lumbar spinal cord section from 200-day-old animals deleted of NuMA exon 22 in motor neurons, and littermate controls. n=3 animals per genotype, 15-22 spinal cord sections per animal, sections spaced approximately 350 µm apart and taken through the entire lumbar cord.

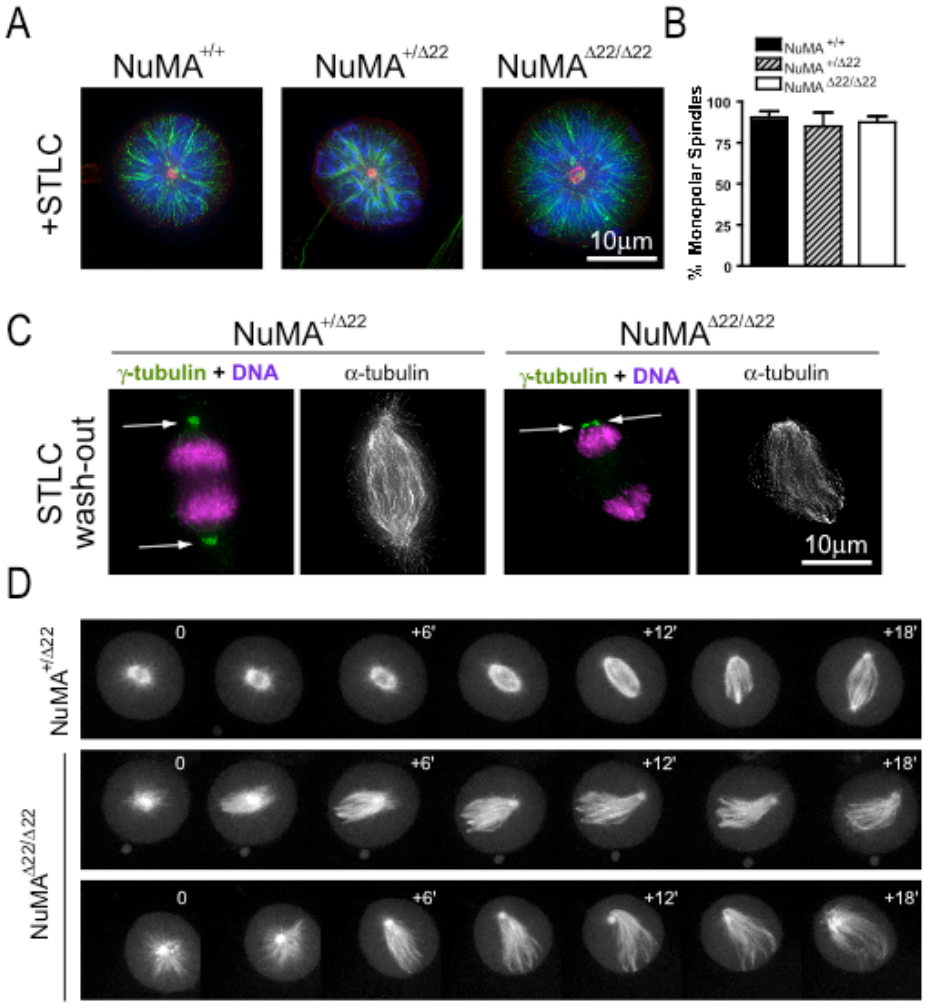

Figure 3.11 Prometaphase centrosome separation and centrosome independent spindle-pole focusing require NuMA

Primary MEFs were arrested in mitosis by treatment with 5 μm STLC for >3h and (A) processed for immunofluorescence. α-tubulin, green; DNA, blue; γ-tubulin, red. Scale bar = 10μm. (B) Frequencies of monopolar spindles shown in (A). n=2 independent cell lines per genotype, >200 mitoses per genotype counted.

(C) Anaphases in heterozygous control and NuMA-disrupted cells 1 hour following wash out of STLC. In merged images, DNA, purple; γ-tubulin, green. Scale bar = 10 μm.

(D) Stills from movies of primary embryo fibroblasts transduced with retrovirus encoding tubulin-YFP, undergoing mitosis following wash out of STLC after a 3-4 hour arrest. Each time point shows a maximum intensity projection of 12 confocal fluorescence Z-sections acquired in 1 μm intervals.

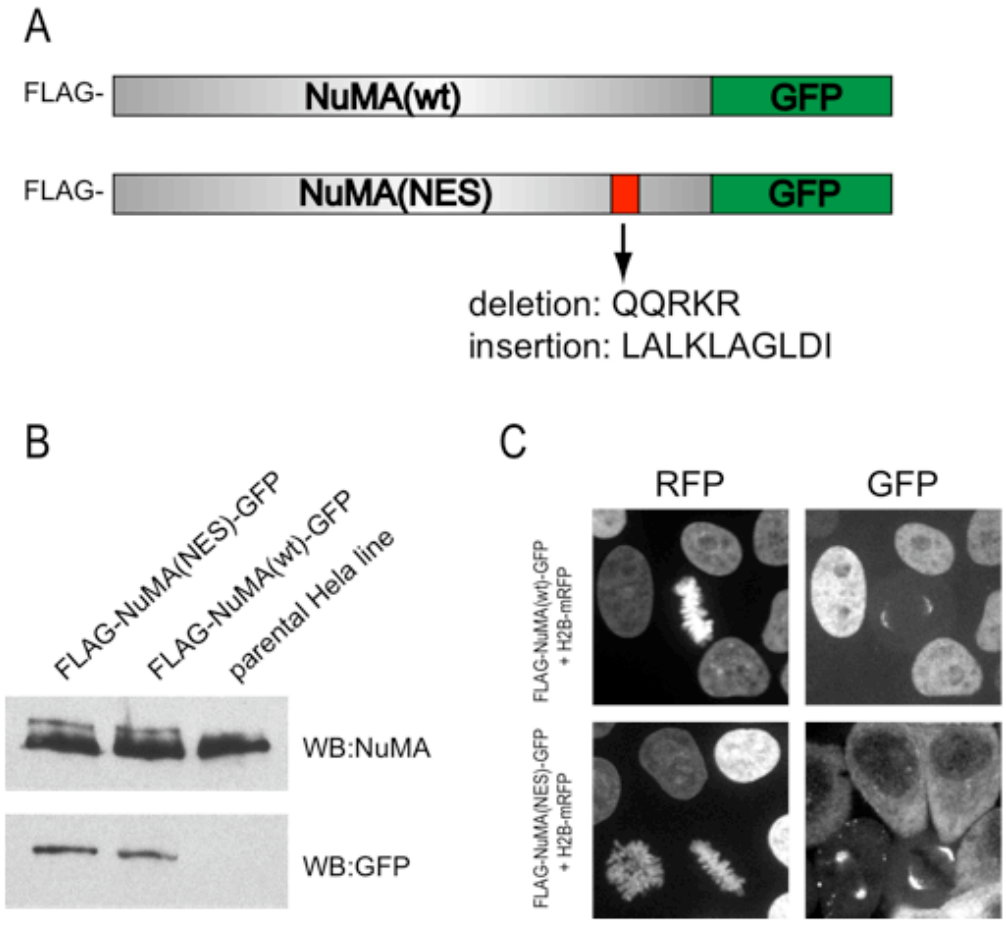

Figure 3.12 Creation and characterization of wild-type and cytoplasmic NuMA-GFP expressing stable HeLa cell lines

(A) Full length wild-type human NuMA cDNA was tagged at the N-terminus with the FLAG epitope and at the C-terminus with GFP. A cytoplasmically-localized variant "NuMA(NES)" was generated by replacement of five amino acids implicated in nuclear localization with a characterized ten residue nuclear export sequence.

(B) Immunoblot of parental HeLa cells and clonal lines stably expressing GFP-tagged wild-type or NuMA(NES) . Lysates were probed with antibodies to NuMA and GFP.

(C) Fluorescence images of wild-type NuMA-GFP and NuMA(NES)-GFP cell lines after transduction with a retrovirus to confer expression of mRFP tagged histone H2B. Images are maximum intensity projection of five confocal Z-sections spaced 2 µm apart.

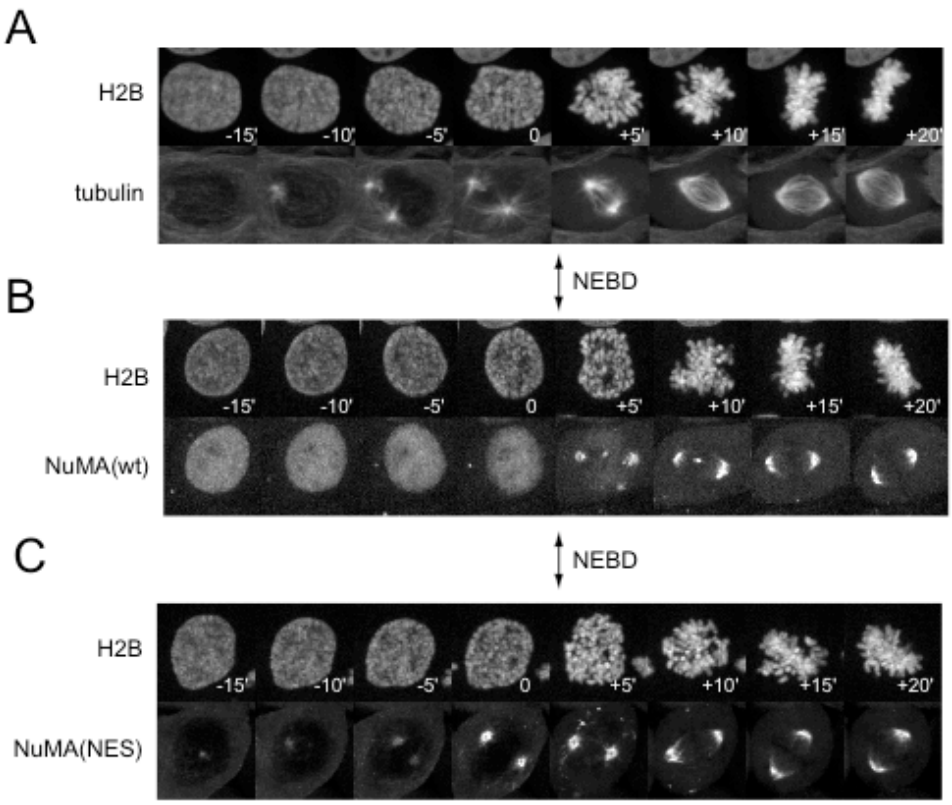

Figure 3.13 Kinetochore-fiber independent localization of NuMA to centrosomes

Still images from movies of HeLa cells expressing H2B-mRFP and also (A) tubulin-YFP, or (B) wild-type NuMA-GFP, or (C) cytoplasmic NuMA(NES)-GFP. Movies were time-aligned by chromosome morphology and degree of chromatin condensation, and NEBD identified by loss of nuclear GFP signal in the wild-type NuMA-GFP movie (B). Images are maximum intensity projection of five confocal Z-sections spaced 2 µm apart.

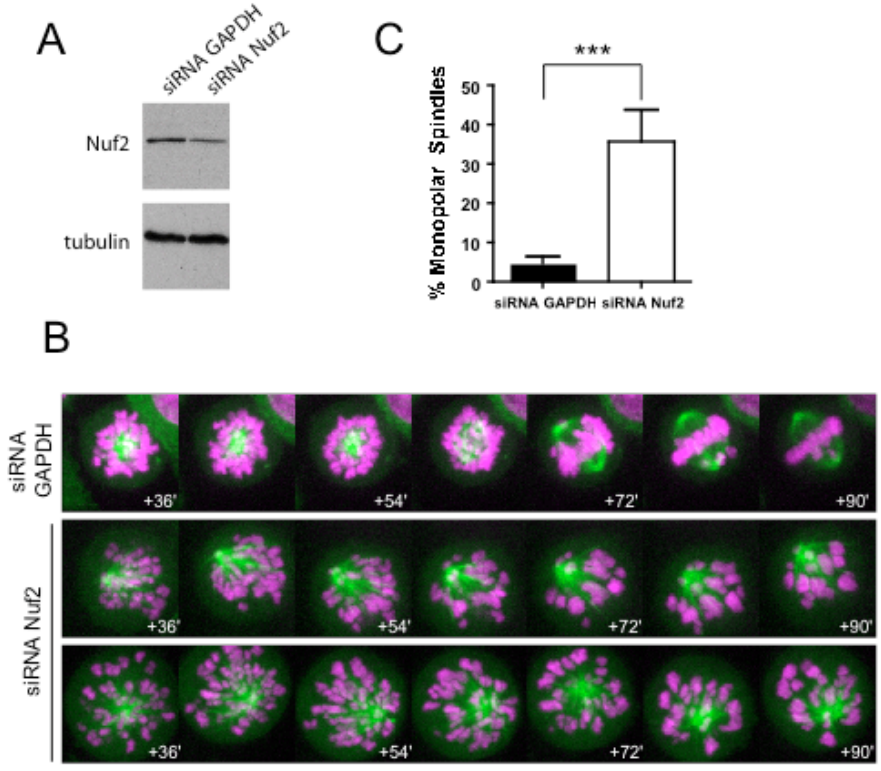

Figure 3.14 Kinetochore-microtubule attachments are required for centrosome separation in prometaphase

(A) Immunoblot of HeLa cells 48 hours after transfection with siRNA oligos against GAPDH or Nuf2, with antibodies to Nuf2 and tubulin.

(B) Still images from movies of HeLa cells expressing H2B-mRFP and also tubulin-YFP, transfected with siRNA oligos against GAPDH or Nuf2, after release from STLC arrest. Time is given in minutes relative to STLC wash-out. Images are maximum intensity projections of five confocal Z-sections spaced 2 µm apart. Green, tubulin; purple, histone H2B.

(C) Quantification of the frequency of spindles which remained monopolar 90 minutes after release from STLC, in cells treated with siRNA to GAPDH or Nuf2. Bars represent the mean and SEM of 3 separate experiments, n=192 cells GAPDH siRNA; n=228 cells Nuf2 siRNA; *** = p<.0001, Fisher's exact test.

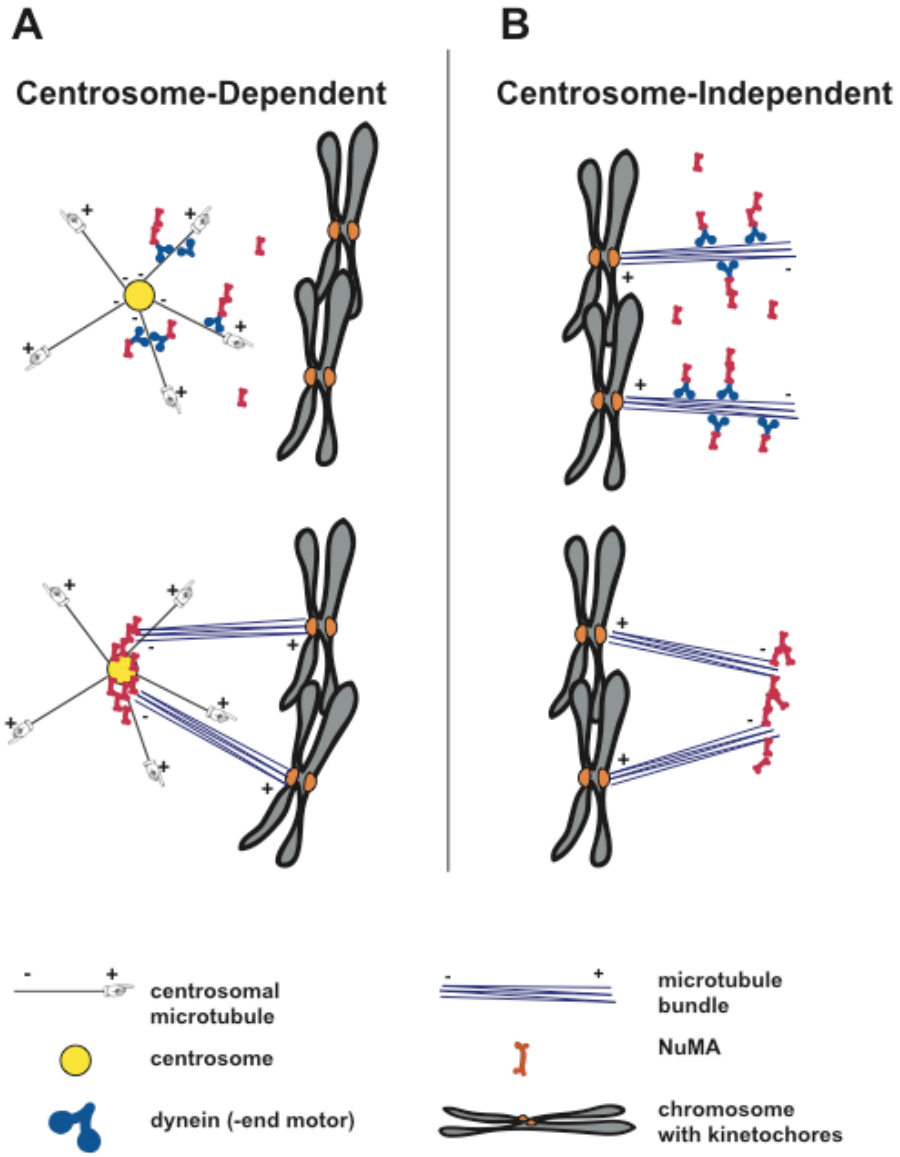

Figure 3.15 Functions of NuMA in centrosome-dependent and –independent spindle pole focusing

(A) In centrosome-dependent spindle pole formation, NuMA is transported to microtubule minus ends along centrosomal microtubules by dynein. Kinetochore-microtubule bundles that reach the pole are tethered there throughout mitosis by NuMA.

(B) Formation of spindle poles in the absence of centrosomes is likely to rely on minus-end directed transport of NuMA on kinetochore fibers, followed by self-assembly of NuMA oligomers (Harborth et al., 1999) into a polymerized matrix.

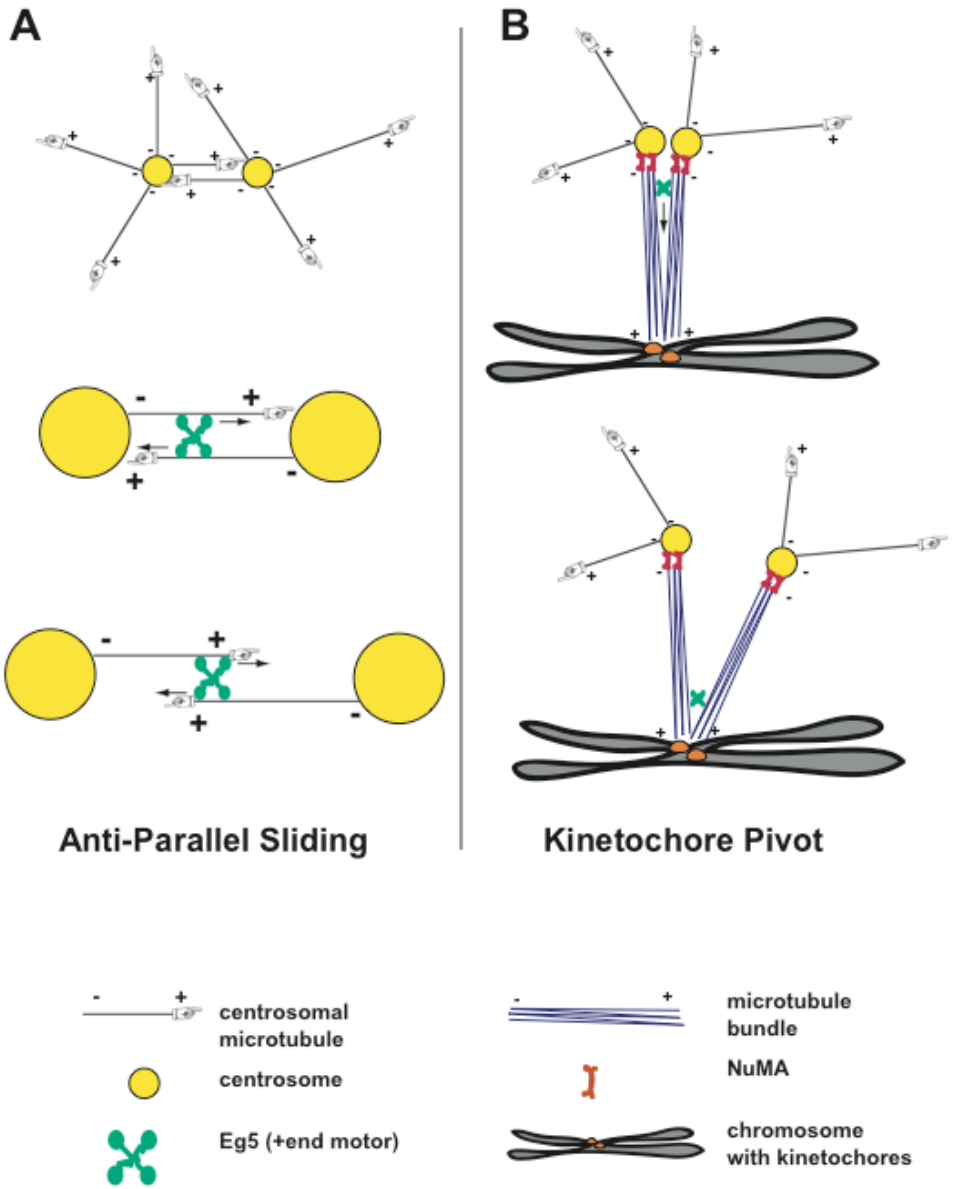

Figure 3.16 Two models for Eg5 mediated centrosome separation
(A) Plus-end directed movement by an Eg5 homotetramer which cross-bridges antiparallel centrosomal microtubules serves to slide microtubules apart, and thereby separate centrosomes
(B) In the "kinetochore pivot" model, Eg5 moves along parallel microtubule bundles from closely spaced centrosomes towards the two kinetochores of a single chromosome, and acts as a wedge, forcing kinetochore fibers, and thereby centrosomes apart. This relies on connections between microtubule bundles and centrosomes, by NuMA, and kinetochores, by components such as Nuf2.

Table 3.1 Genotype Incidence and Frequencies of Pups and Embryos from NuMA$^{Neo/+}$, NuMA$^{flox/+}$, and NuMA$^{\Delta 22/+}$ Heterozygous Crosses

Parental Genotypes[a]		Progeny Genotypes[a]						
		+ / +	Neo / +	Neo / Neo	flox / +	flox / flox	Δ22 / +	Δ22 / Δ22
Neo/+ X Neo/+	pups[b]	23 (26%)	65 (74%)	0				
	embryos[c]	21 (42%)	29 (58%)	0				
flox/+ X flox/+	pups	34 (31%)			53 (47%)	25 (22%)		
Δ22/+ X Δ22/+	pups	14 (33%)					28 (67%)	0
	embryos	7 (32%)					15 (68%)	0

[a] NuMA alleles are abbreviated as follows: "Neo"= NuMA^{Neo}, "flox"= NuMA^{flox}, "Δ22"= NuMA$^{\Delta 22}$, and "+" represents the wild-type NuMA allele
[b] mouse pups were genotyped at post-natal day 21
[c] embryos were collected between embryonic days 9.5 and 14.5

Chapter 3, in part, is in preparation for publication of the material as it may appear in *The Journal of Cell Biology*, 2008, Silk AD, Holland AJ, and Cleveland DW. The dissertation author was the primary researcher and author of this paper.

Chapter 4: Conclusions and Future Directions

4.1 Consequences of aneuploidy

Making use of animals that experience increased rates of single chromosome missegregation events due to reduced levels of the mitotic motor and checkpoint protein CENP-E, I (along with Dr. Beth Weaver) have demonstrated that whole-chromosome aneuploidy serves either to drive or inhibit tumorigenesis in a context dependent manner. The three principal outcomes of this work are: 1) a direct test of the 100 year old hypothesis that aneuploidy, a salient characteristic of solid tumors, drives tumorigenesis; 2) the first demonstration that increased levels of aneuploidy can mediate suppression of tumorigenesis, initiated either chemically by a known carcinogen or genetically by loss of a tumor suppressor; and 3) the surprising finding that aneuploidy is a common and well-tolerated feature of many cell types in normal adult animals. These discoveries have important implications for understanding human tumors and the evolution of the molecular mechanisms that act during mitosis to preserve the diploid state.

4.1.1 How does aneuploidy drive tumorigenesis?

While it has been widely assumed, given the prevalence of aneuploid figures in a wide variety of human cancers, that altered whole chromosome number contributes to tumorigenesis, only now with this work has an

unambiguous test been applied to demonstrate that this is indeed the case. However, our data also make it clear that simply altering the fidelity of chromosome segregation alone is a relatively weak stimulus for tumorigenesis. Aneuploid mice do not suffer from fatal or debilitating early-onset tumors, as do animals lacking key tumor suppressors, such as mice deleted of p53 (Jacks et al., 1994). This is almost certainly a consequence of how alterations in chromosome number affect the complex development of cancer. The easiest way to imagine a direct contribution of aneuploidy to a single-step in the process of tumor formation is that mitotic chromosome missegregation could serve to drive loss heterozygosity of a tumor suppressor. I have initiated a direct test of this mechanism, by introducing CENP-E heterozygosity into animals that are also heterozygous for a loss of function mutation in p53. Heterozygosity for p53 results in the development of tumors after long latencies, and all of these tumors have inactivated the remaining p53 allele (Jacks et al., 1994). I expect that increased rates of aneuploidy will result in a more rapid transition to homozygous p53 loss, and decrease the tumor free lifespan of CENP-$E^{+/-}$ $p53^{+/-}$ compound heterozygotes relative to control littermates. A more indirect effect of aneuploidy on tumor formation might also derive from gene dosage effects that arise as a consequence of simultaneously duplicating or halving the copy number of thousands of genes through a single mitotic error. This might subtly affect aspects of cell cycle progression, apoptotic signaling, or pathways of DNA replication and repair

and thereby render cells either more resistant to tumor-prevention checkpoints or contribute to the generation of additional, potentially tumorigenic mutations.

4.1.2 Aneuploidy therapy for cancer

The contribution to tumorigenesis by aneuploidy-based mutation, whether direct or indirect, serves as a reminder that in order to become cancerous, tumor cells must mutate. Tumor suppression by aneuploidy, one of the most surprising findings described here, highlights the paradox faced by most tumor cells: mutation is necessary but can also be deleterious. Most types of cancers are genomically unstable, whether because of increased frequencies of point-mutation, microsatellite instability, chromosome rearrangement, whole chromosome number alteration, or combinations of any of these possibilities and more (Sieber et al., 2003). Evolution of tumors through constant mutation selects for cells that have the greatest proliferative capacity, but it also produces genetic changes that can be growth inhibitory. Genomic instability in cancer is therefore a double-edged sword that must be well balanced in order to provide sufficient diversity to produce the cancer genotype while not interfering with its relatively stable propagation. By decreasing the fidelity of chromosome segregation, heterozygosity for CENP-E may exert a unique suppressive effect on tumorigenesis by introducing a significant chance of losing oncogenic mutations. Other forms of genomic instability do not so easily provide this destabilizing mutagenic potential. For example, the likelihood of reverting or inactivating a mutant oncogene or

eliminating gene amplification by point-mutation is very, very small (nearly non-existent) relative to the potential to lose, during mitosis, the chromosome carrying these changes. This may explain why, relative to other pathways of genomic instability, so few mutations in mitotic checkpoint genes have been identified in human cancers (Weaver and Cleveland, 2006). In collaboration with Dr. Beth Weaver, I have recently been exploring the exciting possibility of harnessing aneuploidy as an anti-tumor strategy, so called “aneuploidy therapy” for cancer, using genetic and xenograft tumor models in mice.

4.1.3 The myth of normal diploidy

At first glance, it may seem that the demonstration of chromosome segregation errors driving tumorigenesis conflicts with the therapeutic potential of aneuploidy. However, the additional finding that a relatively high level of aneuploidy is a common situation for a variety of cell types in normal adult animals indicates that the condition of a non-diploid karyotype is surprisingly well tolerated. Further, in CENP-E heterozygous animals, which experience even greater levels of multi-tissue aneuploidy than wild-type mice, organ development and function, animal growth, fertility, and life span are relatively unimpaired. This complements the observations that there are no gross phenotypic consequences of aneuploidy caused by reduced levels of Mad2 or Bub3 (Baker et al., 2006; Michel et al., 2001) and reinforces the pioneering results of Chun and colleagues demonstrating that normal mice contain significant levels of single chromosomal aneuploidy both in developing and

adult neurons (Kaushal et al., 2003; McConnell et al., 2004; Rehen et al., 2001; Yang et al., 2003) and that these aneuploid neurons are functional (Kingsbury et al., 2005). Further, homozygous deletion of CENP-E from the adult liver produces disastrous failure of chromosome segregation but has no effect on the rate of liver regeneration or any measurable aspect of liver function (Putkey et al., 2002). All of this challenges the assumption of a requirement for strict diploidy in adult mammals.

During early development, however, tight control over chromosome segregation is absolutely essential – homozygous deletions of mitotic checkpoint genes in mice are not viable (Dobles et al., 2000; Putkey et al., 2002). It may be that signaling gradients crucial for proper development are highly sensitive to gene dosage effects. A threshold level of mitotic errors is permitted but cannot be surpassed. This suggests that differing cell types have varying mitotic checkpoint strengths, and during embryonic divisions where maintenance of diploidy seems to be most essential, the most stringent checkpoints may exist. Indeed, mouse embryonic stem cells maintain diploidy in culture over multiple passages to a far greater degree than primary fibroblasts, which experience rapid divergence from the 2n state under similar growth conditions. In summary, the existence and tolerance of aneuploidy in adult cells and tissues but not in embryonic development or stem cells suggests that the mammalian mitotic checkpoint may have evolved to protect primarily against chromosome gain or loss in early developmental and stem

cell divisions, and be more relaxed in differentiated cell types. It will be interesting to determine whether a high-stringency mitotic checkpoint contributes as a feature of stem cell identity.

4.2 Mitotic spindle architecture

The mammalian spindle is an incredibly complex force-producing biological machine, upon which cells are dependent in order to segregate chromosomes during mitosis. The spindle is composed of a variety of motor and non-motor proteins, and by creating and studying a selectively disruptable allele of the coiled-coil spindle-pole protein NuMA, I have provided key insights into multiple aspects of spindle assembly and function, including: 1) an understanding of the role of centrosomes in the establishment of spindle poles and the identification of NuMA as a key component of a back-up pathway for generating focused poles in the absence of centrosomes; 2) discovery of a mechanism of prometaphase centrosome separation that has implications for cancer therapy; and 3) the demonstration that anaphase chromosome segregation does not require microtubule anchoring at spindle poles, which has implications for deciphering spindle forces and adds to the long-standing debate about the existence of a putative “spindle matrix”.

4.2.1 The relationship between centrosomes and spindle poles

The focused hubs of microtubule minus-ends found at the terminal vertices of the spindle during mitosis are commonly defined as the spindle

poles. During a normal mitosis, in each spindle half, the pole and centrosome are always superimposed, and this makes differentiating one from the other effectively impossible. This has led to the misconception that in somatic cells, the centrosomes are equivalent to the poles of the spindle. It is clear however, that microtubules can become focused after centrosome ablation in cells that would otherwise be thought to rely on centrosomes for pole formation (Khodjakov et al., 2000). This indicates that centrosomes are not synonymous with spindle poles, but if not centrosomes, then what are the critical components of the spindle pole? My work shows that a defining feature of mammalian spindle poles is NuMA, and that while centrosomes serve to mark the future location of spindle poles by acting as a destination for dynein dependent transport of NuMA in early mitosis, it is ultimately NuMA that is responsible for maintaining the focused nature of the pole. Additionally, I have demonstrated that a spindle pole forming in the absence of a centrosome requires NuMA to become effectively focused. This indicates that NuMA is required differentially for the establishment (when there are no centrosomes) and maintenance (when pole focusing is initiated by centrosomes) of spindle poles in the mammalian mitotic spindle. To extend these findings, I have established a collaboration with the laboratory of Dr. Marie-Hélène Verlhac at the Université Pierre et Marie Curie in Paris, to study the function of NuMA in a physiologically acentrosomal system, the mouse oocyte. These studies have the potential to yield fundamental insights into the mechanisms of

acentrosomal spindle pole focusing and the regulation of meiotic spindle formation and function.

4.2.2 Separation of centrosomes in prometaphase

In mitotic prophase, prior to nuclear envelope breakdown, two duplicated centrosomes can crawl across the nuclear envelope in a dynein-dependent manner to diametrically oppose each other in anticipation of bipolar spindle formation (Gonczy et al., 1999). Maintenance of centrosome separation following nuclear envelope breakdown requires the plus end directed motor Eg5, and centrosomes collapse together when its activity is inhibited, triggering an extended mitotic delay (Skoufias et al., 2006). Small molecule inhibition of Eg5 activity is a major focus of anti-mitotic chemotherapy (Weaver and Cleveland, 2005). Reestablishment of centrosome separation and spindle bipolarity following release from Eg5 inhibition occurs without the advantage of a nuclear envelope, and therefore must rely on a mechanism at least partially distinct from the one that acts during prophase. I, along with Dr. Andrew Holland, have demonstrated that restoration of Eg5 activity during prophase is not sufficient to allow escape from a monopolar state. More importantly, the efficient recovery of normal spindle structure is dependent on microtubule linkage of kinetochores and centrosomes, which requires NuMA at spindle poles and the core microtubule attachment function of the Ndc80 complex at kinetochores. These discoveries may yield insight into the mechanisms of resistance to Eg5 inhibiting chemotherapeutics.

Further, it is clear that not all cells make equal use of dynein dependent prophase mechanisms to separate centrosomes during mitotic entry. This might represent an exploitable weakness in certain types of cancer for the development of prometaphase centrosome separation inhibitors. Further study of the reliance of normal and transformed cells on prophase vs. prometaphase mechanisms of centrosome separation may provide more evidence to drive the development of novel anti-tumor agents.

4.2.3 In support of a spindle "matrix"

Upon anaphase initiation, cohesion between chromatids is relieved and sister chromatids segregate in opposite directions towards spindle poles. Chromosome movement during segregation is powered by a number of activities that provide a poleward force, directed through kinetochore fibers to chromosomes. From this it follows that there must be an opposite force exerted on microtubules and spindle poles from chromosomes (Koshland et al., 1988). This anti-poleward pulling by kinetochores must be resisted so that chromosome movements are possible. Otherwise as Nicklas initially asked, why does the pole does not simply move towards the chromosomes (Nicklas, 1989). The simplest way to envision resistance of kinetochore-pulling forces is by anchoring kinetochore fibers to centrosomes at spindle poles and then attaching centrosomes with astral microtubules to the cell cortex. However, experimental removal of centrosomes, and therefore a connection between

the spindle and the cortex, does not prevent chromosome segregation (Khodjakov et al., 2000).

This begs the question: how are chromosome derived pulling forces on kinetochore fibers resisted to permit chromosome segregation? One prospect is the internal stabilization of the spindle by inter-polar microtubules that cross-bridge kinetochore fibers from the two spindle halves. Microtubule binding proteins might cross-link inter-polar microtubules and kinetochore fibers to provide this underlying framework (Gordon et al., 2001). It might be possible to model resistance to chromosome segregation forces using these stabilizing elements, although whether there are sufficient numbers of these spindle microtubules to allow for this effect is unknown. A second possibility for the resistance of spindle forces is the existence of a “spindle matrix”, an underlying network to which the spindle is linked. The idea of such a matrix has been debated for almost 40 years, and multiple protein and non-protein components proposed (Johansen and Johansen, 2007). Analysis of spindle matrix candidates in NuMA deficient mitoses, which lack cortical spindle-anchoring that may be redundant with such a matrix, may help to confirm the existence of this proposed structural network.

4.3 Functional organization of the mammalian nucleus

A remaining unanswered problem is the determination of the nuclear function of NuMA. The NuMA$^{\Delta 22}$ allele was specifically designed so as not to interfere with the nuclear function of NuMA, but creation of an early deletion

within the NuMA gene might serve to accomplish this goal. A myriad of possibilities for a nuclear role of NuMA exist, perhaps most likely is that of a nuclear structural protein, although much like the spindle matrix, the existence of a structural “nuclear matrix” that might contribute to nuclear organization is far from well accepted. Clearly, the identification of nuclear role for NuMA is not a trivial problem, especially given the complete lack of evidence for any one specific interphase function of NuMA and the diversity of molecular systems in the nucleus in which NuMA might participate. A promising direction is the use of global genome/transcriptome/proteome analysis. For example, microarrays to assess alterations in transcriptional regulation in cells lacking nuclear NuMA. This might even be possible using $NuMA^{\Delta 22/\Delta 22}$ cells, which have reduced accumulation of the mutant NuMA protein relative to wild-type cells, and this may be reflected in subtle changes in NuMA-dependent nuclear processes that could be detected by global transcriptional analysis. Evidence that supports using these types of approaches to understand NuMA function comes from the description of a putative interphase interaction of NuMA with components of the cohesin complex (Gregson et al., 2001), which is known to be involved in transcriptional insulation (Koch et al., 2008; Wendt et al., 2008). Preliminary ChIP-CHIP experiments are underway in collaboration with the laboratory of Bing Ren at the Ludwig Institute for Cancer Research to investigate the possibility of NuMA and cohesin co-localization at known

insulator binding sites on chromatin. Further work should provide clues towards unlocking the mystery of a nuclear function for NuMA.

Methods

NuMA targeting and in vivo recombination

A mouse 129S6/SvEvTac BAC genomic library (RPCI-22, CHORI) was screened for the NuMA gene with a probe to the largest single exon of NuMA. This probe was amplified by PCR from mouse tail DNA with primers ex14for (5'-CCAGTTGACCTCTATGACAGGGCTCAATGCCA-3') and ex14rev (5'-CCTTTCGCCCAGCCTTCTCTTGCTCTAACTCCTT-3') and cloned into pGEM (Promega). A single clone was identified and confirmed by PCR to contain the entire NuMA gene.

To generate the exon 22 targeting vector, a 8.9kb *EcoRV-ScaI* fragment containing exons 16 through 25 was subcloned from the NuMA containing BAC into the *EcoRV* site of pBluescript. A loxP site and 3' *SacII* and *AscI* restriction sites were introduced downstream of exon 21 by cloning an oligonucleotide linker into a *BstEII* site. The resulting construct was digested first with *AscI* and *XhoI* to yield a linearized 9.5kb fragment containing the long homology arm, and separately with *SacII* and re-ligated to produce a circular vector containing only the short homology arm. This circular plasmid was digested with *StuI*, and a blunt ended *FRT-PGKNeo-FRT-loxP* cassette from pK-11 (Meyers et al., 1998) was inserted into this site. A 4.2kb fragment comprised of the short homology arm and Neomycin cassette was liberated by *AscI-XhoI* digest and ligated with the previously generated 9.5kb long arm

vector. Finally, the DT negative selection marker (Yanagawa et al., 1999) was inserted into the *XhoI* site of the targeting construct, downstream of the short arm. The targeting vector was linearized with *NotI* before electroporation in to ES cells.

ES culture, electroporation and DNA preparation were carried out essentially as described (Putkey et al., 2002). DNA from G418 resistant ES clones was screened using PCR and Southern blot and clones carrying the appropriate genetic modification were injected into C57/Bl6 embryos by the UCSD transgenic mouse and gene targeting core facility. Pups from chimeric mice were screened by coat color and PCR to identify germline transmission. The Neomycin cassette was removed by *in vivo* recombination through breeding with FlpeR transgenic mice (Rodriguez et al., 2000) and germline removal of exon 22 was effected by breeding with Zp3Cre mice (Lewandoski et al., 1997).

DNA preparation and Genotyping

Mouse tail DNA was prepared by digestion in 10 mM Tris-HCl (pH 7.5), 100 mM NaCl, 10 mM EDTA, and 0.5% SDS with 0.4 μg/μl proteinase K (Roche) overnight at 55°C. DNA was extracted first with phenol:chloroform:isoamyl alcohol (25:24:1) and next with chloroform:isoamyl alcohol (24:1) and precipitated with 2 volumes of ethanol and 1/10 volume of 3 M sodium acetate (pH 5.2). DNA was resuspended in 10 mM Tris and 0.1 mM EDTA (pH 8.0). ES and fibroblast DNA was prepared identically except ES

cells were collected and lysed directly in the tail digestion buffer, with no overnight proteinase K step.

DNA Blotting and PCR Genotyping

For DNA blotting, ES cell DNA was digested with either *EcoRI* alone, or *EcoRI* + *SacII*, run for 24h at 40V at 4°C in TAE buffer on a 0.8% agarose gel, and transferred to Hybond N+ membranes (Amersham) using standard methods. Membranes were hybridized with 32P-dATP-labeled DNA fragments and exposed to X-ray film. The probe for targeting of exon22 was amplified from R1 ES cell DNA using primers pr13for (5'-TTTGGTGGTGGTTTGGTC-3') and pr13rev (5'-TGATAAGCAATGCCACGG-3') and cloned into pGEM. ES cells were genotyped for exon 11 targeting by PCR with 0.2 μM each of primers 11.5 (5′-TCAGCCATTGAATCTGTAGGC-3′) and NeoB (5′-GCTGCTAAAGCGCATGCTCC-3′). ES cells were genotyped for exon 22 targeting by PCR with 0.2 μM each of primers Neo1 (5′-ATGCTCCAGACTGCCTTGGG-3′) and 22.3 (5′-GGAGGTCATTCTACTGGAAG-3′). Mice, embryos and cells were genotyped for exon 22 targeted alleles by PCR with 0.2 μM each of primers ex22F.2 (5′-AACCGCATCGCAGAGTTGCAG-3′) ex24rev (5′-GAGGAGTGGTGGCAACAGTAG-3′), and NeoA (5′-ACTGCCTTGGGAAAAGCGCC-3′). Additional reaction components include

0.2 mM dATPs (Takara) and 0.5 units ExTaq polymerase (Takara) in 1X reaction buffer (Takara). Reaction conditions were: 95°C for 5 min, 35 cycles of 95°C for 30 s, 55°C for 30 s, 72°C for 2 min, and a final extension step at 72°C for 7 min. PCR products were resolved on 1.5% agarose gels in TAE.

Mouse Embryonic Fibroblast Preparation and Culture

MEFs were cultured in DMEM (Gibco) containing 15% fetal bovine serum (Omega Scientific), 100 mM glutamine (Gibco), 50 μg/ml penicillin/streptomycin (Gibco), 0.1mM non-essential amino acids (Gibco), 1mM sodium pyruvate (Gibco) and β-mercaptoethanol (ES cell 100x stock, Chemicon). Mouse embryonic fibroblasts were prepared as previously described (Putkey et al., 2002). Briefly, a pregnant female was sacrificed and the uterus containing embryos was removed. Embryos were carefully dissected away from the uterus and the amniotic sac, head, liver, and tail were removed, and the embryo was transferred to a dish containing 0.05% trypsin (Gibco) and minced into small pieces with fine scissors. Following 10 minutes at 37°C, the tissue fragments were dispersed by pipetting and additional trypsin was added to the embryo for an additional 10 minute incubation. The trypsin and digested embryo were then transferred to a conical tube containing MEF media. After allowing large tissue pieces to settle (2-3 min), the supernatant was transferred to a new tube and spun at 1000 rpm in a clinical centrifuge. The cell pellet was resuspended in 5 ml of media and plated into a 6 cm dish. Primary fibroblasts were maintained and passaged in an incubator

set at 10% CO_2, 37°C and maintained at 3% O_2 by a continuous flow of additional nitrogen gas, to increase replicative lifespan as described (Parrinello et al., 2003). For use in all experiments described, primary fibroblasts were grown for no more than 2 cumulative weeks in culture following derivation.

To induce growth arrest, MEFs were cultured to confluence and then shifted to media containing 2% serum. In fibroblasts carrying the Cre-ER^{TM} transgene (Hayashi and McMahon, 2002) 4-hydroxy-tamoxifen (Sigma, 10 mg/ml stock in ethanol) was added to a final concentration of 0.1μM (unless otherwise indicated) to cause nuclear translocation of Cre.

Xenograft tumors

Xenograft tumor formation experiments were performed by subcutaneous injection of 5 x 10^6 cells in PBS, into 4- to 5- week old nude mice. All experiments were performed in accordance with standards established by the Institutional Animal Care and Use Committee at UCSD.

Transfections and creation of stable NuMA-GFP cell lines

A Flag-tag (DYKDDDDK octapeptide) was inserted at the N-terminus of the full length NuMA cDNA (Compton et al., 1992), and the C-terminus was fused in-frame with a fluorescent LAP tag (Cheeseman and Desai, 2005). A nuclear localization deficient NuMA was generated by site-directed mutagenesis using a primer to replace the putative NLS with a characterized NES. These constructs were cloned into pCNDA6 (Invitrogen) to acquire a Blasticidin resistance marker. The resultant plasmids were linearized and

transfected into HeLa cells using the Effectene reagent (Qiagen) as per the manufacturer's directions. After 12 hours media were replaced, and 48 hours post-transfection, blasticidin-S was added at 5μg/ml. After two weeks of selection, cells were subjected to flow cytometry at the UCSD flow cytometry core facility, and single cells sorted into individual wells of a 96 well plate. Clones were expanded and screened for expression and localization of fluorescent NuMA fusion proteins.

Retrovirus preparation and infections

Retroviral plasmids (pBABE variants) were cotransfected into 293-GP cells, which harbor *gag* and *pol* genes from the Moloney murine leukemia retroviral genome, along with the VSV-G pseudotyping plasmid for the production of amphotropic retrovirus (Morgenstern and Land, 1990). Transient transfection of cDNAs was accomplished using of the Fugene reagent (Roche) according to the manufacturer's recommended protocol. For retroviral infection of immortalized cells, the resulting retroviral supernatant was mixed with 8 μg/ml hexadimethrine bromide (Polybrene) (Sigma-Aldrich) and incubated with cells for 48 hr. Media were replaced, and the cells were split for selection in 5 μg/ml blasticidin or 1μg/ml puromycin. Surviving cells were maintained as polyclonal populations. For retroviral infection of primary MEFs, cells grown in 12-well plates were washed with PBS and incubated for 15' in a humidified incubator with retroviral supernatant mixed with 8μg/ml Polybrene. Plates of cells with were then wrapped in parafilm and spun at 1100g for 30min at room

temperature, after which the supernatant was replaced with primary MEF media and cells returned to the incubator. This generally resulted in greater than 50% infection efficiency of primary mouse fibroblasts.

Preparation of RNA and cDNA

RNA was prepared from mouse fibroblasts using the RNeasy Mini kit (Qiagen) according to the supplied protocol, or alternately from cells and tissues using TRIZOL reagent (Invitrogen) according to the supplied protocol. Briefly, for TRIZOL preparation of RNA, adherent cells were washed in PBS, collected in TRIZOL and passed through a pipette tip several times to lyse. Five-minute room temperature incubation was followed by addition of 0.2 volumes chloroform and an additional 15-30 minute RT incubation. Aqueous and organic phases were separated by 15 minutes of centrifugation at 12000rpm, 4°C, and RNA was subsequently precipitated from the aqueous phase by addition of 0.5 volumes cold isopropanol. The RNA pellet was washed with 1 volume of 75% ethanol and resuspended in RNAse free water. cDNA was prepared using the SuperScript III First-Strand Synthesis kit (Invitrogen) according to the manufacturer's instructions.

Detection of Aberrant Splice Products

Splicing events were detected in NuMA$^{Neo/+}$ cells and tissues using cDNA as a template (prepared as described above) and by PCR amplification with primers pr4for (5'-GTTTCAGAGAACTCGCGGCAGG-3') and Neo31 (5'-GGATTCATCGACTGTGGCCGGCTGGGT-3'). As a control, the C-terminal

half of the NuMA cDNA was amplified, from the $NuMA^{+}$, allele using primers pr4for and ex24rev (5′-GAGGAGTGGTGGCAACAGTAG-3′). A “touchdown” reaction was run as follows: 95°C for 5 min, followed by 2 cycles of 95°C for 30 s, 70° for 30s and 72° for 150s. Two additional cycles were performed at each of the following annealing temperatures: 68°C, 66°C, 64°C and 62°C, followed by 30 cycles of 95°C for 30 s, 60° for 30s and 72° for 150s, with a final extension step of 72° for 7 min.

Quantitative PCR

RNA from cells and tissues prepared using TRIZOL was additionally treated with the RNAse-Free DNase set (Qiagen) in combination with the RNeasy Mini Kit (Qiagen). The loss of full length NuMA mRNA from $NuMA^{Neo/+}$ cells and tissues was measured with 0.4 μM each of the forward and reverse primers 22f.2 (5′-AACCGCATCGCAGAGTTGCAG-3′) and 23r.2(5′-TTACGTCCTTCATGCCGGTCC-3’), 1μl of cDNA transcribed in a 20μl reaction from 1ug total RNA, and the SybrGreen Supermix qPCR reagent (Bio-Rad). Cyclophilin A was amplified as a normalizer using 0.4μM each of the forward and reverse primers cycloAfor (5′-TTCACCTTCCCAAAGACCAC-3′) and cycloArev (5′-AGCACTGGAGAGAAAGGATT-3’). Reaction conditions were: 95°C for 3 min, followed by 40 cycles of 95°C for 10 s, and 55°C for 30s. Reaction efficiencies for NuMA and cyclophilin reactions were calculated from a 3 or 4-step 2-fold dilution series carried out independently for cultured cells

and each tissue type using wild-type cDNA, and determined to average between 97% (NuMA) and 107% (cyclophilin A). The degree of excision was calculated using the Comparative C_t method by normalizing the signal produced from a normally processed NuMA cDNA relative to the unexcised gene cyclophilin A, and comparing $NuMA^{Neo/+}$ and $NuMA^{+/+}$ samples

For measurements of Cre mediated NuMA deletion in fibroblasts, DNA was prepared using the DNeasy Blood and Tissue Kit (Qiagen). The loss of the conditional NuMA allele from genomic DNA was measured in a reaction using 0.4 μM each of the forward and reverse primers 22f.4 (5′-CTTGCTCTATACAGTTGGGCC-3′) and 22rev (5′-GGTGGGTCTCAGAGGAAACTCG-3’). The mouse γ-actin gene was amplified as a normalizer using 0.4μM each of the forward and reverse primers 6590 (5′-TGGATCAGCAAGCAGGAGTATG-3′) and 6591 (5′-CCTGCTCAGTCCATCTAGAAGCA-3’). Reactions were carried out using 40ng genomic DNA and the SybrGreen Supermix qPCR reagent (Bio-Rad). Cycling conditions were: 95°C for 3 min, followed by 40 cycles of 95°C for 10 s, and 60°C for 10s. Reaction efficiencies for NuMA and γ-actin reactions were calculated from three or four independent, 4-step, 5-fold dilution series of wild-type genomic DNA, and determined to average between 95% (γ-actin) and 102% (NuMA). The degree of excision was calculated using the Pfaffl method (Pfaffl, 2001) by normalizing the signal produced from an experimental sample to the unexcised gene, γ-actin, and comparing experimental samples to DNA

extracted from NuMA$^{+/+}$ MEFs. All qPCR reactions were run using the Bio-Rad iCycler (Bio-Rad).

Rotorod Testing

Mice were tested in an accelerating Roto-Rod (SDI, San Diego) assay at 100 and 200 days of age. All trials were carried out between 3pm and 6pm. Animals were placed on the rod and habituated for 30s before rotation was started. Animals were generally given 3 trials per test day, with 15-30 minutes between trials. During trials, mice were placed on the stationary horizontal rod, which increased in speed at a constant acceleration, from 0-50 rpm, over a 5-minute period. The time each animal spent on the rod before falling was recorded. Mice that hung on the rod and passively rotated were scored as falling once they rotated through 360°. Animals that remained on the rod once it had reached maximum velocity were given the maximum time score and returned to their cages. The apparatus was wiped thoroughly with 70% ethanol between trials.

Live Cell Microscopy

HeLa and MEF cells were seeded onto 35-mm glass-bottom dishes (MatTek) and incubated in CO2-independent medium (Gibco) supplemented as described above for immortalized or primary cells respectively. Dishes were placed in a heat-controlled stage set at 37°C. Time-lapse sequences were taken every 3 or 5 minutes. Fluorescence imaging was conducted using a spinning disk confocal (McBain Instruments) attached to a Nikon TE2000e

inverted microscope equipped with a 60x /1.4NA objective lens. Fluorescence excitation was controlled by Metamorph software (Molecular Devices). Z-series images (five images at 2 μm intervals, or 12 images at 1μm intervals) were acquired using a Hamamatsu Orca ER camera (Bridgewater) at 3- or 5-minute intervals. Z-stacks were compiled by maximum intensity projection for presentation.

Tumor and CNS Tissue Histology

For analysis of tumors in aged animals, mice were sacrificed by cervical dislocation following anesthetization with isofluorane (Sigma). Necropsies were performed, and tissues as well as tumors observed by gross inspection were fixed in 10% formalin overnight at room temperature and the stored at 4°C before being embedded in paraffin. Hematoxylin-and-eosin-stained, 5μm thick sections were prepared by the UCSD histology core facility and analyzed by Dr. Nissi Varki.

For indirect immunofluorescence analysis, animals were anaesthetized with Avertin (2-2-2 Tribromoethanol) (Sigma-Aldrich) and perfused with cold 4% formaldehyde in PBS. Spinal cords and brains were dissected and post-fixed, and then cryoprotected by immersion in a solution of 30% sucrose in PBS for 1-2 days at 4°C. Tissues were embedded in Tissue-Tek O.C.T (Sakura, Japan), frozen in -40°C isopentane and stored at -80°C. 30μm thick sections were cut on a Jung 2800 E cryostat (Leica, Germany), floated in PBS + .3% TX-100, and washed three times in the same buffer. Antibodies were

diluted in this buffer and staining was performed overnight at room temperature. Sections were mounted on Fisher Superfrost Plus slides (Fisher) in a solution of 0.2% gelatin in PBS, dried overnight, then covered with ProLong antifade reagent (Invitrogen) and glass coverslips.

For X-gal or Cresyl violet staining, tissues sections were prepared as described for immunofluorescence staining. Staining for B-gal expression was performed by overnight incubation in a solution of 1mg/ml X-gal, 5μm each potassium ferrocyanide and potassium ferricyanide, 2μm $MgCl_2$ and 0.02% NP-40. Staining with Cresyl violet was performed on sections that had been mounted on slides and dried overnight, by rinsing in water and staining for 30s in a solution of 4% Cresyl Violet and 0.3% acetic acid, followed by 1 minute of destaining in each of 70% ethanol (50ml + 15 drops acetic acid), 95% ethanol and 100% ethanol, completed by a 5 min incubation in Toluene before covering with Permount (Fisher) and a glass coverslip.

Antibodies and Fixation

Rabbit polyclonal antibodies used in these studies include: anti-*Xenopus* NuMA tail (1:250) (Merdes et al., 1996), anti-human NuMA tail (1:500) (Gaglio et al., 1995), anti-CENP-E HpX (Yao et al., 1997) (1:200), anti-lamin A/C (courtesy of L. Gerace, Scripps Research Institute, San Diego) (1:500) and anti-Mad2 (1:250).

Monoclonal antibodies used include: SMI-32 (Sternberger Monoclonals, Maryland) (1:1000), GTU88 (Sigma-Aldrich) (1:1000), DM1A (Abcam)

(1:1000), GNS1 (Santa Cruz) (1:100), $p150^{Glued}$ (BD Transduction Labs) (1:100), and 5F9 (Taylor et al., 2001) (1:500). These antibodies identify neurofilaments, γ-tubulin, α-tubulin, cyclin B1, dynein-complex component $p150^{Glued}$, and BubR1 respectively. Additionally, antibodies isolated from human auto-antiserum available as ACA (Antibodies Incorporated, Davis, CA) (1:100) were used to identify centromeres.

Cells were grown on hydrochloric acid washed, poly-L-lysine (Sigma) coated 18mm glass coverslips and fixed in either 1% (for NuMA staining of fibroblasts) or 4% formaldehyde (for most antibodies) in PBS for 10 minutes, or -20°C methanol for 10 minutes (γ-tubulin and cyclin B1 staining); and blocked in Triton Block (0.2M glycine, 2.5% FBS, 0.1% TX-100, in 1x PBX) overnight. Primary and secondary antibodies incubations were carried out in Triton Block for 30- to 60- minutes at room temperature or 37°C, and followed by two 5-minute washes in PBS + 0.1% TX-100. DNA was visualized by staining with 4',6-diamidino-2-phenylindole (DAPI). Coverslips were mounted in ProLong (Invitrogen) and dried overnight before imaging.

Images of fixed cells were acquired using a DeltaVision-modified inverted microscope (IX70; Olympus) and Softworx software (Applied Precision) and were deconvolved unless otherwise indicated.

References

Babu, J. R., Jeganathan, K. B., Baker, D. J., Wu, X., Kang-Decker, N., and van Deursen, J. M. (2003). Rae1 is an essential mitotic checkpoint regulator that cooperates with Bub3 to prevent chromosome missegregation. J Cell Biol *160*, 341-353.

Baek, K. H., Shin, H. J., Jeong, S. J., Park, J. W., McKeon, F., Lee, C. W., and Kim, C. M. (2005). Caspases-dependent cleavage of mitotic checkpoint proteins in response to microtubule inhibitor. Oncol Res *15*, 161-168.

Baker, D. J., Jeganathan, K. B., Cameron, J. D., Thompson, M., Juneja, S., Kopecka, A., Kumar, R., Jenkins, R. B., de Groen, P. C., Roche, P., and van Deursen, J. M. (2004). BubR1 insufficiency causes early onset of aging-associated phenotypes and infertility in mice. Nat Genet *36*, 744-749.

Baker, D. J., Jeganathan, K. B., Malureanu, L., Perez-Terzic, C., Terzic, A., and van Deursen, J. M. (2006). Early aging-associated phenotypes in Bub3/Rae1 haploinsufficient mice. J Cell Biol *172*, 529-540.

Becker, B. E., Romney, S. J., and Gard, D. L. (2003). XMAP215, XKCM1, NuMA, and cytoplasmic dynein are required for the assembly and organization of the transient microtubule array during the maturation of Xenopus oocytes. Dev Biol *261*, 488-505.

Boveri, T. (1902). Ueber mehrpolige Mitosen als Mittel zur Analyse des Zellkerns. Vehr d phys med Ges zu Wurzburg, NF *Bd. 35*.

Boveri, T. (1914). Zur Frage der Entstehung maligner Tumoren. The origin of malignant tumors. Gustav Fischer, Jena.

Bowman, S. K., Neumuller, R. A., Novatchkova, M., Du, Q., and Knoblich, J. A. (2006). The Drosophila NuMA Homolog Mud regulates spindle orientation in asymmetric cell division. Dev Cell *10*, 731-742.

Brown, K. D., Coulson, R. M., Yen, T. J., and Cleveland, D. W. (1994). Cyclin-like accumulation and loss of the putative kinetochore motor CENP-E results from coupling continuous synthesis with specific degradation at the end of mitosis. J Cell Biol *125*, 1303-1312.

Burke, B., and Stewart, C. L. (2002). Life at the edge: the nuclear envelope and human disease. Nat Rev Mol Cell Biol *3*, 575-585.

Campbell, M. S., Chan, G. K., and Yen, T. J. (2001). Mitotic checkpoint proteins HsMAD1 and HsMAD2 are associated with nuclear pore complexes in interphase. J Cell Sci *114*, 953-963.

Chang, P., Jacobson, M. K., and Mitchison, T. J. (2004). Poly(ADP-ribose) is required for spindle assembly and structure. Nature *432*, 645-649.

Chang, W., Dynek, J. N., and Smith, S. (2005). NuMA is a major acceptor of poly(ADP-ribosyl)ation by tankyrase 1 in mitosis. Biochem J *391*, 177-184.

Cheeseman, I. M., and Desai, A. (2005). A combined approach for the localization and tandem affinity purification of protein complexes from metazoans. Sci STKE *2005*, pl1.

Chen, M., and Shen, X. (2007). Nuclear actin and actin-related proteins in chromatin dynamics. Curr Opin Cell Biol *19*, 326-330.

Compton, D. A. (1998). Focusing on spindle poles. J Cell Sci *111 (Pt 11)*, 1477-1481.

Compton, D. A., and Cleveland, D. W. (1993). NuMA is required for the proper completion of mitosis. J Cell Biol *120*, 947-957.

Compton, D. A., and Luo, C. (1995). Mutation of the predicted p34cdc2 phosphorylation sites in NuMA impair the assembly of the mitotic spindle and block mitosis. J Cell Sci *108 (Pt 2)*, 621-633.

Compton, D. A., Szilak, I., and Cleveland, D. W. (1992). Primary structure of NuMA, an intranuclear protein that defines a novel pathway for segregation of proteins at mitosis. J Cell Biol *116*, 1395-1408.

Compton, D. A., Yen, T. J., and Cleveland, D. W. (1991). Identification of novel centromere/kinetochore-associated proteins using monoclonal antibodies generated against human mitotic chromosome scaffolds. J Cell Biol *112*, 1083-1097.

Dai, W., Wang, Q., Liu, T., Swamy, M., Fang, Y., Xie, S., Mahmood, R., Yang, Y. M., Xu, M., and Rao, C. V. (2004). Slippage of mitotic arrest and enhanced tumor development in mice with BubR1 haploinsufficiency. Cancer Res *64*, 440-445.

Dasso, M. (2001). Running on Ran: nuclear transport and the mitotic spindle. Cell *104*, 321-324.

Dobles, M., Liberal, V., Scott, M. L., Benezra, R., and Sorger, P. K. (2000). Chromosome missegregation and apoptosis in mice lacking the mitotic checkpoint protein Mad2. Cell *101*, 635-645.

Du, Q., and Macara, I. G. (2004). Mammalian Pins is a conformational switch that links NuMA to heterotrimeric G proteins. Cell *119*, 503-516.

Elbashir, S. M., Harborth, J., Lendeckel, W., Yalcin, A., Weber, K., and Tuschl, T. (2001). Duplexes of 21-nucleotide RNAs mediate RNA interference in cultured mammalian cells. Nature *411*, 494-498.

Fang, Y., Liu, T., Wang, X., Yang, Y. M., Deng, H., Kunicki, J., Traganos, F., Darzynkiewicz, Z., Lu, L., and Dai, W. (2006). BubR1 is involved in regulation of DNA damage responses. Oncogene.

Ferhat, L., Cook, C., Kuriyama, R., and Baas, P. W. (1998). The nuclear/mitotic apparatus protein NuMA is a component of the somatodendritic microtubule arrays of the neuron. J Neurocytol *27*, 887-899.

Fisk Green, R., Lorson, M., Walhout, A. J., Vidal, M., and van den Heuvel, S. (2004). Identification of critical domains and putative partners for the Caenorhabditis elegans spindle component LIN-5. Mol Genet Genomics *271*, 532-544.

Fukasawa, K. (2005). Centrosome amplification, chromosome instability and cancer development. Cancer Lett *230*, 6-19.

Gaglio, T., Dionne, M. A., and Compton, D. A. (1997). Mitotic spindle poles are organized by structural and motor proteins in addition to centrosomes. J Cell Biol *138*, 1055-1066.

Gaglio, T., Saredi, A., and Compton, D. A. (1995). NuMA is required for the organization of microtubules into aster-like mitotic arrays. J Cell Biol *131*, 693-708.

Gasser, S. M. (2002). Visualizing chromatin dynamics in interphase nuclei. Science *296*, 1412-1416.

Gonczy, P., Pichler, S., Kirkham, M., and Hyman, A. A. (1999). Cytoplasmic dynein is required for distinct aspects of MTOC positioning, including centrosome separation, in the one cell stage Caenorhabditis elegans embryo. J Cell Biol *147*, 135-150.

Gordon, M. B., Howard, L., and Compton, D. A. (2001). Chromosome movement in mitosis requires microtubule anchorage at spindle poles. J Cell Biol *152*, 425-434.

Goshima, G., Nedelec, F., and Vale, R. D. (2005). Mechanisms for focusing mitotic spindle poles by minus end-directed motor proteins. J Cell Biol *171*, 229-240.

Gregson, H. C., Schmiesing, J. A., Kim, J. S., Kobayashi, T., Zhou, S., and Yokomori, K. (2001). A potential role for human cohesin in mitotic spindle aster assembly. J Biol Chem *276*, 47575-47582.

Hahn, W. C., Counter, C. M., Lundberg, A. S., Beijersbergen, R. L., Brooks, M. W., and Weinberg, R. A. (1999). Creation of human tumour cells with defined genetic elements. Nature *400*, 464-468.

Hanks, S., Coleman, K., Reid, S., Plaja, A., Firth, H., Fitzpatrick, D., Kidd, A., Mehes, K., Nash, R., Robin, N.*, et al.* (2004). Constitutional aneuploidy and cancer predisposition caused by biallelic mutations in BUB1B. Nat Genet *36*, 1159-1161.

Harborth, J., Elbashir, S. M., Bechert, K., Tuschl, T., and Weber, K. (2001). Identification of essential genes in cultured mammalian cells using small interfering RNAs. J Cell Sci *114*, 4557-4565.

Harborth, J., Wang, J., Gueth-Hallonet, C., Weber, K., and Osborn, M. (1999). Self assembly of NuMA: multiarm oligomers as structural units of a nuclear lattice. Embo J *18*, 1689-1700.

Harborth, J., Weber, K., and Osborn, M. (1995). Epitope mapping and direct visualization of the parallel, in-register arrangement of the double-stranded coiled-coil in the NuMA protein. Embo J *14*, 2447-2460.

Haren, L., and Merdes, A. (2002). Direct binding of NuMA to tubulin is mediated by a novel sequence motif in the tail domain that bundles and stabilizes microtubules. J Cell Sci *115*, 1815-1824.

Hayashi, S., and McMahon, A. P. (2002). Efficient recombination in diverse tissues by a tamoxifen-inducible form of Cre: a tool for temporally regulated gene activation/inactivation in the mouse. Dev Biol *244*, 305-318.

Heald, R., Tournebize, R., Blank, T., Sandaltzopoulos, R., Becker, P., Hyman, A., and Karsenti, E. (1996). Self-organization of microtubules into bipolar spindles around artificial chromosomes in Xenopus egg extracts. Nature *382*, 420-425.

Heald, R., Tournebize, R., Habermann, A., Karsenti, E., and Hyman, A. (1997). Spindle assembly in Xenopus egg extracts: respective roles of centrosomes and microtubule self-organization. J Cell Biol *138*, 615-628.

Heun, P., Laroche, T., Shimada, K., Furrer, P., and Gasser, S. M. (2001). Chromosome dynamics in the yeast interphase nucleus. Science *294*, 2181-2186.

Huang, X., Gollin, S. M., Raja, S., and Godfrey, T. E. (2002). High-resolution mapping of the 11q13 amplicon and identification of a gene, TAOS1, that is amplified and overexpressed in oral cancer cells. Proc Natl Acad Sci U S A *99*, 11369-11374.

Hutchison, C. J. (2002). Lamins: building blocks or regulators of gene expression? Nat Rev Mol Cell Biol *3*, 848-858.

Iouk, T., Kerscher, O., Scott, R. J., Basrai, M. A., and Wozniak, R. W. (2002). The yeast nuclear pore complex functionally interacts with components of the spindle assembly checkpoint. J Cell Biol *159*, 807-819.

Izumi, Y., Ohta, N., Hisata, K., Raabe, T., and Matsuzaki, F. (2006). Drosophila Pins-binding protein Mud regulates spindle-polarity coupling and centrosome organization. Nat Cell Biol *8*, 586-593.

Jacks, T., Remington, L., Williams, B. O., Schmitt, E. M., Halachmi, S., Bronson, R. T., and Weinberg, R. A. (1994). Tumor spectrum analysis in p53-mutant mice. Curr Biol *4*, 1-7.

Johansen, K. M., and Johansen, J. (2007). Cell and molecular biology of the spindle matrix. Int Rev Cytol *263*, 155-206.

Kalab, P., Pralle, A., Isacoff, E. Y., Heald, R., and Weis, K. (2006). Analysis of a RanGTP-regulated gradient in mitotic somatic cells. Nature *440*, 697-701.

Kalab, P., Weis, K., and Heald, R. (2002). Visualization of a Ran-GTP gradient in interphase and mitotic Xenopus egg extracts. Science *295*, 2452-2456.

Kalitsis, P., Fowler, K. J., Griffiths, B., Earle, E., Chow, C. W., Jamsen, K., and Choo, K. H. (2005). Increased chromosome instability but not cancer predisposition in haploinsufficient Bub3 mice. Genes Chromosomes Cancer.

Kallajoki, M., Weber, K., and Osborn, M. (1991). A 210 kDa nuclear matrix protein is a functional part of the mitotic spindle; a microinjection study using SPN monoclonal antibodies. Embo J *10*, 3351-3362.

Kapitein, L. C., Peterman, E. J., Kwok, B. H., Kim, J. H., Kapoor, T. M., and Schmidt, C. F. (2005). The bipolar mitotic kinesin Eg5 moves on both microtubules that it crosslinks. Nature *435*, 114-118.

Kapoor, T. M., Mayer, T. U., Coughlin, M. L., and Mitchison, T. J. (2000). Probing spindle assembly mechanisms with monastrol, a small molecule inhibitor of the mitotic kinesin, Eg5. J Cell Biol *150*, 975-988.

Karsenti, E. (2004). Cytoskeleton: spindle saga. Nature *432*, 563-564.

Kaushal, D., Contos, J. J., Treuner, K., Yang, A. H., Kingsbury, M. A., Rehen, S. K., McConnell, M. J., Okabe, M., Barlow, C., and Chun, J. (2003). Alteration of gene expression by chromosome loss in the postnatal mouse brain. J Neurosci *23*, 5599-5606.

Kempf, T., Bischoff, F. R., Kalies, I., and Ponstingl, H. (1994). Isolation of human NuMA protein. FEBS Lett *354*, 307-310.

Khodjakov, A., Cole, R. W., Oakley, B. R., and Rieder, C. L. (2000). Centrosome-independent mitotic spindle formation in vertebrates. Curr Biol *10*, 59-67.

Khodjakov, A., Copenagle, L., Gordon, M. B., Compton, D. A., and Kapoor, T. M. (2003). Minus-end capture of preformed kinetochore fibers contributes to spindle morphogenesis. J Cell Biol *160*, 671-683.

Kim, M., Murphy, K., Liu, F., Parker, S. E., Dowling, M. L., Baff, W., and Kao, G. D. (2005). Caspase-mediated specific cleavage of BubR1 is a determinant of mitotic progression. Mol Cell Biol *25*, 9232-9248.

Kingsbury, M. A., Friedman, B., McConnell, M. J., Rehen, S. K., Yang, A. H., Kaushal, D., and Chun, J. (2005). Aneuploid neurons are functionally active and integrated into brain circuitry. Proc Natl Acad Sci U S A *102*, 6143-6147.

Koch, B., Kueng, S., Ruckenbauer, C., Wendt, K. S., and Peters, J. M. (2008). The Suv39h-HP1 histone methylation pathway is dispensable for enrichment and protection of cohesin at centromeres in mammalian cells. Chromosoma *117*, 199-210.

Koshland, D. E., Mitchison, T. J., and Kirschner, M. W. (1988). Polewards chromosome movement driven by microtubule depolymerization in vitro. Nature *331*, 499-504.

Lechler, T., and Fuchs, E. (2005). Asymmetric cell divisions promote stratification and differentiation of mammalian skin. Nature *437*, 275-280.

Lein, E. S., Hawrylycz, M. J., Ao, N., Ayres, M., Bensinger, A., Bernard, A., Boe, A. F., Boguski, M. S., Brockway, K. S., Byrnes, E. J.*, et al.* (2007). Genome-wide atlas of gene expression in the adult mouse brain. Nature *445*, 168-176.

Lengauer, C., Kinzler, K. W., and Vogelstein, B. (1998). Genetic instabilities in human cancers. Nature *396*, 643-649.

Levesque, A. A., Howard, L., Gordon, M. B., and Compton, D. A. (2003). A functional relationship between NuMA and kid is involved in both spindle organization and chromosome alignment in vertebrate cells. Mol Biol Cell *14*, 3541-3552.

Lewandoski, M., Wassarman, K. M., and Martin, G. R. (1997). Zp3-cre, a transgenic mouse line for the activation or inactivation of loxP-flanked target genes specifically in the female germ line. Curr Biol *7*, 148-151.

Li, R., Sonik, A., Stindl, R., Rasnick, D., and Duesberg, P. (2000). Aneuploidy vs. gene mutation hypothesis of cancer: recent study claims mutation but is found to support aneuploidy. Proc Natl Acad Sci U S A *97*, 3236-3241.

Li, R., Yerganian, G., Duesberg, P., Kraemer, A., Willer, A., Rausch, C., and Hehlmann, R. (1997). Aneuploidy correlated 100% with chemical transformation of Chinese hamster cells. Proc Natl Acad Sci U S A *94*, 14506-14511.

Loncarek, J., Kisurina-Evgenieva, O., Vinogradova, T., Hergert, P., La Terra, S., Kapoor, T. M., and Khodjakov, A. (2007). The centromere geometry essential for keeping mitosis error free is controlled by spindle forces. Nature *450*, 745-749.

Lorson, M. A., Horvitz, H. R., and van den Heuvel, S. (2000). LIN-5 is a novel component of the spindle apparatus required for chromosome segregation and cleavage plane specification in Caenorhabditis elegans. J Cell Biol *148*, 73-86.

Lydersen, B. K., and Pettijohn, D. E. (1980). Human-specific nuclear protein that associates with the polar region of the mitotic apparatus: distribution in a human/hamster hybrid cell. Cell *22*, 489-499.

Maekawa, T., Leslie, R., and Kuriyama, R. (1991). Identification of a minus end-specific microtubule-associated protein located at the mitotic poles in cultured mammalian cells. Eur J Cell Biol *54*, 255-267.

Mahoney, N. M., Goshima, G., Douglass, A. D., and Vale, R. D. (2006). Making microtubules and mitotic spindles in cells without functional centrosomes. Curr Biol *16*, 564-569.

Maiato, H., Khodjakov, A., and Rieder, C. L. (2005). Drosophila CLASP is required for the incorporation of microtubule subunits into fluxing kinetochore fibres. Nat Cell Biol *7*, 42-47.

Maiato, H., Rieder, C. L., and Khodjakov, A. (2004). Kinetochore-driven formation of kinetochore fibers contributes to spindle assembly during animal mitosis. J Cell Biol *167*, 831-840.

Manning, A. L., and Compton, D. A. (2008). Structural and regulatory roles of nonmotor spindle proteins. Curr Opin Cell Biol *20*, 101-106.

Mao, Y., Abrieu, A., and Cleveland, D. W. (2003). Activating and silencing the mitotic checkpoint through CENP-E-dependent activation/inactivation of BubR1. Cell *114*, 87-98.

Mao, Y., Desai, A., and Cleveland, D. W. (2005). Microtubule capture by CENP-E silences BubR1-dependent mitotic checkpoint signaling. J Cell Biol *170*, 873-880.

Marx, J. (2002). Debate surges over the origins of genomic defects in cancer. Science *297*, 544-546.

Matsuura, S., Matsumoto, Y., Morishima, K., Izumi, H., Matsumoto, H., Ito, E., Tsutsui, K., Kobayashi, J., Tauchi, H., Kajiwara, Y.*, et al.* (2006). Monoallelic BUB1B mutations and defective mitotic-spindle checkpoint in seven families with premature chromatid separation (PCS) syndrome. Am J Med Genet A *140*, 358-367.

McConnell, M. J., Kaushal, D., Yang, A. H., Kingsbury, M. A., Rehen, S. K., Treuner, K., Helton, R., Annas, E. G., Chun, J., and Barlow, C. (2004). Failed clearance of aneuploid embryonic neural progenitor cells leads to excess aneuploidy in the Atm-deficient but not the Trp53-deficient adult cerebral cortex. J Neurosci *24*, 8090-8096.

McEwen, B. F., Chan, G. K., Zubrowski, B., Savoian, M. S., Sauer, M. T., and Yen, T. J. (2001). CENP-E is essential for reliable bioriented spindle attachment, but chromosome alignment can be achieved via redundant mechanisms in mammalian cells. Mol Biol Cell *12*, 2776-2789.

Meaburn, K. J., and Misteli, T. (2007). Cell biology: chromosome territories. Nature *445*, 379-781.

Merdes, A., and Cleveland, D. W. (1998). The role of NuMA in the interphase nucleus. J Cell Sci *111 (Pt 1)*, 71-79.

Merdes, A., Heald, R., Samejima, K., Earnshaw, W. C., and Cleveland, D. W. (2000). Formation of spindle poles by dynein/dynactin-dependent transport of NuMA. J Cell Biol *149*, 851-862.

Merdes, A., Ramyar, K., Vechio, J. D., and Cleveland, D. W. (1996). A complex of NuMA and cytoplasmic dynein is essential for mitotic spindle assembly. Cell *87*, 447-458.

Meyers, E. N., Lewandoski, M., and Martin, G. R. (1998). An Fgf8 mutant allelic series generated by Cre- and Flp-mediated recombination. Nat Genet *18*, 136-141.

Michel, L. S., Liberal, V., Chatterjee, A., Kirchwegger, R., Pasche, B., Gerald, W., Dobles, M., Sorger, P. K., Murty, V. V., and Benezra, R. (2001). MAD2 haplo-insufficiency causes premature anaphase and chromosome instability in mammalian cells. Nature *409*, 355-359.

Misawa, H., Nakata, K., Toda, K., Matsuura, J., Oda, Y., Inoue, H., Tateno, M., and Takahashi, R. (2003). VAChT-Cre.Fast and VAChT-Cre.Slow: postnatal expression of Cre recombinase in somatomotor neurons with different onset. Genesis *37*, 44-50.

Misteli, T. (2001). Protein dynamics: implications for nuclear architecture and gene expression. Science *291*, 843-847.

Morgenstern, J. P., and Land, H. (1990). Advanced mammalian gene transfer: high titre retroviral vectors with multiple drug selection markers and a complementary helper-free packaging cell line. Nucleic Acids Res *18*, 3587-3596.

Morrison, S. J., and Kimble, J. (2006). Asymmetric and symmetric stem-cell divisions in development and cancer. Nature *441*, 1068-1074.

Myung, K., Smith, S., and Kolodner, R. D. (2004). Mitotic checkpoint function in the formation of gross chromosomal rearrangements in Saccharomyces cerevisiae. Proc Natl Acad Sci U S A *101*, 15980-15985.

Nicklas, R. B. (1989). The motor for poleward chromosome movement in anaphase is in or near the kinetochore. J Cell Biol *109*, 2245-2255.

Norden, C., Mendoza, M., Dobbelaere, J., Kotwaliwale, C. V., Biggins, S., and Barral, Y. (2006). The NoCut pathway links completion of cytokinesis to spindle midzone function to prevent chromosome breakage. Cell *125*, 85-98.

O'Connell, C. B., and Khodjakov, A. L. (2007). Cooperative mechanisms of mitotic spindle formation. J Cell Sci *120*, 1717-1722.

Olave, I. A., Reck-Peterson, S. L., and Crabtree, G. R. (2002). Nuclear actin and actin-related proteins in chromatin remodeling. Annu Rev Biochem *71*, 755-781.

Parrinello, S., Samper, E., Krtolica, A., Goldstein, J., Melov, S., and Campisi, J. (2003). Oxygen sensitivity severely limits the replicative lifespan of murine fibroblasts. Nat Cell Biol *5*, 741-747.

Pfaffl, M. W. (2001). A new mathematical model for relative quantification in real-time RT-PCR. Nucleic Acids Res *29*, e45.

Putkey, F. R., Cramer, T., Morphew, M. K., Silk, A. D., Johnson, R. S., McIntosh, J. R., and Cleveland, D. W. (2002). Unstable kinetochore-microtubule capture and chromosomal instability following deletion of CENP-E. Dev Cell *3*, 351-365.

Qi, H., Rath, U., Ding, Y., Ji, Y., Blacketer, M. J., Girton, J., Johansen, J., and Johansen, K. M. (2005). EAST interacts with Megator and localizes to the putative spindle matrix during mitosis in Drosophila. J Cell Biochem *95*, 1284-1291.

Quintanilla, M., Brown, K., Ramsden, M., and Balmain, A. (1986). Carcinogen-specific mutation and amplification of Ha-ras during mouse skin carcinogenesis. Nature *322*, 78-80.

Quintyne, N. J., Reing, J. E., Hoffelder, D. R., Gollin, S. M., and Saunders, W. S. (2005). Spindle multipolarity is prevented by centrosomal clustering. Science *307*, 127-129.

Rao, C. V., Yang, Y. M., Swamy, M. V., Liu, T., Fang, Y., Mahmood, R., Jhanwar-Uniyal, M., and Dai, W. (2005). Colonic tumorigenesis in BubR1+/-ApcMin/+ compound mutant mice is linked to premature separation of sister chromatids and enhanced genomic instability. Proc Natl Acad Sci U S A *102*, 4365-4370.

Rehen, S. K., McConnell, M. J., Kaushal, D., Kingsbury, M. A., Yang, A. H., and Chun, J. (2001). Chromosomal variation in neurons of the developing and adult mammalian nervous system. Proc Natl Acad Sci U S A *98*, 13361-13366.

Rieder, C. L. (2005). Kinetochore fiber formation in animal somatic cells: dueling mechanisms come to a draw. Chromosoma *114*, 310-318.

Rodriguez, C. I., Buchholz, F., Galloway, J., Sequerra, R., Kasper, J., Ayala, R., Stewart, A. F., and Dymecki, S. M. (2000). High-efficiency deleter mice show that FLPe is an alternative to Cre-loxP. Nat Genet *25*, 139-140.

Sbodio, J. I., and Chi, N. W. (2002). Identification of a tankyrase-binding motif shared by IRAP, TAB182, and human TRF1 but not mouse TRF1. NuMA contains this RXXPDG motif and is a novel tankyrase partner. J Biol Chem *277*, 31887-31892.

Shi, J., Orth, J. D., and Mitchison, T. (2008). Cell type variation in responses to antimitotic drugs that target microtubules and kinesin-5. Cancer Res *68*, 3269-3276.

Shi, Q., and King, R. W. (2005). Chromosome nondisjunction yields tetraploid rather than aneuploid cells in human cell lines. Nature *437*, 1038-1042.

Shin, H. J., Baek, K. H., Jeon, A. H., Park, M. T., Lee, S. J., Kang, C. M., Lee, H. S., Yoo, S. H., Chung, D. H., Sung, Y. C*., et al.* (2003). Dual roles of human BubR1, a mitotic checkpoint kinase, in the monitoring of chromosomal instability. Cancer Cell *4*, 483-497.

Shopland, L. S., and Lawrence, J. B. (2000). Seeking common ground in nuclear complexity. J Cell Biol *150*, F1-4.

Sieber, O. M., Heinimann, K., and Tomlinson, I. P. (2003). Genomic instability--the engine of tumorigenesis? Nat Rev Cancer *3*, 701-708.

Siller, K. H., Cabernard, C., and Doe, C. Q. (2006). The NuMA-related Mud protein binds Pins and regulates spindle orientation in Drosophila neuroblasts. Nat Cell Biol *8*, 594-600.

Skoufias, D. A., DeBonis, S., Saoudi, Y., Lebeau, L., Crevel, I., Cross, R., Wade, R. H., Hackney, D., and Kozielski, F. (2006). S-trityl-L-cysteine is a reversible, tight binding inhibitor of the human kinesin Eg5 that specifically blocks mitotic progression. J Biol Chem *281*, 17559-17569.

Soriano, P. (1999). Generalized lacZ expression with the ROSA26 Cre reporter strain. Nat Genet *21*, 70-71.

Spector, D. L. (2001). Nuclear domains. J Cell Sci *114*, 2891-2893.

Strate, L. L., and Syngal, S. (2005). Hereditary colorectal cancer syndromes. Cancer Causes Control *16*, 201-213.

Sugimoto, I., Murakami, H., Tonami, Y., Moriyama, A., and Nakanishi, M. (2004). DNA replication checkpoint control mediated by the spindle checkpoint protein Mad2p in fission yeast. J Biol Chem *279*, 47372-47378.

Taylor, S. S., Hussein, D., Wang, Y., Elderkin, S., and Morrow, C. J. (2001). Kinetochore localisation and phosphorylation of the mitotic checkpoint components Bub1 and BubR1 are differentially regulated by spindle events in human cells. J Cell Sci *114*, 4385-4395.

Tousson, A., Zeng, C., Brinkley, B. R., and Valdivia, M. M. (1991). Centrophilin: a novel mitotic spindle protein involved in microtubule nucleation. J Cell Biol *112*, 427-440.

Tulu, U. S., Fagerstrom, C., Ferenz, N. P., and Wadsworth, P. (2006). Molecular requirements for kinetochore-associated microtubule formation in mammalian cells. Curr Biol *16*, 536-541.

Wang, Q., Liu, T., Fang, Y., Xie, S., Huang, X., Mahmood, R., Ramaswamy, G., Sakamoto, K. M., Darzynkiewicz, Z., Xu, M., and Dai, W. (2004). BUBR1 deficiency results in abnormal megakaryopoiesis. Blood *103*, 1278-1285.

Wasser, M., and Chia, W. (2000). The EAST protein of drosophila controls an expandable nuclear endoskeleton. Nat Cell Biol *2*, 268-275.

Weaver, B. A., Bonday, Z. Q., Putkey, F. R., Kops, G. J., Silk, A. D., and Cleveland, D. W. (2003). Centromere-associated protein-E is essential for the mammalian mitotic checkpoint to prevent aneuploidy due to single chromosome loss. J Cell Biol *162*, 551-563.

Weaver, B. A., and Cleveland, D. W. (2005). Decoding the links between mitosis, cancer, and chemotherapy: The mitotic checkpoint, adaptation, and cell death. Cancer Cell *8*, 7-12.

Weaver, B. A., and Cleveland, D. W. (2006). Does aneuploidy cause cancer? Curr Opin Cell Biol *18*, 658-667.

Weaver, B. A., Silk, A. D., and Cleveland, D. W. (2006). Cell biology: nondisjunction, aneuploidy and tetraploidy. Nature *442*, E9-10; discussion E10.

Weaver, B. A., Silk, A. D., Montagna, C., Verdier-Pinard, P., and Cleveland, D. W. (2007). Aneuploidy acts both oncogenically and as a tumor suppressor. Cancer Cell *11*, 25-36.

Wen, W., Meinkoth, J. L., Tsien, R. Y., and Taylor, S. S. (1995). Identification of a signal for rapid export of proteins from the nucleus. Cell *82*, 463-473.

Wendt, K. S., Yoshida, K., Itoh, T., Bando, M., Koch, B., Schirghuber, E., Tsutsumi, S., Nagae, G., Ishihara, K., Mishiro, T.*, et al.* (2008). Cohesin mediates transcriptional insulation by CCCTC-binding factor. Nature *451*, 796-801.

Wijnhoven, S. W., Kool, H. J., van Teijlingen, C. M., van Zeeland, A. A., and Vrieling, H. (2001). Loss of heterozygosity in somatic cells of the mouse. An important step in cancer initiation? Mutat Res *473*, 23-36.

Wong, R. W., Blobel, G., and Coutavas, E. (2006). Rae1 interaction with NuMA is required for bipolar spindle formation. Proc Natl Acad Sci U S A *103*, 19783-19787.

Wood, K. W., Sakowicz, R., Goldstein, L. S., and Cleveland, D. W. (1997). CENP-E is a plus end-directed kinetochore motor required for metaphase chromosome alignment. Cell *91*, 357-366.

Yanagawa, Y., Kobayashi, T., Ohnishi, M., Kobayashi, T., Tamura, S., Tsuzuki, T., Sanbo, M., Yagi, T., Tashiro, F., and Miyazaki, J. (1999). Enrichment and efficient screening of ES cells containing a targeted mutation: the use of DT-A gene with the polyadenylation signal as a negative selection maker. Transgenic Res *8*, 215-221.

Yang, A. H., Kaushal, D., Rehen, S. K., Kriedt, K., Kingsbury, M. A., McConnell, M. J., and Chun, J. (2003). Chromosome segregation defects contribute to aneuploidy in normal neural progenitor cells. J Neurosci *23*, 10454-10462.

Yang, C. H., and Snyder, M. (1992). The nuclear-mitotic apparatus protein is important in the establishment and maintenance of the bipolar mitotic spindle apparatus. Mol Biol Cell *3*, 1259-1267.

Yang, Z., Loncarek, J., Khodjakov, A., and Rieder, C. L. (2008). Extra centrosomes and/or chromosomes prolong mitosis in human cells. Nat Cell Biol *10*, 748-751.

Yao, X., Anderson, K. L., and Cleveland, D. W. (1997). The microtubule-dependent motor centromere-associated protein E (CENP-E) is an integral component of kinetochore corona fibers that link centromeres to spindle microtubules. J Cell Biol *139*, 435-447.

Yen, T. J., Compton, D. A., Wise, D., Zinkowski, R. P., Brinkley, B. R., Earnshaw, W. C., and Cleveland, D. W. (1991). CENP-E, a novel human centromere-associated protein required for progression from metaphase to anaphase. Embo J *10*, 1245-1254.

Yoon, Y. M., Baek, K. H., Jeong, S. J., Shin, H. J., Ha, G. H., Jeon, A. H., Hwang, S. G., Chun, J. S., and Lee, C. W. (2004). WD repeat-containing mitotic checkpoint proteins act as transcriptional repressors during interphase. FEBS Lett *575*, 23-29.

Yucel, J. K., Marszalek, J. D., McIntosh, J. R., Goldstein, L. S., Cleveland, D. W., and Philp, A. V. (2000). CENP-meta, an essential kinetochore kinesin required for the maintenance of metaphase chromosome alignment in Drosophila. J Cell Biol *150*, 1-11.

Zeng, C. (2000). NuMA: a nuclear protein involved in mitotic centrosome function. Microsc Res Tech *49*, 467-477.